~~THE~~ SIGNIFICANCE OF MASS TRANSFER IN THE OXIDATION REACTIONS OF CARBON.

A Thesis submitted for the degree of

DOCTOR OF PHILOSOPHY

in the Faculty of Science

of the

University of London

by

JOHN FRANCIS MICHAEL NAGLE, B.Sc., D.I.C.

Department of Chemical Engineering,
Imperial College of Science and Technology,
London, S.W.7.

June, 1961.

ABSTRACT.

The rates of oxidation of carbon and graphites have been measured in the temperature range 1,000°C. to 2,000°C. at pressures of 0.06 atmospheres to 1 atmosphere with gas velocities varying from 100 cms/sec. to 10,000 cms/sec. Cold gas was directed on to the side of an electrically heated carbon rod, whose temperature was measured by a disappearing filament pyrometer. By timing the retreat of the surface of the rod opposite the gas orifice, the rate of reaction was calculated.

At atmospheric pressure and high temperatures the combustion rate of the most reactive material, the porous carbon, was found to be mass transfer controlled and the mass transfer rates were correlated against the gas velocity, the carbon temperature, the oxygen partial pressure and the total gas pressure. When a less reactive polycrystalline graphite was oxidised at lower total gas pressure a considerable degree of chemical control was achieved and using the previously mentioned correlations the influence of mass transfer on the reaction rates was estimated and the true chemical reaction rates calculated. The least reactive material, pyrographite, seemed to be free from mass transfer control of the combustion rate.

Both the polycrystalline graphite and pyrographite reaction rates reached a maximum about 1,700°C. and then decreased at higher temperatures. Although this effect has been found at low pressures it has never before been reported for the high oxygen pressures used in this work. The position of the maximum rate is 500°C. higher at 0.23 atmospheres of oxygen than at the 2.5×10^{-5} atmospheres of oxygen used in previous experiments.

A simple theory has been proposed to explain the rather unusual kinetic behaviour of graphite and when probable values are chosen for the constants in the kinetic expression the calculated reaction rates agree with both the high pressure and low pressure observed rates.

ACKNOWLEDGEMENTS.

The author wishes to thank Dr.R.F.Strickland-Constable whose guidance and help have been invaluable throughout this research, and to thank Professor D.M.Newitt, F.R.S., in whose department the work was done.

To Mr.A.C.V.Sweeting and his staff the author must express his gratitude for their assistance in building apparatus, and he is also most grateful to Mr.L.R.Barrett, Lecturer in Ceramics, for the loan of the Hackbridge Transformer.

During the course of his research the author has been supported by the North Thames Gas Board and the Esso Petroleum Company and he is most grateful for their generosity. An apparatus grant for this research has been provided by the United Kingdom Atomic Energy Authority, Harwell, to whom the author is very much obliged.

CONTENTS.

	Page
Title Page.	1
Abstract.	2
Acknowledgements.	4
Contents.	5
Introduction.	8
Literature Survey.	11
(A) General Remarks.	11
(B) Gasification of graphite at low temperatures.	11
(C) Gasification of graphite at intermediate temperatures.	15
(D) Gasification of graphite at high temperatures.	32
Experimental.	40
(A) Apparatus.	40
(B) Mensuration.	46
(C) Experimental Procedure.	52
(D) Description of Materials.	54
Analysis of the Experimental Results.	57
(A) Dependence of the apparent mass transfer coefficient on gas velocity and carbon surface temperature.	57
(B) Dependence of the rate of reaction of porous carbon with oxygen on the oxygen partial pressure at a total gas pressure of one atmosphere.	64
(C) Dependence of the reaction rate of porous carbon with oxygen on reduced total gas pressures and partial oxygen pressures.	68

	Page
(D) Dependence of the reaction rate of polycrystalline graphite with oxygen on the graphite temperature and gas velocities in air.	72
(E) Dependence of the reaction rate of polycrystalline graphite with oxygen on the graphite temperature and gas velocities in 50% oxygen-nitrogen at one atmosphere total gas pressure.	75
(F) Dependence of the reaction rate of polycrystalline graphite with oxygen on the graphite temperature, oxygen partial pressure, total gas pressure and gas velocities at reduced pressures.	76
(G) Dependence of the reaction rate of pyrographite with oxygen on the graphite temperature and gas velocity.	94
Theories Proposed to Account for the High Temperature Kinetics of the Graphite Oxidation Reactions.	97
(A) Eyring's Theory.	98
(B) Surface Healing Theory.	100
Discussion.	110
Appendix 1. Experimental Observations.	125
Contents of Appendix 1	125
Table 1.	127
Table 2.	132
Table 3.	136
Table 4.	140
Table 5.	144
Table 6.	147
Table 7.	156
Table 8.	166

Page

Appendix 2. Graphs. 168

Appendix 3. Impact Pressures. 184

Appendix 4. Error Analysis. 186

Appendix 5. Optical Pyrometry. 191

Bibliography. 193

INTRODUCTION.

The oxidation reactions of carbon are of great commercial importance and also of much academic interest.

Many of the carbon gasification products are used as both fuel and as starting materials for the synthesis of organic chemicals and inorganic fertilisers. Carbons and graphites have found increasing use as constructional materials in the chemical industry, in nuclear engineering and in certain branches of aeronautical engineering. The corrosion resistance of graphite combined with its good mechanical strength and thermal shock resistance make it an almost unique high temperature constructional material, which is, however, attacked by oxidising gases to give gaseous products. A good understanding of the chemical kinetic and other factors which influence the rates of the carbon oxidation reactions, under a very wide range of conditions of temperature and pressure, is of obvious industrial importance.

Academic interest in the oxidation reactions of carbon is very great because these reactions are among the few reactions in which a gas reacts with a covalent solid to give gaseous products. The oxidation reactions of carbon are especially interesting because they can be studied over

a very wide range of temperatures. Heterogeneous reactions, because they are partly controlled by physical factors, are very complex. The overall rate of a heterogeneous reaction is determined by the individual rates of several processes, such as the diffusion of the reactant gas through stagnant gas layers to the solid surface, the diffusion of the reactant gas into the porous structure of the solid, the adsorption of the reactant gas on the solid followed by chemical reaction and the subsequent desorption of gaseous products which must then diffuse out of the pores through the boundary layer into the bulk of the gaseous phase.

Some of the previously mentioned processes in the oxidation reactions of carbon have been well studied, but at very high temperatures little has been done to try to distinguish the surface kinetic process from the usually important boundary layer mass transfer process, which is occurring at the same time. The chief difficulty of this problem of studying one process while other processes are going on, is that the rate of the slow process in the succession will obscure the rate of a faster process which may be of interest. If in a particular system several processes contribute to the overall rate and if one of these processes, e.g. the chemical reaction rate, is very slow

compared with the others the system can be said to be in the chemical regime. At high temperatures and high partial pressures of oxygen the carbon-oxygen system is usually in the boundary layer mass transfer regime.

The surface chemical kinetics of the carbon oxidation reactions, when studied at very low pressures where stagnant boundary layers cannot exist, are most unusual. The reaction rate not only goes through a maximum as the solid temperature is raised but it also shows hysteresis. Since at atmospheric pressure, e.g. in air, the reaction between carbon and oxygen is in the mass transfer regime at high temperatures it has not hitherto been possible to tell if the unusual surface chemical kinetics will be found at higher partial pressures of oxygen. This present work was undertaken to provide an answer to this question.

LITERATURE SURVEY.

A. General Remarks.

The processes involved in heterogeneous reactions are not equally important under a given set of conditions of temperature and pressure. Under any set of conditions one process will usually be much slower than any of the others and will inconsequence control the reaction rate. The rate controlling process will change as the prevailing conditions change so that a study of the literature on the oxidation reactions of carbon will show that experiments have been carried out under extreme conditions, e.g. low temperature, low pressure, etc. in the hope of isolating some particular rate controlling process. The literature is best subdivided by consideration of the process of special interest, i.e. by the temperature and pressure range in which the experiments were done. All the oxidising gases show the same patterns of behaviour so that it is usually unnecessary to give them separate attention.

B. Gasification of Graphite at Low Temperatures (ca. 500°C.)

B.1. Possible Reactions of Oxidising Gases with Graphite.

Graphite can react with oxidising gases in the

following ways.

With oxygen $C + O_2 \rightarrow CO_2$

$2C + O_2 \rightarrow 2CO$

With carbon dioxide $C + CO_2 \rightarrow 2CO$

With steam $C + H_2O \rightarrow CO + H_2$

$C + 2H_2O \rightarrow CO_2 + 2H_2$

With nitrous oxide $C + N_2O \rightarrow CO + N_2$

$C + 2N_2O \rightarrow CO_2 + 2N_2$

When graphite and oxygen react carbon monoxide is often the favoured product and carbon dioxide is produced in smaller quantities. This observation is true also of steam but with nitrous oxide reaction about 400°C. favours carbon dioxide production while at higher temperatures the proportion of carbon monoxide increases [1]. The similarity in the reactions suggests that similar reaction mechanisms exist and that since the gases differ greatly the role of the graphite in the reaction mechanism must be very important.

B.2. The Rate Determining Process in the Low Temperature Gasification.

Duval [2] points out that though there have been many studies of the reaction between graphite and oxygen at

temperatures of 400°C. to 1,000°C., pressures of fractions of a millimetre of mercury to one atmosphere, the results are difficult to analyse and compare because at low temperature the reaction rate depends on the structure of the graphite and above all on its purity to a degree only recently recognised. Many authors seems to agree, however, that at temperatures around 500°C. the oxidation reactions of graphite are in the chemical regime [3,4,5].

Gulbransen et alia [3] studied the reactions of pure artificial graphite with oxygen at graphite temperatures of 425°C. to 575°C. and between pressures of 0.15 cms. (mercury) and 9.8 cms. (mercury) of oxygen, and in addition they examined the oxidation of graphite with carbon dioxide at 7.5 cms. (mercury) between 500°C. and 900°C.

For the reaction of graphite with oxygen they found the activation energy of the reaction to be 37 k.cal/mole The magnitude of this activation energy suggests that the reaction rate is controlled by the rate of chemical attack.

Rossberg and Wicke [4,5] in their papers have studied the oxidation of bored out cylinders of spectroscopically pure graphite with oxygen, between temperatures of 520°C. and 1,420°C. In their experiments they measured the surface area of the graphite using the

B.E.T. method of adsorption of krypton. Their plot of Log (effective reaction rate constant) versus 1/T°A shows that below 650°C. the reaction activation energy is 50 k.cal/mole and that in the higher temperature regions half of this value is obtained. These authors conclude from a consideration of Thiele's theory of Pore Diffusion [6] that below 650°C. the reaction rate is controlled by the rate of chemical attack and that above 650°C. pore diffusion rates become important. A further paper by Wicke and Hedden [7] which reports the attack by carbon dioxide on graphite in the temperature range 900°C. to 1,200°C. shows that when the attack is made on very small particles of graphite the activation energy of combustion is twice the activation energy found when the attack is made on a bigger piece of graphite. The Thiele Theory would support the view that the higher activation energy is that of the chemical reaction and that as the size of the graphite increases pore diffusion would be more important and the activation energy could be halved.

B.3. Catalytic Effects at Low Temperatures.

Walker [8] has shown the catalytic effect of traces of iron on the reactions between carbon dioxide and oxygen on graphite "wear dust" at low pressures of about

20 microns of mercury in the temperature range 400°C. to 700°C. for carbon dioxide and 200°C. to 500°C. for oxygen. In the case of carbon dioxide when the traces of iron were removed from the "wear dust" the sample had to be heated a further 300°C. to get the same amount of reaction. The oxygen reaction indicated that the catalytic effect of iron was much less at 500°C. than at 200°C. which is to be expected since the catalyst merely provides a reaction path of lower activation energy to facilitate reaction at lower temperatures. It would seem therefore that at higher temperatures the catalytic effect of iron should not be very great.

At low temperatures the oxidation reactions of graphite seem to be in the chemical regime and to be strongly influenced by traces of catalytic impurities in the graphite.

C. <u>The Gasification of Graphite at Intermediate Temperatures. (700°C. - 1,200°C.)</u>.

In the temperature range 700°C. to 1,200°C. the rate controlling step in the attack of oxidising gases on graphite is thought to be the rate at which the reactant gases and products can diffuse through the pores in big pieces of graphite. Much experimental work has been done on the attack of oxygen, carbon dioxide and steam on graphite in this temperature range. The Thiele Theory of Pore

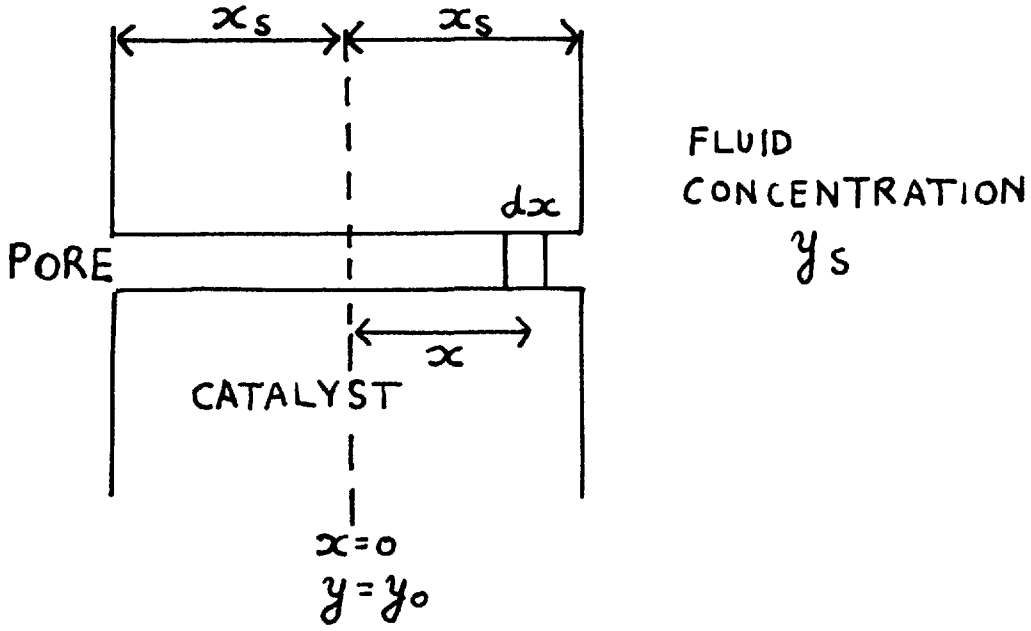
Diffusion upon which most of the interpretations of these works rest will be described first.

C.1. The Thiele Theory of Pore Diffusion [6].

Thiele's Theory of Pore Diffusion was really developed for the interaction of fluid reactants on a porous catalyst and is not strictly applicable to reactions of gases with a porous solid, where the porosity will change and the solid will be consumed. This theory is, however, still the best treatment of the reactions of gases with porous solids and with its predictions many of the experiments are compared to show the existence of pore diffusion as a rate controlling process.

If particles are very small then the fluid reactant will have the same concentration in all the pores, but as the particle size is increased the products will be formed faster than they can be carried out of the pores and the reactant concentration in the pores will be less than the concentration at the surface of the particles. The reaction will now be confined more to the surface of the particle. i.e. in the outer pore region. A consequence of these ideas is that below a certain grain size the activity of porous particles will be proportional to the total mass present but above that particle size the activity will be proportional

FIGURE 1



to the external surface areas of the grains.

To derive expressions for the activity of porous catalysts Thiele had to make a big number of simplifying assumptions of which the most important perhaps is that the pore length is assumed proportional to the shortest dimension of the grains.

The theory will be developed for the simple case of a first order reaction occurring with no volume change on a flat plate (Pore length = $\frac{1}{2}$ thickness of plate). See Figure 1 for an illustration of this simple case.

The reaction is assumed first order with respect to one component only and the other component is ignored. The reverse reaction rate is also assumed to be negligible.

x = distance from centre, measured along the pore (cms)

x_s = distance from centre to surface along the pore(cms)

y = concentration of reactant at x in the pore (moles/cc)

c = the reaction rate constant $\frac{\text{moles}}{\text{sec, cm}^2 \text{ of pore surface, moles/cc of reactant}}$

k = the diffusivity of the reactant (cm^2/sec.)

r = area of pore cross-section per length of perimeter of pore (cms).

a = area of pore cross-section (cm^2)

$h = \sqrt{\frac{c}{k\,r}}$

The reactant diffuses across the right-hand boundary of the element, some reacts and less diffuses across the left-hand boundary of the element.

In any section Diffusion Transfer Rate = k a dy/dx

Difference in diffusion at the two boundaries

$$= k\ a\ d\ (dy/dx)$$

The amount of reaction on the surface of the element of the pore $= a\ c\ y\ dx/r$

where the area of the walls of the element = a dx/r.

Equating $\frac{d}{dx}\left(\frac{dy}{dx}\right) = \frac{cy}{kr}$

$$\frac{d^2y}{dx^2} = \frac{cy}{kr} = h^2y.$$

At the centre the flow by diffusion = 0 (by symmetry)

$dy/dx = 0$ when $x = 0$

and $y = y_s$ when $x = x_s$

$$y = y_s \frac{e^{hx} + e^{-hx}}{e^{hx_s} + e^{-hx_s}} = y_s \frac{\cosh (hx)}{\cosh (hx_s)}$$

The total amount converted by one half pore in unit time, is equal to the amount diffusing into one entrance of the pore in that time

$$\text{i.e.} = k\ a\ (dy/dx)_s$$

This can be shown to be $= k\ a\ h\ y_s\ \text{tansh}\ (hx_s)$

and when x_s is larger = k a h y_s.

The chief features of this result which are used in the interpretation of experiments are :

(a) the reaction rate is proportional to $\sqrt{k}$ and hence is proportional to $\sqrt{\frac{1}{\text{Total gas pressure}}}$

and (b) the reaction rate is proportional to $\sqrt{c}$, i.e. proportional to the square root of the true chemical reaction rate constant. A consequence of this is that the activation energy of a reaction controlled by the rate of pore diffusion is half the activation energy of the true chemical reaction rate.

C.2. Experimental Studies of Intermediate Temperature Range Gasification - Interpretations based on the Thiele Theory of Pore Diffusion.

Wicke and his co-workers have studied the reactions of graphite with oxygen, carbon dioxide and steam in the temperature range 700°C. to 1,200°C. and have interpreted the results on the basis of Thiele's Theory and have suggested that pore diffusion is the rate controlling process of these reactions in this particular temperature range.

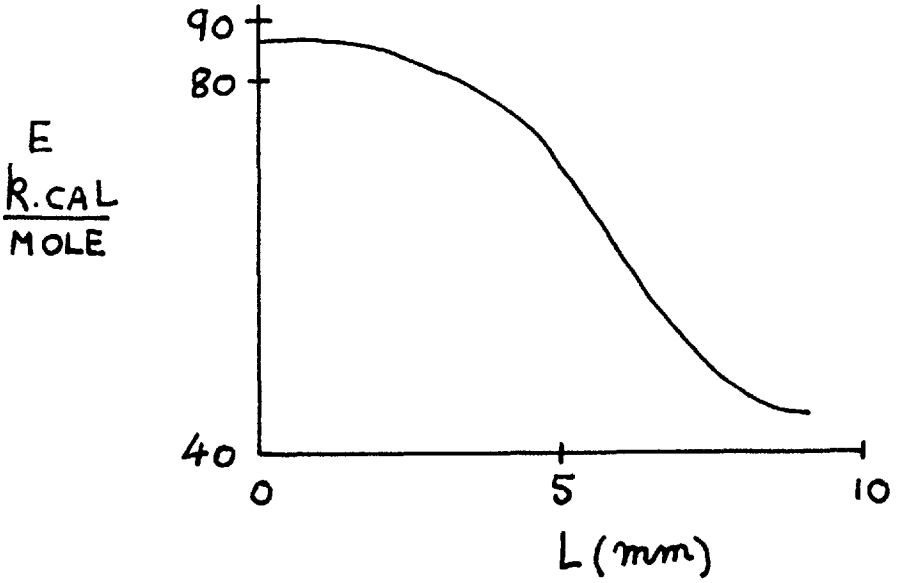
Wicke and Hedden [7] used two types of apparatus in their study of the reactions of oxygen and carbon dioxide with spectroscopically pure graphite. In one apparatus

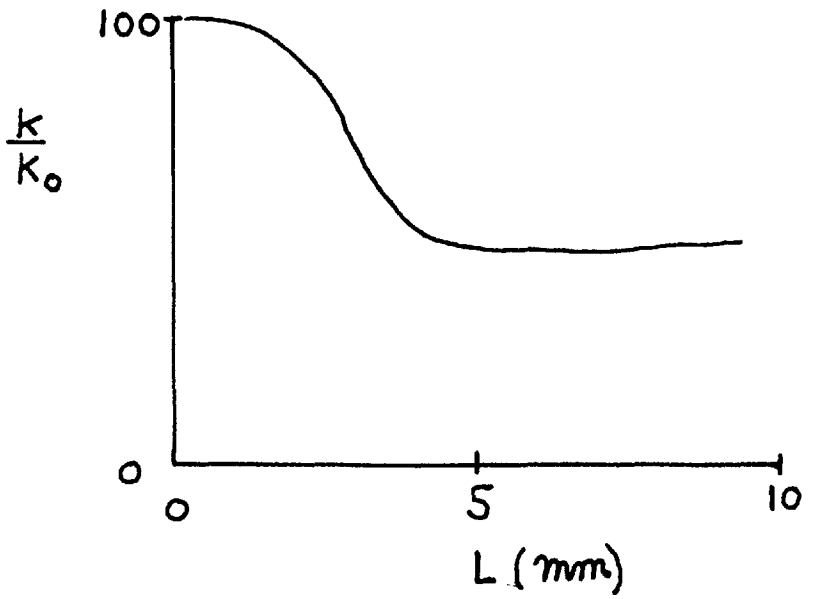
the gases were streamed through cylinders of graphite and in the other the gases were streamed through heaps of very small particles. The purpose of these alternative methods was to demonstrate the influence of porous diffusion on the temperature dependence of the reaction rate. The Thiele theory suggests that with small particles the whole of the inner surface of the graphite is available for reaction and that under these conditions the rate of reaction should be controlled by the rate of chemical combination and not by the rate of pore diffusion. The activation energies of the reactions carried out on the small particles were twice those obtained when measurements were made on larger pieces of graphite.

Reaction	$C + O_2 \rightarrow CO_2$	$C + CO_2 \rightarrow 2CO$	
Temperature	600 - 700°C.	1000 - 1100°C.	
Pressure	0.1 to 0.2 ats. O_2	0.1 to 0.7 ats. CO_2	
Activation Energies	29±1 k cal/mole and	43±1 k cal/mole and	Diffusion Present
	57±3 k cal/mole	85±3 k cal/mole	Diffusion Absent
$k_o = He^{-A/RT}$	$1.5 \times 10^9 \, e^{\frac{-58000}{RT}}$	$2.0 \times 10^9 \, e^{\frac{-86000}{RT}}$	

In other measurements the diffusivity of the carbon dioxide was changed by adding helium to the gas mixture instead of

FIGURE 2





nitrogen and the reaction rate was found to change with the diffusivity.

The activation energies were plotted against particle size for the Boudouard reaction and they fell eventually to one half of their original value. The pore length was taken equal to the particle radius. The effectiveness factor k/k_o fell in a somewhat similar fashion (see Figure 2).

C.3. The Mechanism of Graphite Combustion with Oxygen.

A kinetic mechanism of the reaction of oxygen with pure graphite has been proposed by Rossberg [5]. This mechanism is rather similar to the mechanism of the steam reaction which was proposed by Rossberg and Wicke [9] but which will not be described.

Dry air or oxygen-nitrogen mixtures were streamed through tubes of graphite at a variety of gas speeds of up to 20 metres/second. The inner surface of the graphite was determined by the B.E.T. method and was of the order of 2.5 m^2/gm. The surface temperatures of the graphite were varied in the range 520°C. to 1,420°C. and the outlet gases were analysed. The gas pressures were varied in the range 26 mm. (mercury) to 208 mm. (mercury).

The rate controlling processes in this temperature

range were successively the chemical reaction rate up to 650°C., the pore diffusion rate from 650°C. up to 900°C. and the rate of boundary layer mass transfer above 1,000°C.

Important to an understanding of the kinetics is the ratio of the carbon monoxide concentration in the reaction products to the concentration of the carbon dioxide. Rossberg suggests that the conditions under which his experiments were carried out minimises afterburning of the carbon monoxide and also the Boudouard reaction. It would seem, therefore, that both carbon monoxide and carbon dioxide are primary products of the combustion. The ratio $[CO/CO_2]$ was shown to remain constant at constant pressure even when the inlet gas concentrations were changed. The formation of both carbon monoxide and carbon dioxide must therefore occur by means of reactions which are of the same order. In agreement with the findings of other workers the ratio $[CO/CO_2]$ showed an activation energy of about 15 kcal/mole, depending on the type of graphite, in the temperature range 500°C. to 1,400°C.

Rossberg has established that

1) the complete reaction is first order with respect to the oxygen concentration.
2) the carbon monoxide and carbon dioxide form at the same time on the graphite surface.

3) the CO/CO_2 ratio varies exponentially with temperature and is only slightly dependent on the graphite structure.

4) the CO/CO_2 ratio is independent of the oxygen concentration.

5) transport phenomena in pores and boundary layers leaves the CO/CO_2 ratio practically unchanged.

The fourth finding excludes secondary oxidation of the carbon monoxide. The formation of carbon dioxide would be of a higher order in the gas phase so that the CO/CO_2 ratio would increase with increasing oxygen pressure.

The temperature dependence of the CO/CO_2 ratio permits the following atomic model of the reaction mechanism to be proposed.

Oxygen is adsorbed at random on the surface. The unpaired electrons in the oxygen attract the two adjoining carbon atoms so that the usual interatomic distance of 1.2 A increases. The oxygen molecule can now vibrate with a bigger amplitude and can also rotate rather freely on the surface. Dissociation can now occur in two ways.

Carbon Monoxide Formation : During big vibration the two oxygen atoms separate to about 2.4 A., the distance between two carbon atoms. In this transition state the

bonding between the two oxygen atoms becomes less strong than the fairly stable carbon-oxygen bond and also less strong than the bonding of neighbouring carbon-carbon atoms. Carbon monoxide then desorbs quickly.

Carbon Dioxide Formation : For the formation of the second surface oxide the adsorbed oxygen molecule must be in a sterically favourable position. The transition to the activated intermediate stage occurs immediately if the internuclear direction of the two oxygen atoms falls parallel to the C-axis of the graphite lattice. One can put the ratio of the frequency factors, attained in the transition state for the carbon monoxide and carbon dioxide formation almost equal to the ratio of the vibrational frequency to the rotational frequency of the adsorbed oxygen. Assuming the first frequency as 10^{13} to 10^{14} sec^{-1} and the second as 10^{10} to 10^{11} sec^{-1} the ratio of the frequency factors of the carbon monoxide and carbon dioxide formation is about 10^{3} to 10^{4} which is of the same order as the experimental results.

The difference in the two activation energies ^{A}E = 15 kcal/mole ($\Delta\,^{A}E = {}^{A}E_{CO} - {}^{A}E_{CO_2}$) is in good agreement with the activation energy which has been found for the CO/CO_2 ratio.

Rossberg and Wicke [4] have tested the influence of temperature and pressure changes on the combustion rate of oxygen on pure graphite.

At temperatures around 500°C. the activation energy of the reaction is about 50 kcal/mole and the reaction rate is not influenced by the total gas pressure when the oxygen concentration is constant. Above 700°C. the activation energy of combustion is about 25 to 30 kcal/mole and a clear pressure dependence was established for the combustion rate. The combustion rate varied inversely with the square root of the gas pressure i.e. varied directly with the square root of the oxygen diffusivity. This behaviour is indicative of a pore diffusion controlled reaction as was shown earlier in the section on the Thiele Theory.

C.4. Experiments not Depending Directly on Thiele Theory Interpretations.

Some workers have studied the gasification of graphite by a variety of methods which were not designed to be tested by the Thiele Theory though at times further deductions from the results have been made by using it.

Duval [2] reports an experiment carried out by Serpinet. Two cylinders of graphite taken from the same

block had a difference of a factor of two in the diameters. These cylinders were heated simultaneously in an atmosphere of the reactant gas and the weight losses were measured. At low temperatures in the chemical regime all the internal surface is active in reaction and the loss of weight is in proportion to their volumes that is to say 8. In the pore diffusion regime at higher temperatures the outer surface of the samples becomes more important and the weight losses are in proportion to the ratio of the sample surfaces, i.e. 4.

The rates of gasification of graphite with carbon dioxide at various depths in the graphite sample have been measured by Ramchandra [11] and his co-workers.

Rods of graphite were placed axially in the gas stream and the ends of the rods were protected by porcelain cones so that only the sides of the rods could be attacked. The rods were weighed during gasification. The times at which successive losses of 0.1 gram occurred were noted and after reaction the bulk density profile was determined.

The bulk density profile was determined by taking cuts of 0.25 mm. at various depths in the sample. The difference in density between the unreacted graphite and the reacted graphite is a measure of the amount of reaction. The chief result of this work is that the amount of reaction is less as the distance from the graphite surface increases.

Petersen and Wright [12] using a method similar to that of Ramchandra showed that at 900°C. the bulk density seemed to be uniform throughout the sample. At 1,100°C. the rate of gasification is very much faster at the graphite surface so that in fact the rate of transport of the reactant into the solid is an important rate controlling process. The measured activation energy was about 50 kcal/mole which is about half the activation energy obtained during lower temperature reaction.

C.5. Other Studies of the Intermediate Temperature Range Gasification.

Hennig [13] has studied the rates of reaction of single crystals of graphite at temperatures about 900°C. to 1,000°C. with oxygen at pressures of 10^{-3} atmospheres to one atmosphere. All the crystals examined belonged to two classes which differed in chemical reactivity i.e. crystals with or without excess lattice defects. Even the crystals which were free of excess vacancies had a few twin lines, i.e. narrow ribbons of twinned regions which appear to have no excessive reactivity to oxygen or carbon dioxide. All the crystals had surface steps some of which were at right angles to the cleavage planes, but these steps could be made less steep by treatment with chlorine and could be removed

by flame etching in a carbon monoxide-oxygen flame.

The surface area effective during reaction was estimated by tracing the movement of a step, in an electron microscope, during the oxidation. The number of monolayers removed together with the weight change of the crystal permits the area attacked during oxidation to be found. The reactivity seemed to be different in different crystallographic directions but the differences were small. Single crystals burn only at layer plane edges and the surface is not highly irregular or even channelled as Eyring and Blyholder [14] have suggested.

The activation energy of the reaction was about 43 k cal./mole and the reaction order with respect to oxygen concentration was about one half. The samples were heated to about 900°C. before reaction to get rid of water vapour which was thought to cling strongly to the surface and catalyse the reaction. Hennig found that water had a strongly catalytic effect and that water labelled with tritium would remain on the graphite surface until the temperature was above 1000°C. Traces of chlorine were shown to inhibit the catalytic effect of water but to leave the uncatalysed attack of oxygen on graphite unchanged. Vertical steps are not essential for fast reaction for very low rates of reaction have been found on crystals which

had many steps and very fast rates were often found on completely flame etched crystals. Silicon appeared to protect the surface of the graphite and even at fairly low temperatures this interaction has been found. The protective action of silicon did not seem to arise because of any inhibition but just through direct shielding. Defects which resulted from rapid quenching of the graphite increased the reaction rate greatly.

The reaction between graphite and oxygen has been studied between 600°C. and 800°C. by Blyholder and Eyring [14] These authors suggest that on samples thicker than 0.1 mm. the reaction rate is controlled by the rate of pore diffusion, and that the true surface reaction is of zero order and has an activation energy of about 80 kcal/mole. Carbon monoxide was the primary product of the reaction. Water is thought to inhibit the reaction rate and for this reason the first few layers of graphite were burned off before each run. The graphite for these reactions was rubbed in thin layers on a ceramic rod and the experimental pressure was about 50 microns of mercury. This work disagrees with most other work carried out in the intermediate temperature region in that the value it ascribes to the activation energy is about twice as high as is usually found, and the reaction order of zero instead of unity is another unusual feature.

D. Graphite Gasification at High Temperatures.

The interaction of graphite with oxidising gases at very high temperatures has been studied in two ways, reactions have been carried out in very low pressure gases and reactions have been carried out at atmospheric pressure in fast gas streams. The overall result of these researches is that the temperature dependence of the gasification rate at very high temperatures is very low, but two different explanations of this result are offered.

At very low pressures the mean free paths of the gases are so great that there can be no boundary layer resistance to the reaction rate and the low activation energy of the surface chemical reaction is thought to be the result of some kind of recrystallisation of the graphite surface or, alternatively, as the result of the removal of some catalysing substance so reducing the reaction rate in opposition to the expected Arrhenius temperature dependence.

At atmospheric pressure the low temperature dependence has been explained as a result of the boundary layer mass transfer control of the reaction rate.

D.1. Gasification Reactions at Low Pressures and High Temperatures.

Strickland-Constable [15,16] and Duval [17,18]

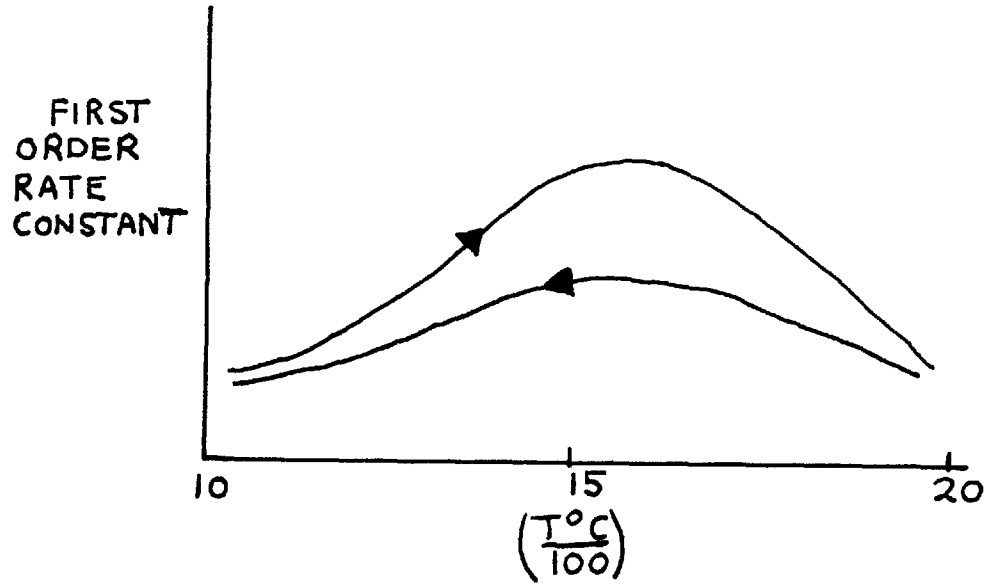
have studied the interaction of gases such as oxygen, carbon dioxide, steam and nitrous oxide with electrically heated carbon filaments in the temperature range 900°C. to 2,000°C., at pressures less than 1 mm. of mercury. In some cases the filaments were coated with pyrolytic carbon made by cracking methane on the heated filaments.

In the temperature range 1,400°C. to 2,000°C. the combustion rate has a negative temperature coefficient and was first order with respect to the oxygen concentration. When filaments were used in the presence of glow discharge the combustion behaviour was very much different; the reaction was zero order and the reaction rate increased sharply with temperature. The quantity of carbon dioxide produced under these conditions was greater than usual. In the absence of glow discharge the values of the calculated first order reaction rate constants show a hysteresis as the temperature is increased and decreased again. This behaviour was also shown by carbon dioxide and steam (See Figure 3).

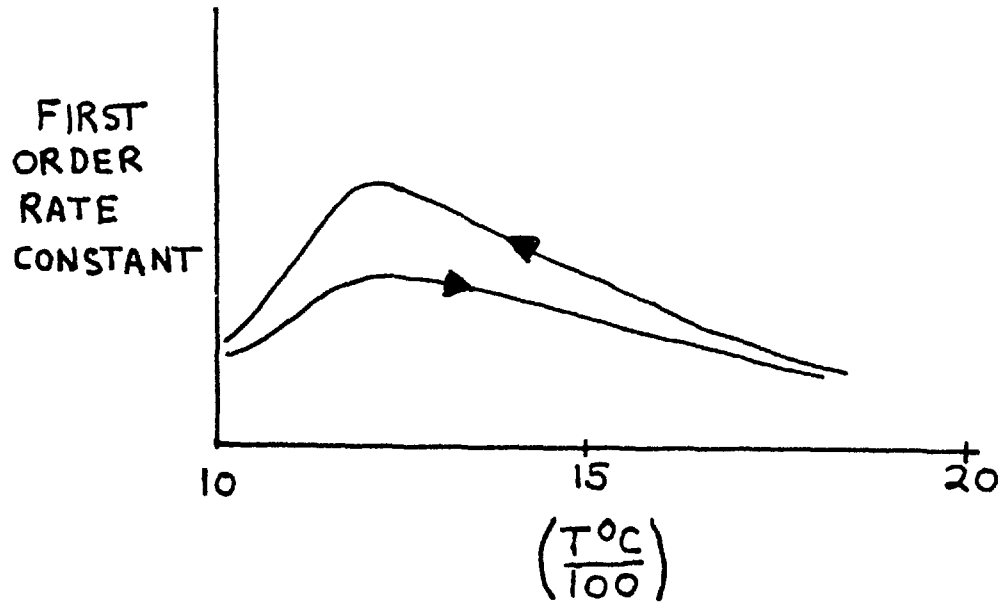
Studies of the gasification of carbon by nitrous oxide, carbon dioxide and steam have been carried out by Strickland-Constable in a manner similar to his investigation of the carbon-oxygen reaction. Care was again taken to

FIGURE 3

STEAM ON CARBON FILAMENTS



OXYGEN ON CARBON FILAMENTS



suppress electronic excitation of the gases. The results obtained by Meyer [19,20] are very different from the results obtained by Strickland-Constable and it would appear that the difference can be explained by the presence of the discharge phenomenon in Meyer's experiments. Duval [17,18] supports Strickland-Constable in this view and has shown that mercury vapour in the experimental system can promote discharge effects.

Two theories have been advanced to explain the results of the high temperature reactions at low pressures. A mathematical development of these theories will be presented later.

One theory [15] suggests that surface roughness on the atomic scale assists the reaction and this roughness is maintained by or created during reaction. At very high temperatures diffusion of carbon atoms can heal the surface making it less reactive. This theory can give a simple account of the hysteresis in the reaction rates of steam, carbon dioxide and nitrous oxide attack on carbon but a further assumption is needed to explain the oxygen reaction behaviour.

Blyholder and Eyring [21] propose the existence of two kinds of edge carbon atoms. Hydrogen associated

with the lattice is thought to activate the surface at low temperatures but at high temperatures this hydrogen is driven off and the attack of the reactants on the pure graphite is much slower. Eyring developed this theory to give an explanation of Meyer's results and thus obtained kinetic expressions which would give zero order reaction at high temperatures.

D.2. Gasification of Graphite at High Temperature and High Pressures.

Wicke and Rossberg [4] have shown that between 1300°C. and 1400°C. the effective temperature coefficient of the graphite-oxygen reaction was zero. In addition, the apparent reaction rate constant was inversely proportional to the total gas pressure at pressures of about 50 mm. of mercury. These facts suggest that the boundary layer mass transfer was the controlling regime under the above conditions. When a large chip of quartz was placed in the gas stream in this experiment the resultant stirring and turbulence increased the apparent reaction rate constant by a factor of about two. The presence of radial concentration gradients in the tube of burning graphite was shown by taking samples of the combustion gases at different distances from the axis of the tube, through a fine quartz probe.

All these findings are consistent with the explanation that the combustion rate is mass transfer controlled.

Watt et alia [22] have studied the reaction of graphite with hot combustion gases which consisted chiefly of water vapour. The gases were passed over a rotating cylinder of graphite placed radially in the gas stream and the rate of reaction was followed by measuring the geometrical retreat of the graphite photographically. The combustion temperature was about 2,400°C. The reacted specimens were tapered towards the centre of the combustion tube; the narrowest point on the specimen was the point nearest the axis of the combustion tube. This tapering was attributed to the effect of the velocity distribution, in the combustion tube, on the rate of mass transfer. The authors related the reaction rate at 2 mm. intervals on the specimen to the corresponding gas velocities and showed that the reaction rate was dependent on the gas velocity to a power varying between 0.25 to 0.35 depending on the reactivity of the particular grade of graphite. An attempt was made to estimate the rate of the surface reaction after the influence of mass transfer had been allowed for by extrapolation.

Spectroscopic grades of graphite [23] in the temperature range 900°C. to 1,200°C. react with oxygen in a partly mass transfer controlled reaction. Above 1,000°C. the reaction rate was dependent on the square root of the gas velocity, but below 1,000°C. some type of chemical resistance to the reaction rate became more important.

The influence of mass transfer in the reaction of oxygen with graphite has been studied in fast gas streams and temperatures of 1,200°C. to 1,700°C. by Walker and his co-workers [24]. Heated reactant gases were blown on to the end of a rod which had been preheated by using it as one of the electrodes of an arc. The graphite rod was fed into the reaction chamber as quickly as it was used so that the position of the graphite relative to the gas inlet nozzle remained constant. The exit gases were analysed and the pit in the carbon was sectioned to find the area. Impact pressures of the gas over the surface of the pit were very different. There would seem to be some possibility that the inlet reactants mixed with the gaseous products of the reaction.

The main results of this work were (a) the reaction was first order with respect to the oxygen concentration;

(b) the reaction rate was dependent on the gas velocity;

(c) the activation energy of the reaction was low and it decreased as the gas velocity was increased.

The gasification of graphite at high temperatures is a complex process combining the physical effects of boundary layer mass transfer with rather unusual surface chemical kinetics.

EXPERIMENTAL.

A. Apparatus.

The reaction enclosure consisted of a cruciform vessel made from welded sections of 6½" diameter and 4" diameter steel pipe. Steel rods of ½" diameter provided electrical connections from the bus-bars of a 30 kilowatt Hackbridge transformer. These rods passed through packed glands made from Sindanyo, placed in the ends of the 4" pipe section. Carbon or graphite rods could be firmly held on moveable contacts attached to the connecting rods and in this way were heated by electrical resistance heating. The Hackbridge transformer had ten tappings to permit stepwise variation of the secondary voltage from 6 to 12 volts. To obtain lower voltage drops across the cabon specimen, resistances of about 0.02 to 0.1 ohm made from parallel strands of 20 S.W.G. nichrome wire were placed in series with the carbon. Carbon surface temperatures in the region 1,000°C. to 2,000°C. were easy to obtain.

The reaction vessel was provided with two windows, one a big removeable window 4" in diameter placed in the front of the vessel. Through this window the carbon specimen could be observed in a travelling microscope, at the point

above the jet through which the attacking gas passed. The temperature of the carbon was measured by an optical pyrometer which could be sighted through this big window. A Cambridge Pyrometer and a Tinsley Pyrometer were used permitting temperature measurements up to 1,900°C. The reaction rate was calculated from the observed rate of retreat of the carbon surface as measured in the eyepiece of the microscope. A smaller window was placed on the top of the vessel to assist the positioning of a pitot tube used to measure the velocity of the gas coming from the jet. The big window also provided the means of access to the vessel to replace the spent carbon specimens.

Connected to the reaction vessel was a tapping for measuring the static pressure of the gas, an adjustable pitot tube to measure the velocity of the reaction gas, a bleed to the atmosphere to assist the control of a reduced gas pressure and of course a reaction gas inlet and oil backing pumps (See Figure 4).

The reaction gas was directed radially across the carbon rod (See Figure 6). A refractory tipped Bray Gas Burner Jet was used as the orifice through which the reaction gas entered to impinge on the carbon. The advantages of using such an orifice were several: (a) the orifice was always

FIGURE 4 SCHEME OF REACTION APPARATUS

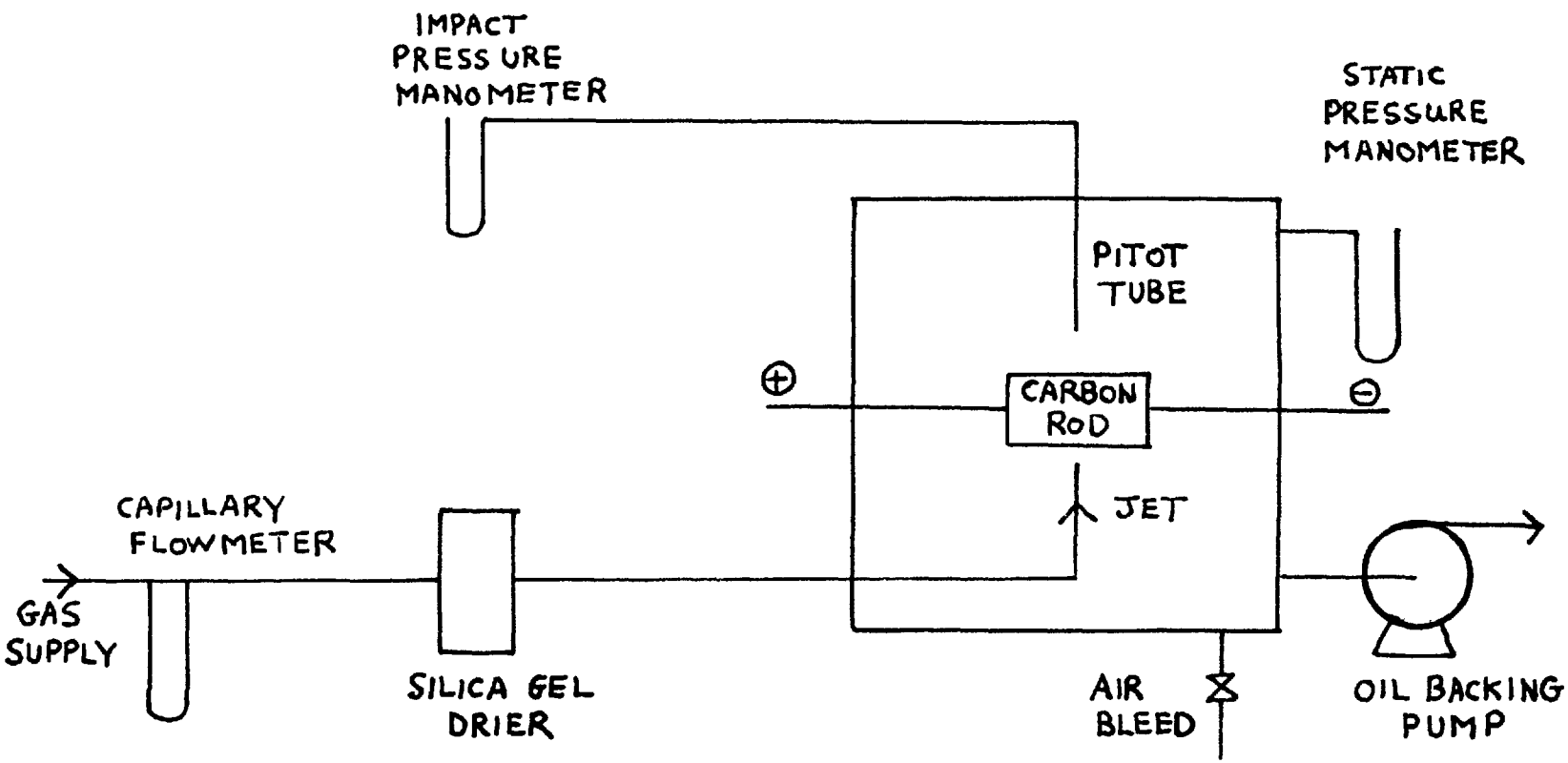


FIGURE 5 SCHEME OF GAS MIXING APPARATUS

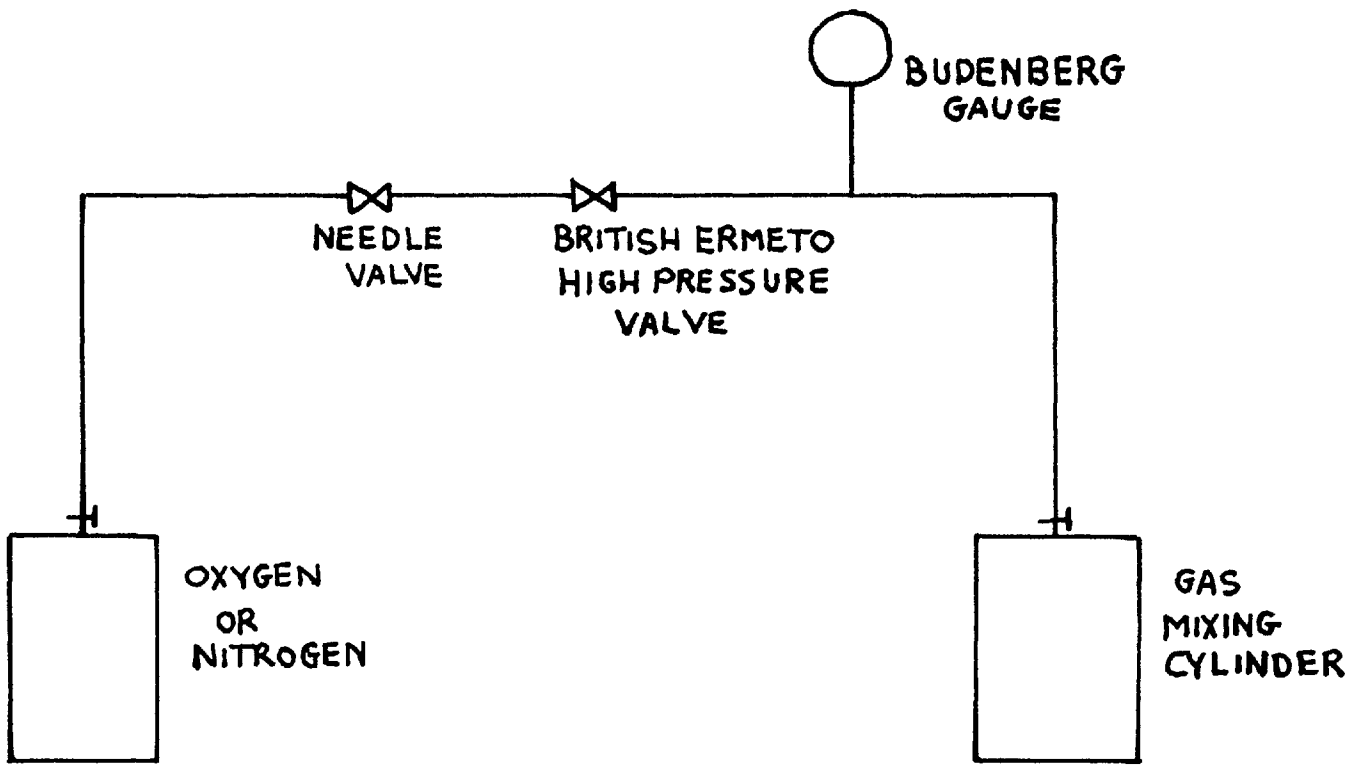
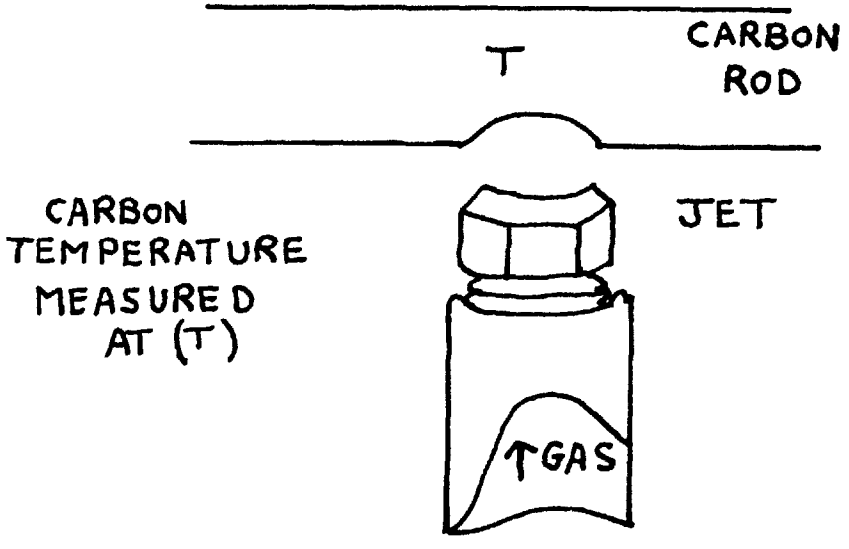


FIGURE 6



about ½ mm. from the hot carbon surface but the refractory was only rarely damaged; (b) if jets had to be replaced replacements were guaranteed similar within narrow tolerances; (c) there was a fairly uniform gas velocity distribution across the jet especially at higher gas flow rates; (d) the jet was small so that at high gas velocities it was not too difficult to provide an adequate gas supply.

Measurements of the gas flows were made in calibrated capillary flowmeters. The linear gas velocities at the jet were measured by a pitot tube placed in the centre of the gas stream and the gas velocities were correlated with the mass throughput of the gases as measured in the capillary flowmeter. The gas velocities could be varied by a factor of about 100 from 100 cms/sec to 10,000 cms/sec. A silica gel drier in which the gases had a residence time of at least 3 minutes was used to dry the gases on the downstream side of the capillary meter.

When gas mixtures of special proportions were required they were prepared by mixing the gases in a storage vessel at pressures up to 100 atmospheres (See Figure 5). This method was chosen because of the difficulty of metering two gases simultaneously and arranging to keep the flow of the mixed gases constant at the desired value. The gas

pressures in the storage vessel were measured by a Budenberg Standard Test Gauge and the pressures at which each component was introduced gave the composition of the mixture.

Graphite rods were cut from blocks of graphite using a thin-walled brass tube of 1/4" I.D. as a corer. Teeth were cut in the tube, which was used with an electric hand drill. Rods about 4 cms. long and 6 mms. in diameter could be made in one minute by this method. There was always a fairly large burn-off at the point of attack on the graphite so that the effect of impurities which may have been introduced on to the surface of the graphite during rod manufacture would not influence the overall combustion rate greatly.

B. Mensuration.

B.1. The Linear Rate of Removal of Carbon.

The amount of carbon removed by the reaction was found by measuring the rate at which the surface of a carbon rod retreated when the reactive gas e.g. air was allowed to impinge on the point under observation. All measurements of the linear removal of the carbon were made in the graticule of a travelling microscope, and a stopwatch was used to find the time of retreat. The combustion time was taken during

the period when the rod appeared to be burning at a steady rate. It was not possible to test the reproducibility of the reaction rate on the same rod because the carbon temperature could not be held at exactly the same value for a series of runs.

The linear retreat of the carbon could be measured to $\pm$ 0.002 cms. and the time of combustion to $\pm$ 0.2 seconds.

The influence of these probable errors on the overall measured reaction rate will be discussed later in the 'Error Analysis'.

B.2. Measurements of the Densities of the Carbons and Graphites.

Two methods were used to measure the densities of the carbons and graphites used in these experiments:

(a) samples were weighed in air and water successively and the density calculated from the upthrust;

(b) the linear dimensions of a cylindrical sample were measured by a micrometer and the sample was weighed.

In some cases density measurements made by others were available.

These methods usually agreed to two places of decimals in the values they gave to the bulk density of the solid. In polycrystalline graphite, however, there can be

variations in density from point to point in a sample and though these variations were never explored it is assumed that in the usual burn-off recorded in the experiments that the density could vary by ± 0.1 gm./cc. from run to run.

B.3. The Velocity of the Reactant Gas.

The velocity of the attacking gas was measured by a pitot tube placed about 1/2 mm. from the nozzle in the centre of the gas stream when the ambient gas pressure in the vessel was 1 atmosphere. The velocities which were measured by the pitot tube were compared with the simultaneous mass flow rates of the gas measured by the calibrated capillary flowmeter. Mass flow rates which were measured when the pressure in the reaction vessel was about 1/10th atmosphere, say, were recorded as the linear gas velocities measured at 1 atmosphere corresponding to the particular gas mass flow rates. Thus the velocities later measured from the capillary flowmeter readings are really nominal gas velocities and since the Reynolds Number depends only on the mass flow rate, and is independent of the pressure these nominal gas velocities provide a measure of the Reynolds Number whatever the pressure in the reaction vessel.

$$Re = \frac{u\ d\ l}{\mu}$$

where u = the linear gas velocity,

d = gas density,

l = some linear dimension of the system. In the case of gas flowing radially over a cylinder it would be the diameter of the cylinder,

μ = the viscosity of the gas.

Now $ud = \frac{\text{mass flow rate}}{\text{unit area}}$ = a constant independent of gas pressure.

μ is dependent on pressure only at very low or very high pressures.

Thus the nominal gas velocity is proportional to the Reynolds Number.

The main variability in the velocity measurements arises in the reading errors of the capillary flowmeter. The probable error is about $\pm$ 1 mm. of water. Different flowmeters were used to measure mass flow rates of very different magnitudes, so that measurements could be made in fairly responsive regions of the flowmeter calibrations. At a velocity of about 900 cms./sec. the probable error in velocity would be about $\pm$ 10 cms./sec.

B.4. Temperature of the Carbon.

Measurements of the temperature had to be made at a point about 2 mm. away from and at an angle of 90° from the point of impact of the attacking gas. This situation

would give rise to some error in temperature and it was not possible to estimate the magnitude of the error. The point at which the temperature was measured was still, however, swept by the attacking gas. Temperature readings were taken about halfway through the period over which the combustion rate was measured. There were obviously two main sources of variance in the temperature measurements; there were reading errors in the optical pyrometers used and these were estimated at ± 10°C. and in addition the temperature could change during the time the combustion rate was being measured, and although no measurements of any such variation were made the probable temperature error could be ± 20°C.

Optical pyrometers measure apparent black body temperatures and therefore with unenclosed imperfect black bodies the measured temperatures are lower than the actual temperatures. The magnitude of this bias increases as the temperature of the body increases. This effect is treated in greater detail in the appendix on 'Optical Pyrometry'.

B.5. Total Ambient Gas Pressure. Partial Oxygen Pressure.

Errors in the ambient gas pressure, the partial pressure in the case of air and pure oxygen, and in the measured impact pressure of the gas on the leading edge of a cylinder could be estimated as ± 1 mm. of mercury. When

mixtures of gases were prepared, the oxygen concentration could vary by ± 2% of its mean value. These gas mixtures were usually made by adding 50 ats. of oxygen to 50 ats. of nitrogen, and the reading errors in each measurement would be ± 1 atm.

The effect of errors in the impact pressure and the impact partial pressure of the oxygen on the error in the reaction rate is discussed in the 'Error Analysis'. No special consideration has been given to the errors in experiments where gas mixtures of 50% oxygen were used but in the case of the mass transfer controlled attack on Morganite Link MS carbons the total measured variance in the reaction order was ± 10%.

B.6. Gas Impact Pressures.

Since the gases impinge at high velocity on the carbon surface, the pressures at the surface will be in excess of the static pressures in the reaction vessel. Impact pressures calculated by the conventional method and based on the velocity of the gas issuing from the jet were found to give results that were too high, probably owing to divergence of the streamlines round the carbon rod. To measure the true pressure at the carbon surface, a steel rod the same size as the carbon had a pressure tapping

inserted diametrically into it at the point where the gas impinged. The corrections to the ambient pressures used in the calculations are shown later. An example of the difference the impact can make to the gas pressure at the point of attack is given below.

When the nominal gas velocity is 7000 cms./sec., the expected gas velocity in the reaction vessel when the ambient pressure is 0.13 ats. is (7000/0.13) cms./sec.

The impact pressure calculated from the formula

$$u_1^2 = 2p_1 v_1 \log_e p_2/p_1$$

where u_1 = gas velocity at pressure p_1,
p_2 = impact pressure,
v_1 = the specific volume of the gas at p_1

is 0.65 atmospheres.

The measured impact pressure under these conditions was only 0.23 atmospheres.

C. Experimental Procedure.

The procedure described below was followed in most cases.

C.1. Measurement of Reaction Rates.

1. The apparatus was set to give the required mass flow rate in the jet and the required pressure in the reaction vessel.

2. The optical pyrometer filament temperature was set at the expected value of the carbon temperature.

3. The current was switched on to heat the carbon rod. When the rod appeared to begin to burn steadily the position of its surface at a point opposite the centre of the orifice was fixed on the graticule of the travelling microscope eyepiece and the stopwatch was started.

4. While the carbon was burning the carbon temperature was measured.

5. The carbon surface position was again noted and the time of burning recorded.

6. A fresh carbon rod was put in place for the next run.

C.2. Preparing Gas Mixtures and Using Them.

1. The mixing vessel was evacuated by an oil backing pump.

2. Gas for mixing was streamed through the connecting tubing to displace air.

3. The first gas was passed into the vessel quickly at the beginning but then slowly as the desired pressure was approached. The valve on the vessel was then closed and the gas pressure noted.

4. The second gas was streamed through the valve of the mixing cylinder very quickly to assist mixing but as the chosen pressure was reached the rate of entry was reduced. The valve was closed and the total gas pressure was noted.

5. The gas mixture was left for about 1/2 an hour to ensure complete mixing.

6. Much of the gas mixture was streamed through the drier, flowmeter, and connecting tubing to displace air.

D. Description of Materials.

Carbons.

The carbon rods were manufactured by the Ship Carbon Company, Grove Road, Chadwell Heath, Essex. These carbon rods were prepared from a lamp black base and a coal tar binder. Nothing seems to be known about the impurity content except that the ash content is always less than 0.1%. The density of the carbon is 1.34 gms./cc. and it is therefore very porous.

Polycrystalline Graphite.

The following properties of this graphite were kindly supplied by the British Coal Utilisation Research Association.

Lump density 1.76 gms./cc.

Helium density 2.154 gms./cc.

X-ray density 2.66 gms./cc.

Total porosity 23%, of which 1/6 is inaccessible to helium or other fluids.

Accessible surface area 0.2 m^2/gm.

Inaccessible surface area 4 m^2/gm.

85-88% of the accessible pore volume is reached through pores of diameter greater than 2 μ while almost all the remainder is located beyond openings of 0.1 μ diameter.

A typical analysis of this kind of graphite.

Ash 0.01 to 0.03%

Fe	10 p.p.m.	All other metallic impurities less
Ca	15 p.p.m.	then 1 p.p.m.
Sr	15 p.p.m.	
Na	2 p.p.m.	
V	10 p.p.m.	

Pyrographite.

This material was manufactured by High Temperature Materials Inc., 31 Antwerp Street, Boston 35, Mass., U.S.A., by cracking hydrocarbon vapour on graphite formers at temperatures about 2,100°C. Pyrographite is a polycrystalline graphite in which there is a high degree of orientation.

Most of the crystallites are oriented parallel to the base of the graphite sheets. The graphite is very pure having less than one part in ten million of impurity and in addition is much less porous than extruded graphite having a density 2.2 gms./cc. The experimental samples were cut 4 mm. wide from sheets 2 mm. thick and were used with the 4 mm. face opposite the jet.

ANALYSIS OF THE EXPERIMENTAL RESULTS.

Introduction.

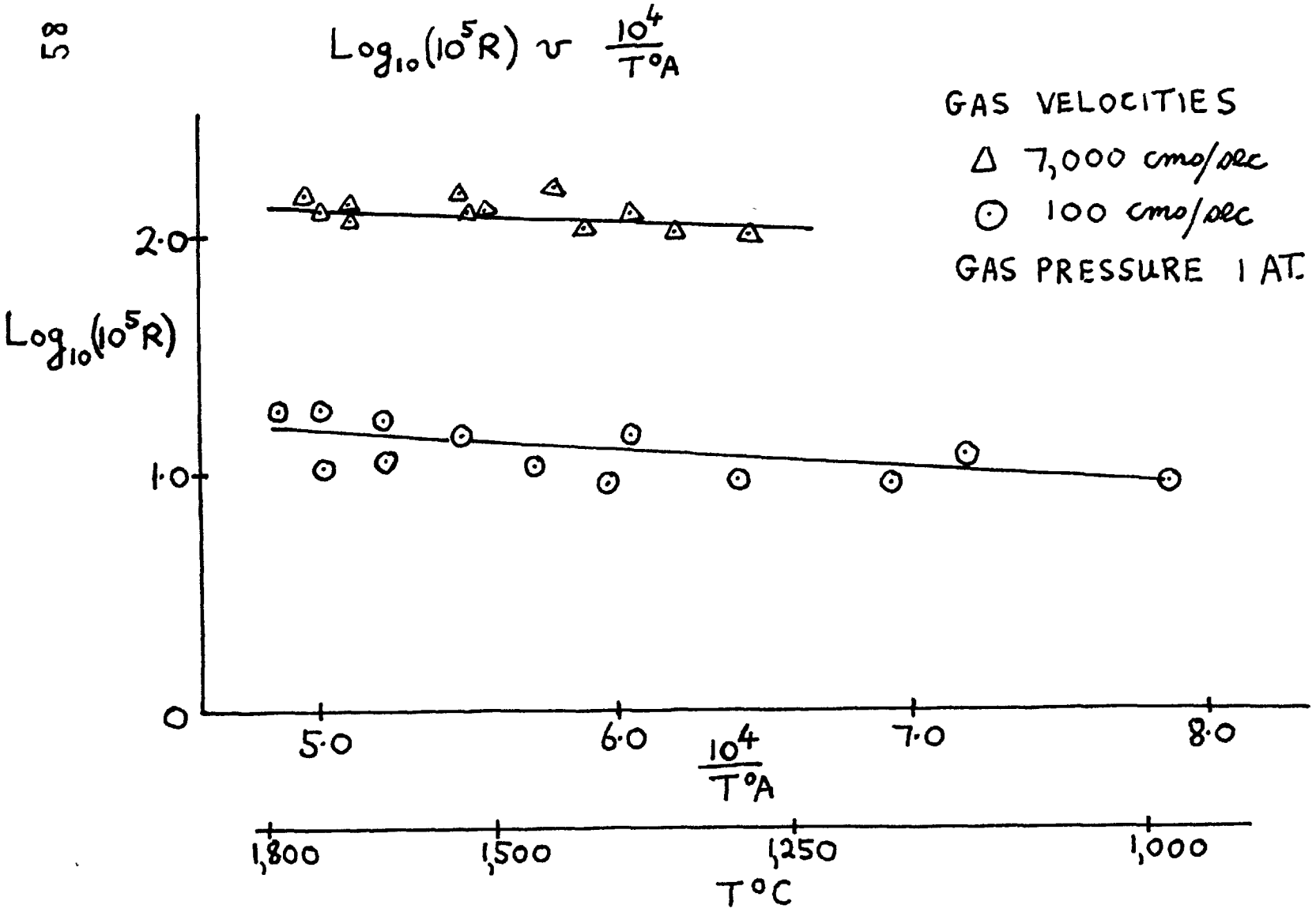
This section will show how the experimental results have been interpreted, but the interpretation and the assumptions upon which it is based will be treated more fully in the 'Discussion' section. Some graphs of the experimental results will be presented in this section and the rest will be included in Appendix 2.

A. The Dependence of the Apparent Mass Transfer Coefficient on Gas Velocity and Carbon Surface Temperature.

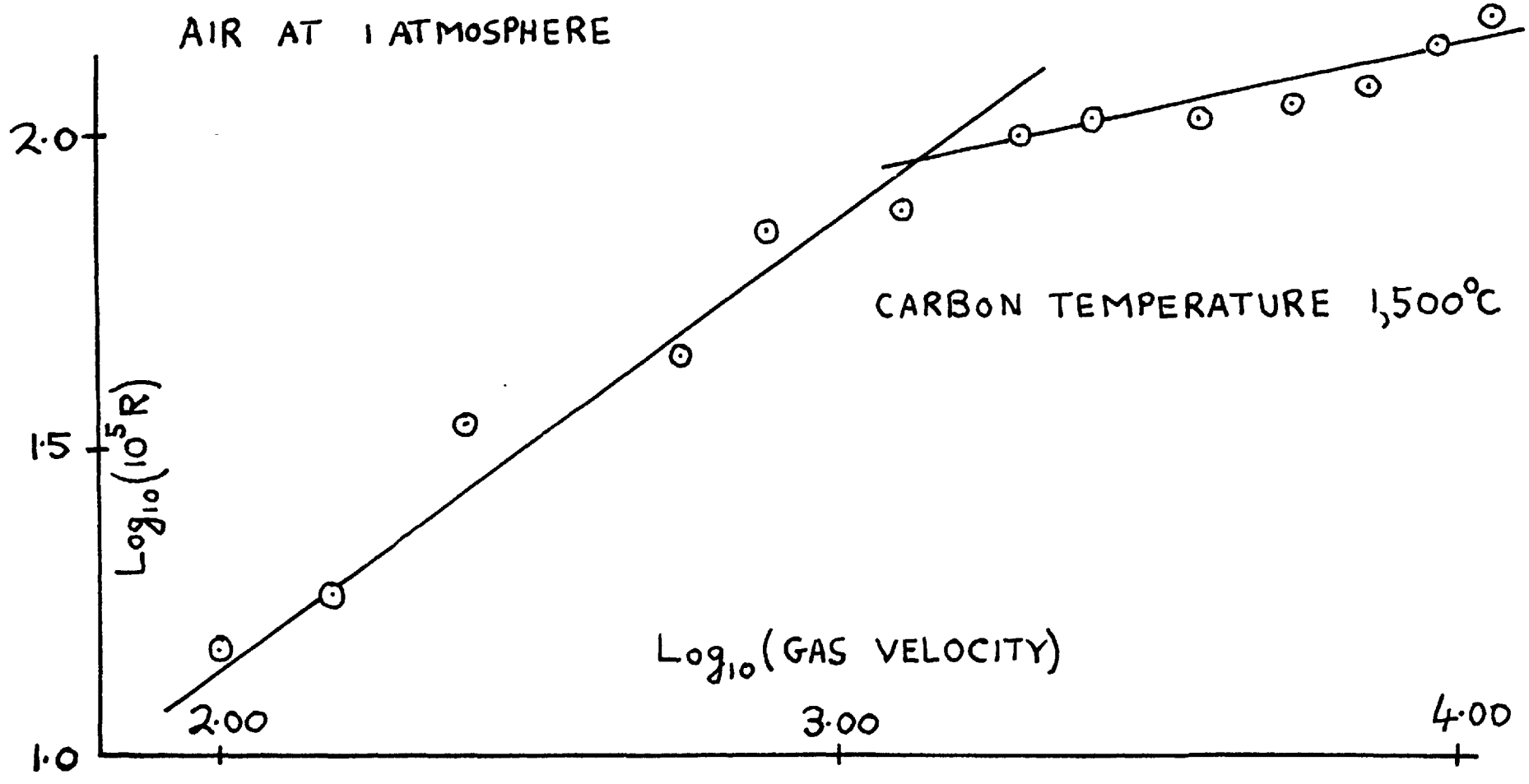
Results taken from Appendix 1, Table 1.

Graphs 1 and 2 give an indication of the dependence of the apparent mass transfer coefficient on the gas velocity and carbon surface temperature. Preliminary experiments have shown that there are two distinct velocity dependences of the apparent mass transfer coefficient. The transition seems to occur about a gas velocity of 1,500 cms/sec. A simultaneous regression of $\log_{10}$ (10^5 x apparent mass transfer coefficient) on $\log_{10}$ (gas velocity) and ($1/T°A \times 10^4$) is calculated for each velocity range. It has been assumed here that the reaction rate depends on the first power of the main stream oxygen concentration and it will be shown later that this assumption is approximately true.

GRAPH 1 ATTACK OF AIR ON POROUS CARBON



GRAPH 2 POROUS CARBON: $Log_{10}(10^5R)$ v Log_{10}(GAS VELOCITY)



If the mass transfer coefficient = h

Suppose $h = \text{constant} \times 10^{-b_2/T} \times (\text{gas velocity})^{b_1}$

Then $\log_{10}(h) = (\text{constant})^1 + b_1 \log_{10}(\text{gas velocity}) - b_2/T$

Put $\log_{10}(10^5 h) = y$ $\qquad Y = y - \bar{y}$

$\log_{10}(\text{gas vel.}) = x_1$ $\qquad X_1 = x_2 - \bar{x}_1$

$1/T°A \times 10^4 = x_2$ $\qquad X_2 = x_2 - \bar{x}_2$

A.1. Results at velocities below 1,500 cms./sec.

Total number of results = 113.

$\sum y = 260.4$	$\sum x_1 = 303$	$\sum x_2 = 681$
$\bar{y} = 2.34$	$\bar{x}_1 = 2.68$	$\bar{x}_2 = 6.00$
$\sum Y^2 = 6.94$	$\sum X_1^2 = 14.15$	$\sum X_2^2 = 89.1$
$\sum YX_1 = 8.79$	$\sum YX_2 = -5.10$	$\sum X_1X_2 = 0.02(\sum X_1X_2)^2 = 4 \times 10^{-4}$

The partial regression coefficients b_1 and b_2 of y on x_1 and x_2 are given by the equations

$$b_1 = \frac{\sum X_2^2 \sum YX_1 - \sum X_1X_2 \sum YX_2}{\sum X_1^2 \sum X_2^2 - (\sum X_1X_2)^2} = 0.62$$

$$b_2 = \frac{\sum X_1^2 \sum YX_2 - \sum X_1X_2 \sum YX_1}{\sum X_1^2 \sum X_2^2 - (\sum X_1X_2)^2} = -0.057$$

Sum of squares of $(y-\bar{y})$ explained by $X_1 = \frac{(\sum YX_1)^2}{\sum X_1^2} = 5.45$

Sum of squares of $(y-\bar{y})$ explained by $X_2 = \frac{(\sum YX_2)^2}{\sum X_2^2} = 0.29$

Sum of squares of $(y-\bar{y})$ due to X_1 and X_2 together

$$= b_1 \sum YX_1 + b_2 \sum YX_2 = 5.74$$

Source of Variance	Sum of Squares	Degrees of Freedom	Mean Squares
Variation due to X_1	5.45	1	5.45
Addition due to X_2	0.29	1	0.29
Total from X_1 and X_2	5.74		
Residual	1.20	110	0.01
Total i.e. $\sum Y^2$	6.94	112	

Significance test on X_2 variance $= \frac{0.29}{0.01} = 29$ at 1 and 110 degrees of freedom. The chance that this ratio was the result of randomness only is less than 1 in 1,000. The regression is therefore a real dependence.

Alternative solution for b_1 and b_2 and to find the variance of b_1 and b_2.

$$b_1 \sum X_1^2 + b_2 \sum X_1X_2 = 1$$

$$b_1 \sum X_1X_2 + b_2 \sum X_2^2 = 0$$

Put c_{a_1} for b_1 and c_{a_2} for b_2 here

$$c_{a_1} = 7.04 \times 10^{-4}, \quad c_{a_2} = -1.58 \times 10^{-5}$$

$$b_1 \sum X_1^2 + b_2 \sum X_1X_2 = 0$$

$$b_1 \sum X_1X_2 + b_2 \sum X_2^2 = 1$$

Put c_{b_1} for b_1 and c_{b_2} for b_2 here.

$$c_{b_1} = -1.59 \times 10^{-5}, \quad c_{b_2} = 1.13 \times 10^{-5}$$

$$b_1 = c_{a_1} \sum YX_1 + c_{a_2} \sum YX_2 = 0.62$$

$$b_2 = c_{b_1} \sum YX_1 + c_{b_2} \sum YX_2 = -0.058$$

From the analysis of variance $S^2_{residual} = 0.01$

$$S_r = 0.1$$

Standard error of $b_1 = S_r \sqrt{c_{a_1}} = 0.03$

Standard error of $b_2 = S_r \sqrt{c_{b_2}} = 0.012$

$$b_1 = 0.62 \pm 0.03$$

$$b_2 = -0.058 \pm 0.012$$

Regression line $(y-\bar{y}) = b_1 (x_1 - \bar{x}_1) + b_2 (x_2 - \bar{x}_2)$

$$y = 1.09 + 0.6\, x_1 - 0.06\, x_2$$

Analysis of Covariance.

Correlation coefficient of b_1 on $b_2 = \dfrac{c_{a_2}}{\sqrt{c_{a_1}\, c_{b_2}}}$

$$= -0.001$$

This correlation coefficient is clearly not significant so that errors in theestimation of b_1 do not affect estimates of b_2.

A.2. Results at velocities above 1,500 cms./sec.

Number of results = 98.

$\sum y$	= 267.8	$\sum x_1$	= 358.6	$\sum x_2$	= 557.1
$\bar{y}$	= 2.74	$\bar{x}_1$	= 3.66	$\bar{x}_2$	= 5.70
$\sum Y^2$	= 0.95	$\sum X_1^2$	= 5.93	$\sum X_2^2$	= 41.2

$\sum YX_1 = 1.54 \quad \sum YX_2 = -5.02 \quad \sum X_1X_2 = -5.85 \quad (\sum X_1X_2)^2 = 34.2$

Calculated as before $b_1 = 0.16$

$b_2 = -0.098$

Source of Variance	Sum of Squares	Degrees of Freedom	Mean Squares
Variance due to X_2	0.61	1	0.61
Due to addition of X_1	0.13	1	0.13
Variance due to X_1 & X_2	0.74		
Residual	0.21	95	2.2×10^{-3}
Total $\sum Y^2$	0.95	97	

The ratio $\frac{0.13}{0.002} = 65$ at 95 and 1 degrees of freedom.

The significance of this ratio shows again that the regression is real.

c_{a_1} etc. are calculated as before.

$c_{a_1} = 0.196, \quad c_{a_2} = 0.028$

$c_{b_1} = 2.8 \times 10^{-2}, \quad c_{b_2} = 2.82 \times 10^{-2}$

Standard error of $b_1 = S_r\sqrt{c_{a_1}} = 0.021$

Standard error of $b_2 = S_r\sqrt{c_{b_2}} = 0.008$

$b_1 = 0.16 \pm 0.02$

$b_2 = -0.10 \pm 0.01$

Regression line $y = 2.72 + 0.16\, x_1 - 0.10\, x_2$

Analysis of Covariance.

$$\text{Correlation coefficient of } b_1 \text{ on } b_2 = \frac{c_{a_2}}{\sqrt{c_{a_1} c_{b_2}}}$$

= 0.38 at 95 degrees of freedom.

This correlation is significant. Errors which cause b_1 to be high will cause b_2 to be high also. There is, however, not a perfect association between these estimates.

Summary.

At gas velocities below 1,500 cms./sec.

$$h \times 10^5 = 12.3 \, (e^{-2700/1.98T}) \, (\text{velocity})^{0.6}$$

At gas velocities above 1,500 cms./sec.

$$h \times 10^5 = 525 \, (e^{-4500/1.98T}) \, (\text{velocity})^{0.16}$$

B. Dependence of the reaction rate of porous carbon with oxygen on the oxygen partial pressure at total gas pressure of 1 atmosphere.

Results taken from Appendix 1, Table 2.

Graph 3 shows the reaction rate depends on the oxygen partial pressure.

If the reaction rate $R = k p^n$

where p = partial pressure of reacting gas
n = order of reaction

As before k will be a function of carbon temperature and gas velocity,

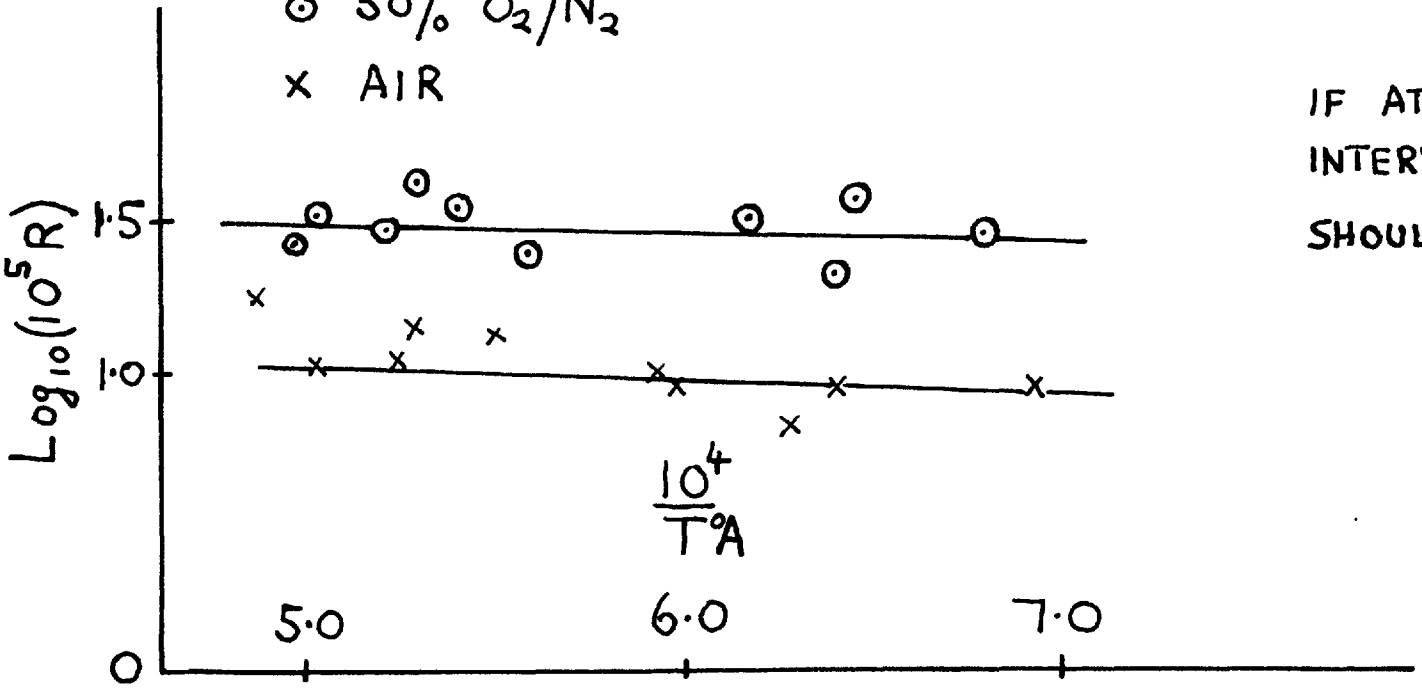
GRAPH 3 $Log_{10}(10^5 R)$ v $\frac{10^4}{T°A}$

THE EFFECT OF PARTIAL OXYGEN PRESSURE ON THE ATTACK OF OXYGEN ON POROUS CARBON

GAS VELOCITY 100 cms/sec

⊙ 50% O_2/N_2

× AIR



IF ATTACK IS FIRST ORDER INTERVAL BETWEEN GRAPHS SHOULD EQUAL 0·4

Put $y = \log_{10}(10^5 R)$ $\quad Y = y - \bar{y}$

$x_1 = \log_{10}$ (gas velocity) $\quad X_1 = x_1 - \bar{x}_1$

$x_2 = 1/T°A \times 10^4$ $\quad X_2 = x_2 - \bar{x}_2$

$x_3 = \log_{10}$(10x oxygen partial pressure in ats.) $\quad X_3 = x_3 - \bar{x}_3$

The gas velocities are less than 1,500 cms/sec.

Total number of results = 128

$\sum y = 221.9 \quad \sum x_1 = 327.9 \quad \sum x_2 = 748.4 \quad \sum x_3 = 64.0$

$\bar{y} = 1.73 \quad \bar{x}_1 = 2.56 \quad \bar{x}_2 = 5.84 \quad \bar{x}_3 = 0.5$

$\sum Y^2 = 14.7 \quad \sum X_1^2 = 20.0 \quad \sum X_2^2 = 84.5 \quad \sum X_3^2 = 5.14$

$\sum X_1X_2 = -31 \quad \sum X_1X_3 = -0.07 \quad \sum X_2X_3 = -6.90$

$\sum YX_1 = +12.5 \quad \sum YX_2 = -12.7 \quad \sum YX_3 = +4.85$

Notation. $X_1^2 = c_{11} \quad X_1X_3 = c_{13} \quad YX_2 = c_{y2}$

To find b_1, b_2 and b_3 and the variances of these regression coefficients.

Set One.

$$c_{11}p_1 + c_{12}q_1 + c_{13}r_1 = 1$$
$$c_{12}p_1 + c_{22}q_1 + c_{23}r_1 = 0$$
$$c_{13}p_1 + c_{23}q_1 + c_{33}r_1 = 0$$

Set Two.

$$c_{11}p_2 + c_{12}q_2 + c_{13}r_2 = 0$$
$$c_{12}p_2 + c_{22}q_2 + c_{23}r_2 = 1$$
$$c_{13}p_2 + c_{23}q_2 + c_{33}r_2 = 0$$

Set Three.

$$c_{11}p_3 + c_{12}q_3 + c_{13}r_3 = 0$$
$$c_{12}p_3 + c_{22}q_3 + c_{23}r_3 = 0$$
$$c_{13}p_3 + c_{23}q_3 + c_{33}r_3 = 1$$

The solutions of Set One corresponding to p_1, q_1, etc. are

$$p_1 = c^{11} \qquad q_1 = c^{12} \qquad r_1 = c^{13}$$

and by symmetry $c^{12} = c^{21}$, $c^{13} = c^{31}$, $c^{23} = c^{32}$

The inverse matrix is

$$\begin{vmatrix} c^{11} & c^{12} & c^{13} \\ c^{21} & c^{22} & c^{23} \\ c^{31} & c^{32} & c^{33} \end{vmatrix} = 10^{-3} \times \begin{vmatrix} 50 & 2.1 & 3.56 \\ 2.1 & 13.4 & 18.0 \\ 3.56 & 18.0 & 220 \end{vmatrix}$$

$$b_1 = c^{11} c_{y_1} + c^{12} c_{y_2} + c^{13} C_{y_3} = 0.62$$

$$b_2 = c^{21} c_{y_1} + c^{22} c_{y_2} + c^{23} c_{y_3} = -0.06$$

$$b_3 = c^{31} c_{y_1} + c^{32} c_{y_2} + c^{33} c_{y_3} = 0.9$$

The residual variance S^2 is given by

$$S^2 = \frac{1}{n - p - 1} \left(c_{yy} - b_1 c_{y_1} - b_2 c_{y_2} \ldots - b_p c_{yp} \right)$$

$$S^2 = 1.6 \times 10^{-2} \qquad S = 0.13$$

Standard Error of b_1 = $S\sqrt{c^{11}}$ = 0.03

Standard Error of b_2 = $S\sqrt{c^{22}}$ = 0.015

Standard Error of b_3 = $S\sqrt{c^{33}}$ = 0.06

$b_1 = 0.62 \pm 0.03$ Mean $b_1 = 0.6$

$b_2 = -0.06 \pm 0.015$ Mean $b_2 = -0.06$

$b_3 = 0.9 \pm 0.06$ Mean $b_3 = 1.0$

Note. The value of b_3 is close enough to 1, which is the value suggested by mass transfer theory.

Test of Interaction.

The values of b_2 and b_3 were found to be correlated.

$$r_{23} = \frac{c^{23}}{\sqrt{c^{22}\ c^{33}}} = 0.3 \text{ at 124 degrees of freedom.}$$

The correlation coefficient is very significant. Errors in the estimation of the influence of temperature cause errors in the estimation of the influence of concentration.

Regression Line.

$$(y-\bar{y}) = b_1(x_1-\bar{x}_1) + b_2(x_2-\bar{x}_2) + b_3(x_3-\bar{x}_3)$$

$$\underline{y = 0.6x_1 - 0.06x_2 + x_3 + 0.03}$$

At gas velocities below 1,500 cms./sec.

$$10^5 R = 1.07\ (\text{velocity})^{0.6}\ (e^{-2700/1.98T})\ (10p)$$

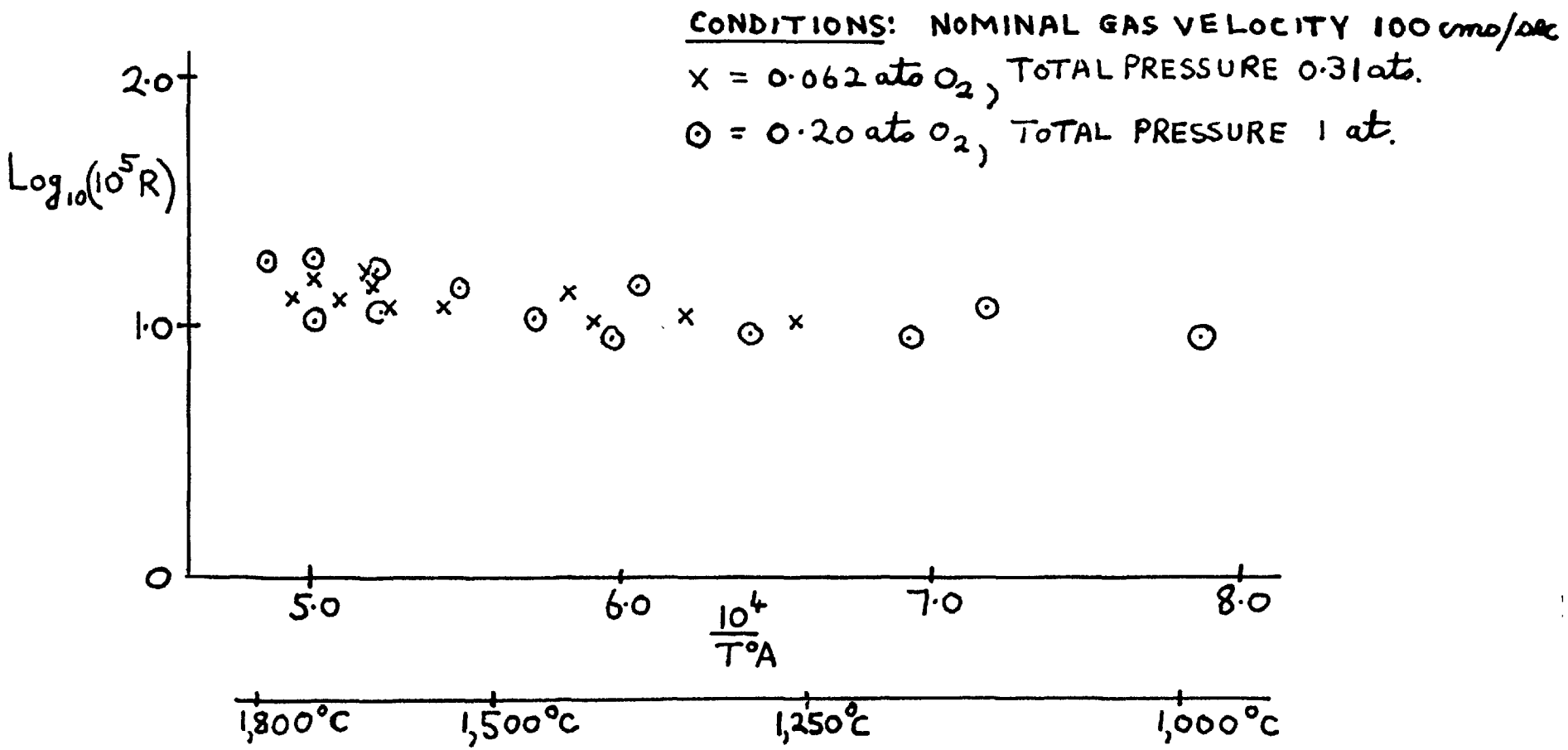
C. Dependence of the reaction rate of porous carbon with oxygen on reduced total gas pressures and partial oxygen pressures.

Results taken from Appendix 1, Table 3.

Graph 4 will show that the reaction rate does not change much when a constant composition oxygen-nitrogen mixture (air) is used at reduced pressures. The rate of mass transfer depends on the diffusivity of the reactant

GRAPH 4 $\quad \mathrm{Log}_{10}(10^5 R) \upsilon \frac{10^4}{T°A}$

THE EFFECT OF TOTAL PRESSURE AND PARTIAL OXYGEN PRESSURE ON THE ATTACK OF OXYGEN ON POROUS CARBON



gas and the diffusivity of a gas is a function of the absolute gas pressure (P). It would seem that the increased diffusivity cancels the effect of reduced oxygen partial pressure in the main gas stream.

$$R = k_o V^m e^{-A/1.98T} p^n P^z$$

The notation is as follows:

$y = \log_{10} (10^5 R)$ $x_1 = \log_{10}$(gas velocity)

$x_2 = 1/T°A \times 10^4$

$x_3 = \log_{10}$ (100 x oxygen partial pressure in ats.)

$x_4 = \log_{10}$ (10 x total gas pressure in ats.).

All gas velocities below 1,500 cms./sec.

The total number of results = 120.

$\sum y = 191.2$ $\sum x_1 = 315.6$ $\sum x_2 = 689.1$ $\sum x_3 = 126.2$ $\sum x_4 = 90.2$

$\bar{y} = 1.59$ $\bar{x}_1 = 2.62$ $\bar{x}_2 = 5.75$ $\bar{x}_3 = 1.05$ $\bar{x}_4 = 0.75$

$\sum Y^2 = 6.43$ $\sum X_1^2 = 15.9$ $\sum X_2^2 = 56.6$ $\sum X_3^2 = 7.40$ $\sum X_4^2 = 7.40$

$\sum X_1X_2 = 0.36$ $\sum X_1X_3 = 4.32$ $\sum X_1X_4 = 4.32$ $\sum X_2X_3 = 5.54$

$\sum X_2X_4 = 5.54$ $\sum X_3X_4 = 7.40$ $\sum YX_1 = 7.58$ $\sum YX_2 = -2.30$

$\sum YX_3 = 2.00$ $\sum YX_4 = 2.00$.

The values of certain terms are equal because in the experiment $X_3 = X_4$, so that in fact three variables will be tested, b_1, b_2 and $(b_3 + b_4)$; the last will be called t.

Using the method outlined in the last analysis

the inverse matrix is

$$\begin{vmatrix} c^{11} & c^{12} & c^{13} \\ c^{21} & c^{22} & c^{23} \\ c^{31} & c^{32} & c^{33} \end{vmatrix} = 10^{-3} \times \begin{vmatrix} 76.5 & 4.32 & -47.5 \\ 4.32 & 19.7 & -16.7 \\ -47.5 & -16.7 & 176 \end{vmatrix}$$

$$b_1 = 0.5$$
$$b_2 = -0.05$$
$$t = 0.03$$

The residual variance $S^2 = 2.2 \times 10^{-3}$ $S = 0.15$

Standard error of $b_1 = 0.15 \sqrt{c^{11}} = 0.04$

Standard error of $b_2 = 0.15 \sqrt{c^{22}} = 0.02$

Standard error of $t = 0.15 \sqrt{c^{33}} = 0.06$

Since $t = 0.03 \pm 0.06 = 0$

$$b_3 = -b_4$$

But in the earlier experiment $b_3 = 1$

$$b_4 = -1$$

i.e. the lower the total gas pressure the higher the reaction rate; a result consistent with the idea of a diffusion controlled reaction.

$$b_1 = 0.5 \pm 0.04$$
$$b_2 = -0.05 \pm 0.02$$
$$b_3 = 1.0 \pm 0.06$$
$$b_4 = -1.0 \pm 0.06$$

Regression Line.

$$(y-\bar{y}) = b_1 (x_1-\bar{x}_1) + b_2 (x_2-\bar{x}_2) + b_3 (x_3-\bar{x}_3) + b_4 (x_4-\bar{x}_4)$$

$$y = 0.27 + 0.5x_1 - 0.05x_2 + x_3 - x_4$$

At gas velocities below 1,500 cms./sec.

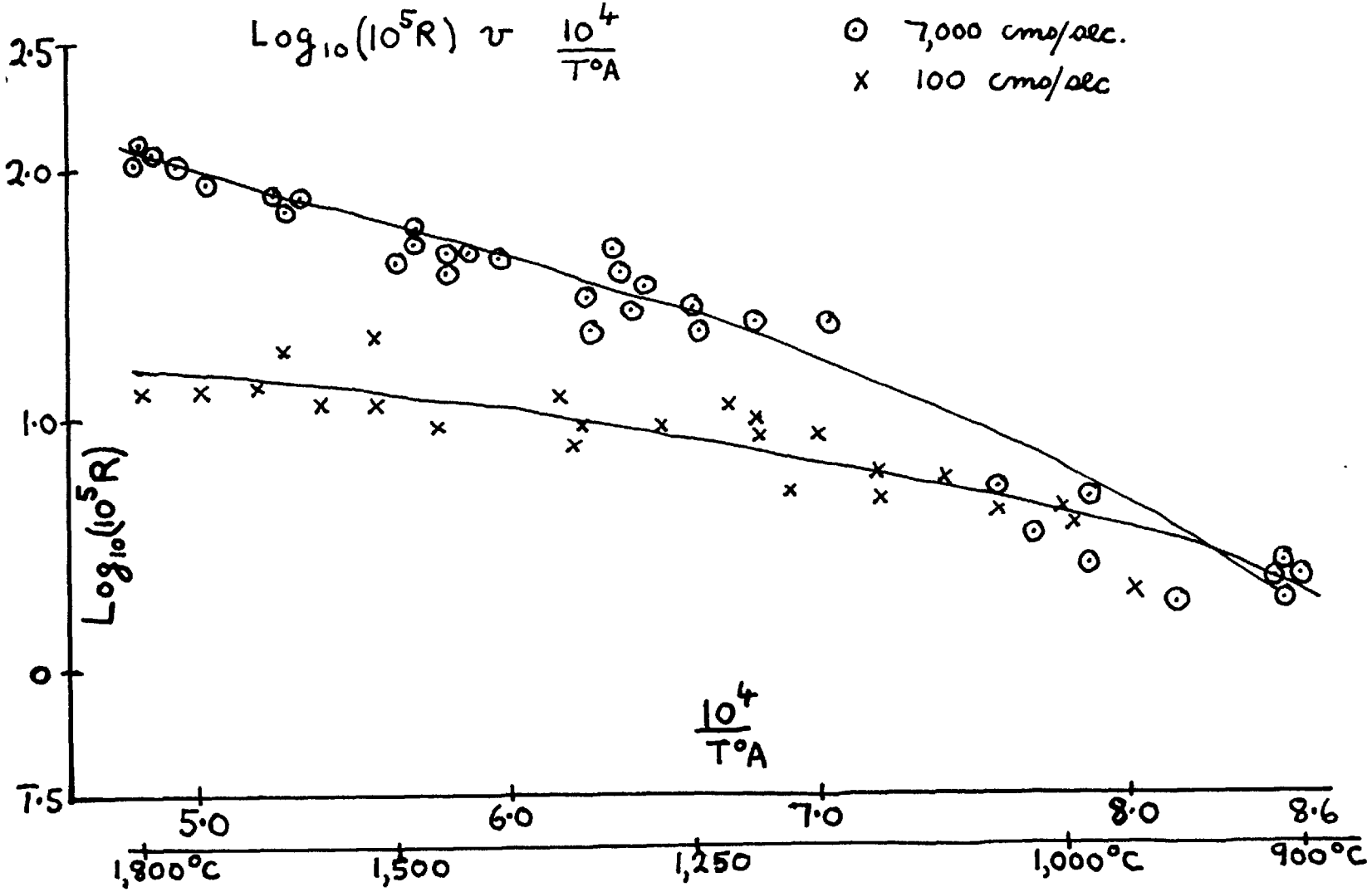
$$10^5 R = \frac{1.86(\text{velocity})^{0.5} \ (e^{-2000/1.98T}) \ (100p)}{(10P)}$$

D. Dependence of the reaction rate of polycrystalline graphite with oxygen on the graphite temperature and gas velocities.

Results taken from Appendix 1, Table 4.

The rates of reaction of graphite with air and oxygen-nitrogen mixtures are partly controlled by mass transfer especially at high temperatures and low gas velocities as Graph 5 indicates. A consequence of the changing regime is that the apparent activation energy of the reaction should decrease as the temperature is increased for any fixed gas velocity. The influence of change of velocity on the reaction rate should be greatest at high temperatures. To show this effect, curves for each velocity will be fitted to the experimental results and differentiated to give the change of activation energy with temperature. These curves should tend to become coincident at low temperature.

GRAPH 5 ATTACK OF AIR ON POLYCRYSTALLINE GRAPHITE



D.1. Air at 100 cms./sec.

$y = \log_{10}(10^5 R)$ $\quad x_1 = 1/T°A \times 10^4$ $\quad x_2 = (x_1^2) = (1/T°A \times 10^4)^2$

$Y = y - \bar{y}$ $\quad x_1 = x_1 - \bar{x}_1$ $\quad x_2 = x_2 - \bar{x}_2$

Total number of results = 30

$\sum y = 27.6$ $\quad \sum x_1 = 197.7$ $\quad \sum x_2 = 1329$

$\bar{y} = 0.92$ $\quad \bar{x}_1 = 6.6$ $\quad \bar{x}_2 = 44$

$\sum Y^2 = 1.84$ $\quad \sum X_1^2 = 26.6$ $\quad \sum X_2^2 = 4522$

$\sum YX_1 = -5.14$ $\quad \sum YX_2 = -68.7$ $\quad \sum X_1 X_2 = 338.5$

In a manner similar to that used for the multiple linear regressions b_1 and b_2 are found.

$$b_1 = 0 \qquad b_2 = -1.67 \times 10^{-2}$$

Regression $\quad y = 1.65 - 1.67 \times 10^{-2} x_1^2$

Analysis of Variance

Variance due to regression = $b_1 c_1 y + b_2 c_2 y = 1.14$

Variance due to linear term = $(c_1 y)^2 / c_{11} = 0.99$

(This linear term is ox_1)

Source of Variance	Degrees of Freedom	Sum of Squares	Mean Squares
Linear term	1	0.15	0.15
Parabolic term	1	0.99	0.99
Regression	2	1.14	
Residual	27	0.70	2.6×10^{-2}
Total $\sum Y^2$	29	1.84	

F ratio for the parabolic term = $\frac{15}{2.6}$ = 5.8 at 1 and 27 degrees of freedom. This term is significant at the 1% level.

Activation Energies change with Temperature.

$$\frac{d(\log_{10} 10^5 R)}{dx_1} = -3.34 \times 10^{-2} x_1$$

When $x_1 = 5.0$ Slope = -0.17 Activation energy = 7.5 $\frac{\text{kcal}}{\text{mole}}$

$x_1 = 8.5$ Slope = -0.28 Activation energy = 13 kcal/mole

Similar analyses were carried out for air velocities of 250 cms/sec., 1090 cms/sec. and 7,000 cms/sec.

Summary. Attack of Air at atmospheric pressure on graphite.

Gas Velocity cms/sec	Regression Equations	Activation Energies kcal/mole	
		$x_1 = 5.0$	$x_1 = 8.5$
100	$y=1.65 - 1.67\times10^{-2} x_1^2$	7.5	13
250	$y=0.55 + 0.6x_1 - 7.5\times10^{-2}x_1^2$	6.3	30
1090	$x = 7.40 + 1.14y - 1.28y^2$	12	25
7000	$y = 2.93 - 0.036 x_1^2$	16	26

E. Results taken from Appendix 1, Table 5.

Summary. Attack of 50% oxygen-nitrogen at atmospheric pressure on graphite.

Gas Velocity cms/sec.	Regression Equations	Activation Energies kcal/mole	
		$x_1 = 5.0$	$x_1 = 8.0$
100	$x= 7.75 +2.08y - 2.16y^2$	7	30
250	$x= 8.59 +0.67y - 1.2y^2$	11	27
1090	$x= 7.65 +2y -1.45y^2$	10	32
7000	$x= 8.93 -0.71y^2$	14	28

F. Dependence of the reaction rates of polycrystalline graphite with oxygen on the graphite temperature, oxygen partial pressure, total gas pressure and gas velocity at reduced pressures.

Results taken from Appendix 1, Tables 6 and 7.

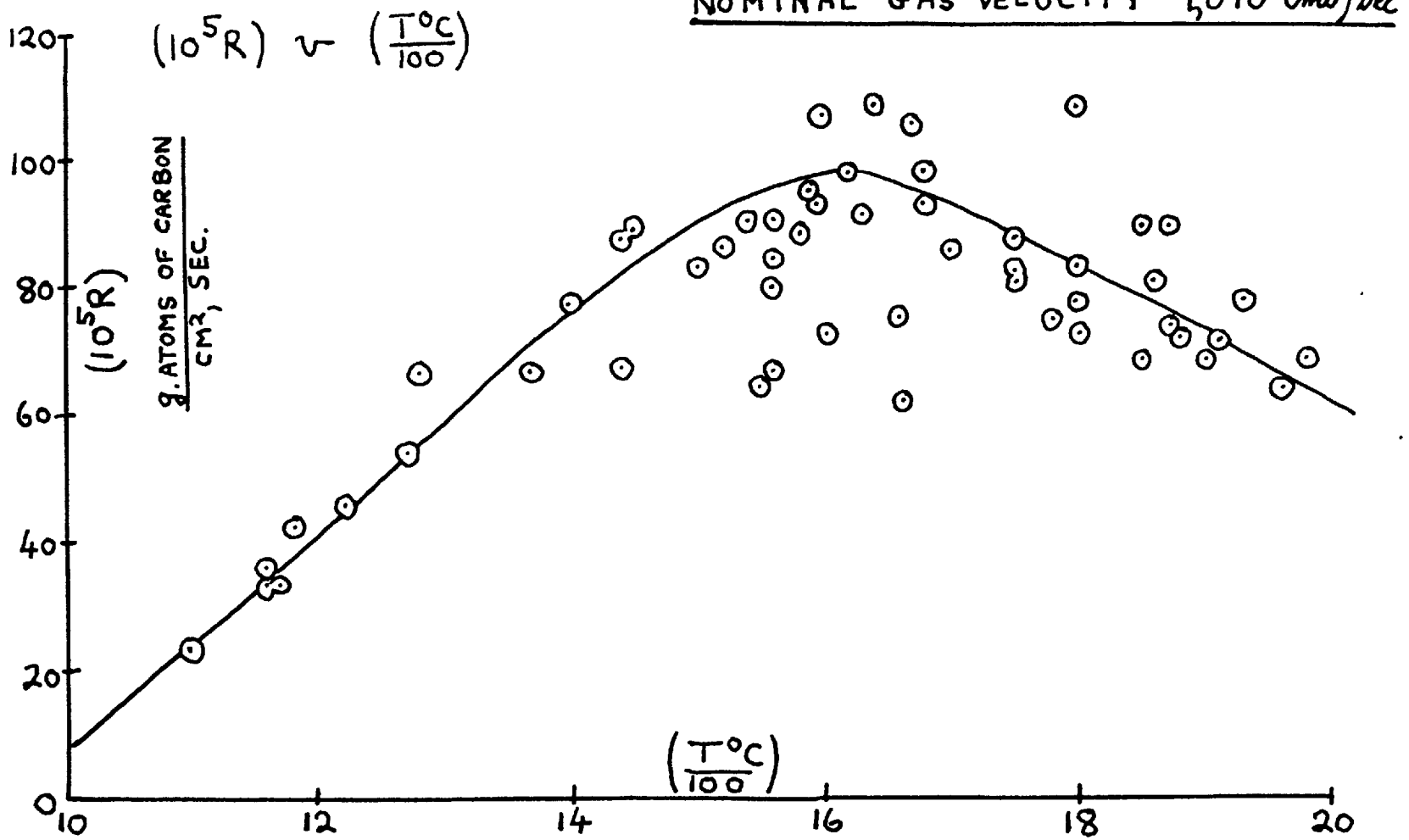
Typical results obtained are shown on Graphs 6 and 7.

At different reaction rates under the same conditions in the gas phase, different fractions of the main gas phase oxygen partial pressure are used to drive oxygen to the carbon surface. The higher the reaction rate the lower will be the partial pressure of oxygen on the carbon surface. To find the partial pressure of the oxygen on the carbon surface an estimate of the mass transfer coefficient will be used.

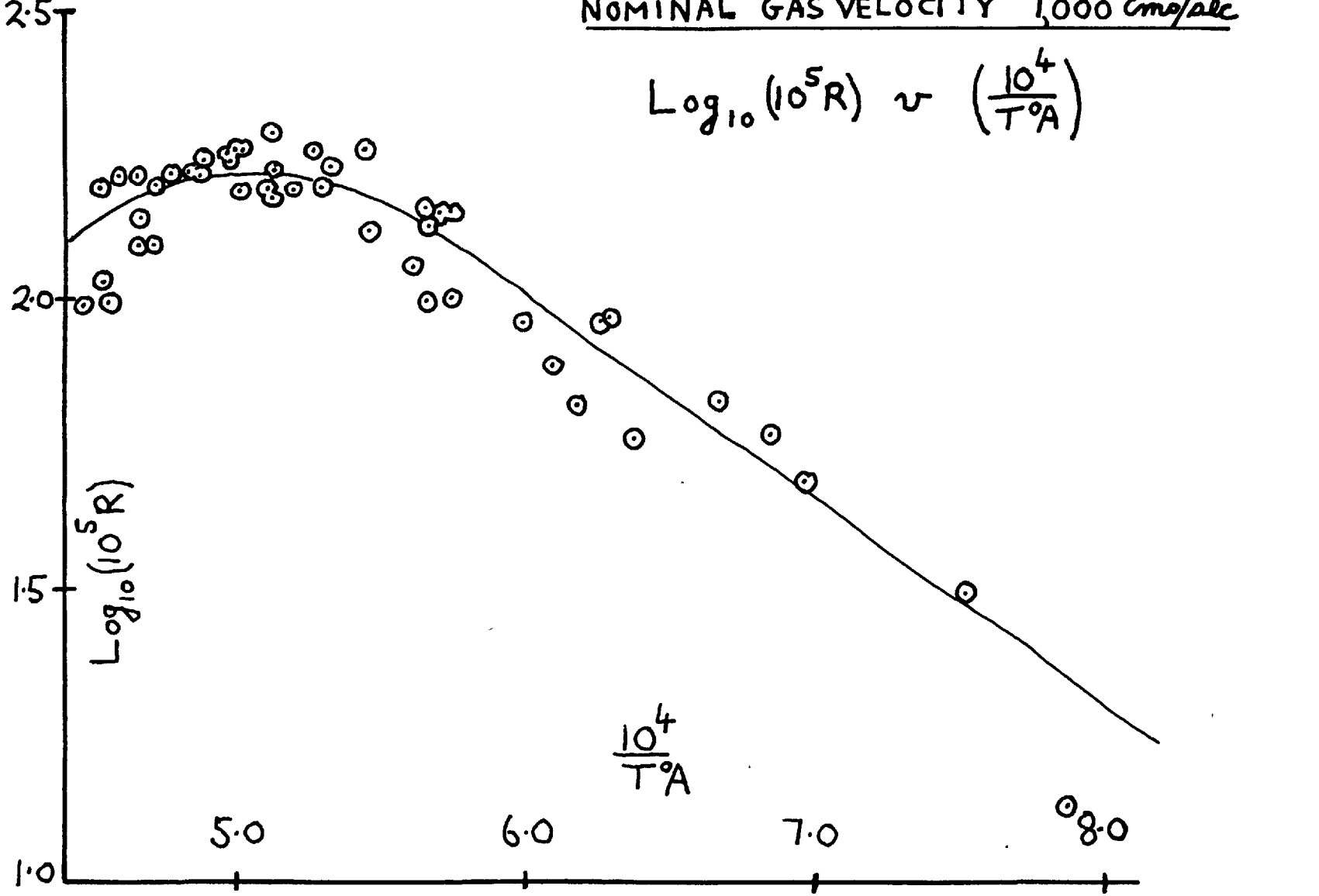
$$h\ (p_o - p) = k\ p^n = R$$

h = mass transfer coefficient
p_o = main gas oxygen partial pressure
p = partial pressure of oxygen on the carbon surface
n = the reaction order
k = the surface reaction rate constant
R = the measured reaction rate.

GRAPH 6 POLYCRYSTALLINE GRAPHITE, OXYGEN AT 0·20 ATS., NOMINAL GAS VELOCITY 4,090 cmo/sec



GRAPH 7 POLYCRYSTALLINE GRAPHITE. OXYGEN AT 0·13 ATS.,
NOMINAL GAS VELOCITY 7,000 cms/sec



From an estimate of h and a knowledge of R it is possible to find p for any value of p_o.

Estimation of the Mass Transfer Coefficients.

The reaction of porous carbon with oxygen has been shown to behave as a mass transfer controlled process, especially at high temperatures and low gas velocities. The measured reaction rates of oxidation of porous carbon are approximately equal to the rate of mass transfer of oxygen to the carbon surface. When a slower reacting graphite is used in place of porous carbon it is assumed that under conditions of geometrical, dynamic and thermal similarity that the mass transfer coefficient is unchanged.

The gas velocities quoted are nominal gas velocities which are measured from a mass gas flow rate - gas velocity correlation and these nominal gas velocities are therefore proportional to the Reynolds Number no matter what the linear gas velocity in the reaction vessel may be.

It has been found necessary to extrapolate values of the mass transfer coefficients obtained at atmospheric pressure to the expected values at reduced pressure on the basis of an inverse pressure dependence. The previously discussed results show that the measured mass transfer coefficients are approximately inversely proportional to the

total gas pressure.

At nominal gas velocities below 1,500 cms/sec. the possible mass transfer rates are correlated by

$y = 0.27 + 0.5x_1 - 0.05x_2 + x_3 - x_4$ as was shown in section C.

It is possible to write an analogous expression for gas velocities greater than 1,500 cms/sec. using the same nomenclature $y = 1.72 + 0.16x_1 - 0.1x_2 + x_3 - x_4$ The symbols y, x_1, etc. have the meaning given to them in section C.

The mass transfer coefficients are calculated thus

$$h \times 10^5 = \frac{R \times 10^5}{p_o}$$

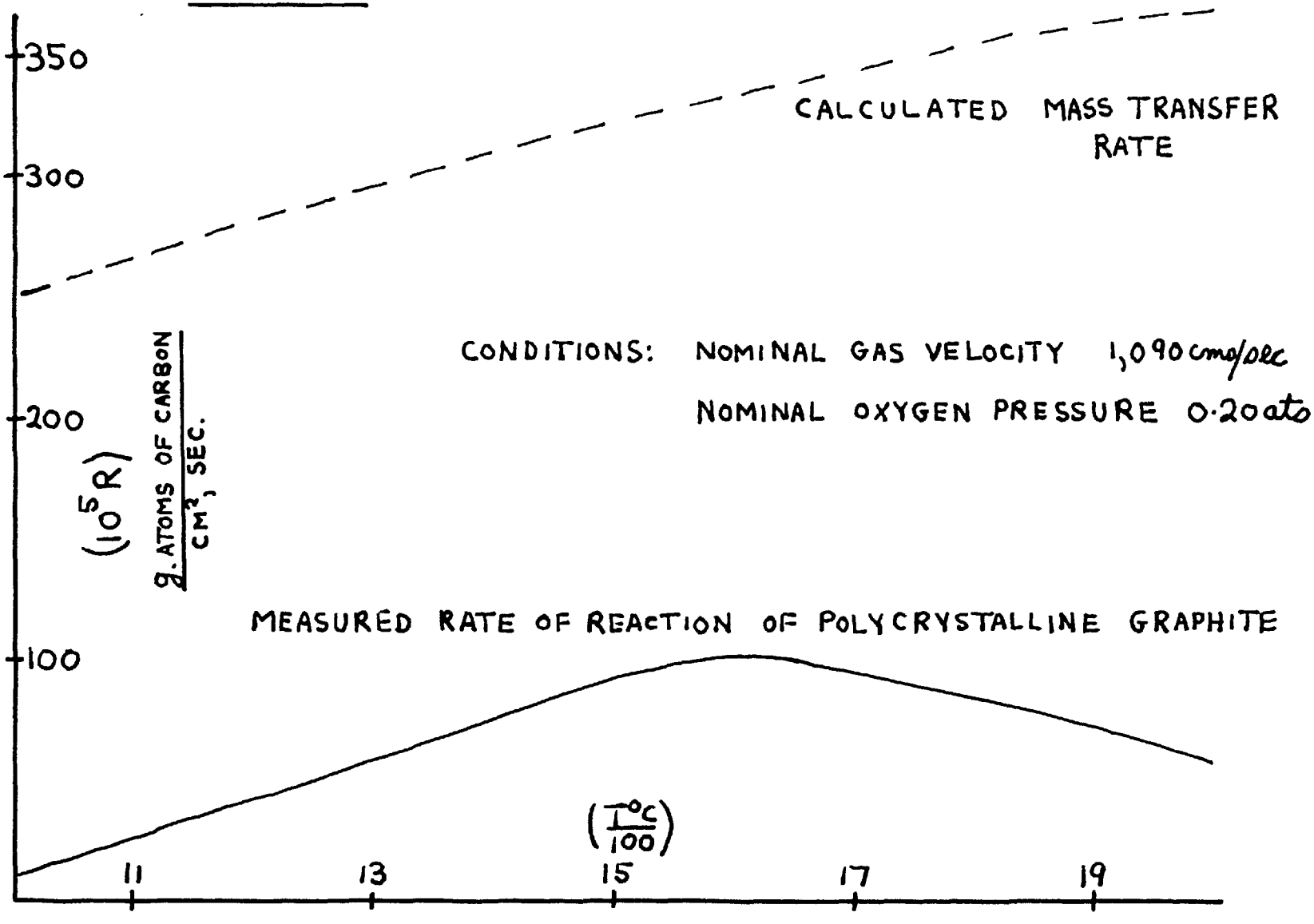
Although these mass transfer coefficients measure the rate at which oxygen diffuses, they are referred to the amount of carbon burned at any carbon temperature and gas velocity

$$h = \frac{\text{gm. atoms of carbon}}{\text{cm}^2\text{, sec, atmosphere of oxygen}}$$

It is assumed that with the graphite and carbon that about the same proportion of carbon monoxide to carbon dioxide is produced at the same temperature.

Graph 8 shows how the reaction rates of graphite with oxygen compare with the calculated possible mass transfer rates.

GRAPH 8


350
300
200
100
CALCULATED MASS TRANSFER RATE
CONDITIONS: NOMINAL GAS VELOCITY 1,090 cm/sec
NOMINAL OXYGEN PRESSURE 0·20 ata
$(10^5 R)$ g. ATOMS OF CARBON / CM², SEC.
MEASURED RATE OF REACTION OF POLYCRYSTALLINE GRAPHITE
$\left(\frac{T°C}{100}\right)$
11
13
15
17
19

From plots of reaction rate versus temperature at any fixed gas phase condition, reaction rates at different temperatures have been taken from the line which appears to fit the experimental observations.

To find the values of p corresponding to R and p_o

(T°C/100)	10^5R	10^5h	(p_o-p)ats	p ats.
Conditions. Total Pressure = 0.13 ats. Partial oxygen pressure = 0.026 ats. Nominal gas velocity 1090 cms/sec.				
10	0.4	1920	0.0002	0.026
11	1.5	2080	0.0007	0.025
12	3.4	2160	0.0016	0.024
13	6.5	2280	0.0028	0.023
14	11.5	2380	0.0044	0.022
15	17	2500	0.0071	0.019
16	19.5	2540	0.0081	0.018
17	17	2660	0.0061	0.020
18	14	2720	0.0051	0.021
19	10	2770	0.0041	0.022
20	6	2840	0.0021	0.024
Conditions. Total pressure = 0.13 ats. Partial oxygen pressure = 0.13 ats. (p_o). Nominal gas velocity 1090 cms/sec.				
10	3	1920	0.002	0.128
11	9	2080	0.004	0.126
12	16	2160	0.007	0.123
13	26	2280	0.011	0.119
14	43	2380	0.018	0.112
15	65	2500	0.026	0.104
16	75	2540	0.030	0.100

(T°C/100)	10^5R	10^5h	(p_o-p)ats	p ats.
17	73	2660	0.027	0.103
18	63	2720	0.023	0.107
19	52	2770	0.019	0.111
20	38	2840	0.013	0.117

Conditions. Total Pressure 0.20 ats. Partial oxygen pressure 0.20 ats(p_o). Nominal gas velocity 1090 cms/sec.

10	10	1250	0.008	0.19
11	24	1340	0.018	0.18
12	42	1410	0.030	0.17
13	60	1480	0.040	0.16
14	76	1540	0.050	0.15
15	90	1620	0.055	0.14
16	99	1660	0.060	0.14
17	94	1730	0.055	0.14
18	84	1780	0.048	0.15
19	73	1820	0.040	0.16
20	62	1850	0.033	0.17

Conditions. Total pressure 0.30 ats. Partial oxygen pressure 0.06 ats(p_o). Nominal gas velocity 1090 cms/sec.

10	2	840	0.002	0.058
11	5.5	900	0.006	0.054
12	9.5	940	0.010	0.050
13	14.5	985	0.015	0.045
14	19	1030	0.018	0.042
15	26.5	1080	0.024	0.036
16	33.5	1100	0.030	0.030
17	35	1160	0.030	0.030
18	31	1190	0.026	0.034
19	24.5	1210	0.020	0.040
20	17.5	1240	0.014	0.046

(T°C/100)	10^5R	10^5h	(p_o-p)ats	p ats.

Conditions. Total pressure 0.30 ats. Partial oxygen pressure 0.30 ats(p_o). Nominal gas velocity 1090 cms/sec.

10	12	840	0.014	0.29
11	36	900	0.04	0.26
12	60	940	0.064	0.24
13	83	985	0.084	0.22
14	105	1030	0.102	0.20
15	119	1080	0.110	0.19
16	125	1100	0.113	0.19
17	120	1160	0.103	0.20
18	110	1190	0.093	0.21
19	100	1210	0.083	0.22
20	88	1240	0.071	0.23

Conditions. Total Pressure 0.20 ats. Partial oxygen pressure 0.04 ats(p_o). Nominal gas velocity 1090 cms/sec.

10	0.5	1250	0.0004	0.040
11	1.5	1340	0.0011	0.039
12	6.5	1410	0.005	0.035
13	10.5	1480	0.007	0.033
14	15.5	1540	0.010	0.030
15	20.5	1620	0.013	0.027
16	24	1660	0.014	0.026
17	24.5	1730	0.014	0.026
18	21	1780	0.012	0.028
19	15.5	1820	0.009	0.031
20	9	1850	0.005	0.035

($T°C/100$)	10^5R	10^5h	(p_o-p) ats	p ats.
Conditions. Nominal pressure 0.063 ats. Impact Pressure 0.069 ats. Partial oxygen pressure 0.069 ats. Nominal gas velocity 1090 cms/sec.				
10	1	3380	0.0003	0.069
11	6	3610	0.0017	0.067
12	12	3780	0.0032	0.066
13	21	3960	0.0053	0.064
14	33	4140	0.0080	0.061
15	46	4350	0.0105	0.058
16	50	4450	0.011	0.058
17	48	4650	0.0104	0.059
18	42	4750	0.008	0.061
19	33	4840	0.007	0.062
20	22	4990	0.004	0.064
Conditions. Nominal pressure 0.13 ats. Impact Pressure 0.23 ats Partial oxygen pressure 0.046 ats. Gas velocity 7000 cms/sec.				
10	1	1470	0.0007	0.045
11	4.5	1700	0.003	0.043
12	8.5	1900	0.005	0.041
13	13.5	2070	0.007	0.039
14	20	2280	0.009	0.037
15	31	2440	0.013	0.033
16	45	2680	0.017	0.029
17	47	2800	0.017	0.029
18	41	3000	0.014	0.032
19	33	3160	0.010	0.036
20	24	3280	0.007	0.039

(T°C/100)	10^5R	10^5h	(p_o-p) ats.	p ats.
Conditions. Nominal pressure 0.13 ats. Impact pressure 0.23 ats				
Partial oxygen pressure 0.23 ats.				
Gas velocity 7000 cms/sec.				
10	16	1470	0.011	0.22
11	35	1700	0.021	0.21
12	50	1900	0.026	0.20
13	70	2070	0.034	0.20
14	90	2280	0.039	0.19
15	116	2440	0.048	0.18
16	146	2680	0.055	0.17
17	165	2800	0.059	0.17
18	172	3000	0.058	0.17
19	140	3160	0.044	0.18
20	105	3280	0.032	0.20
Conditions. Nominal pressure 0.20 ats. Impact Pressure 0.30				
Partial oxygen pressure 0.30 ats. Gas velocity 7000 cms/sec.				
10	18	1130	0.016	0.28
11	44	1300	0.034	0.27
12	72	1460	0.049	0.25
13	105	1600	0.067	0.23
14	130	1750	0.075	0.22
15	150	1870	0.079	0.22
16	160	2060	0.078	0.22
17	165	2160	0.076	0.22
18	164	2300	0.072	0.23
19	158	2420	0.066	0.23
20	140	2530	0.056	0.24

($T°C/100$)	$10^5 R$	$10^5 h$	$(p_o - p)$ ats	p ats.

Conditions. Nominal pressure 0.20 ats. Impact pressure 0.30
Partial oxygen pressure 0.06 ats. Gas velocity 7000 cms/sec.

10	0.5	1130	0.0005	0.059
11	5	1300	0.004	0.056
12	12.5	1460	0.008	0.052
13	19.5	1600	0.012	0.048
14	28	1750	0.016	0.044
15	41	1870	0.022	0.038
16	54	2060	0.026	0.034
17	62	2160	0.029	0.031
18	60	2300	0.026	0.034
19	52	2420	0.022	0.038
20	43	2530	0.017	0.043

Conditions. Nominal pressure 0.60 ats. Impact pressure 0.65
Partial oxygen pressure 0.65 ats. Gas velocity 7000 cms/sec.

10	15	520	0.03	0.62
11	56	600	0.09	0.56
12	104	672	0.15	0.50
13	146	734	0.20	0.45
14	188	810	0.23	0.42
15	230	864	0.27	0.38
16	264	950	0.28	0.37
17	263	990	0.27	0.38
18	246	1060	0.23	0.42
19	220	1120	0.20	0.45
20	190	1160	0.11	0.54

(T°C/100)	10^5R	10^5h	(p_o-p) ats	p ats.
Conditions. Nominal pressure 0.40 ats. Impact pressure 0.44 Partial oxygen pressure 0.44 ats. Gas velocity 7000 cms/sec.				
10	10	770	0.01	0.43
11	53	890	0.06	0.38
12	96	990	0.10	0.34
13	140	1080	0.13	0.31
14	186	1190	0.16	0.28
15	220	1270	0.17	0.27
16	244	1440	0.18	0.26
17	236	1460	0.16	0.28
18	214	1560	0.14	0.30
19	184	1650	0.11	0.33
20	154	1710	0.09	0.35
Conditions. Nominal gas pressure 0.50 ats. Impact pressure 0.54 ats. Partial oxygen pressure 0.54 ats. Gas velocity 7000 cms/sec.				
10	12	626	0.02	0.52
11	55	725	0.08	0.46
12	100	805	0.12	0.42
13	148	880	0.17	0.38
14	190	970	0.20	0.34
15	228	1040	0.22	0.32
16	250	1140	0.22	0.32
17	244	1190	0.20	0.34
18	220	1270	0.17	0.37
19	190	1340	0.14	0.40
20	156	1390	0.11	0.43

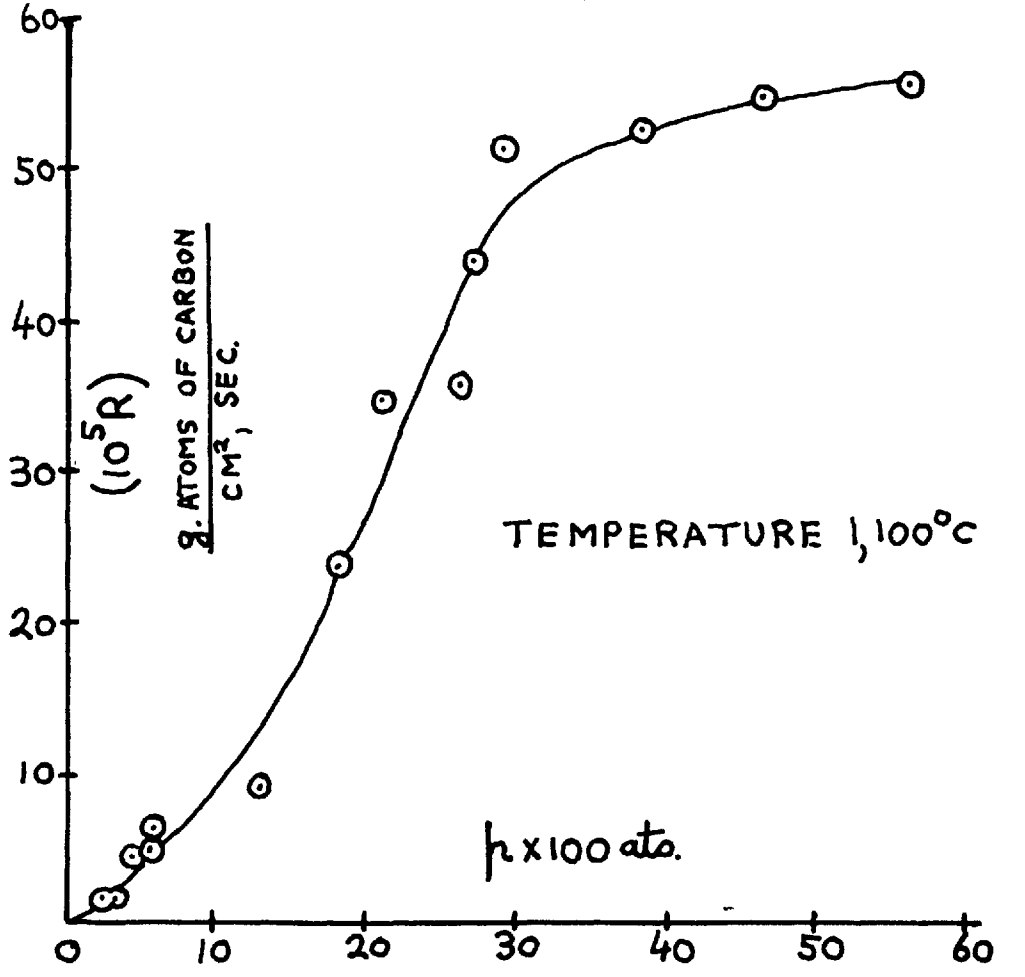
($T°C/100$)	10^5R	10^5h	(p_o-p) ats.	p ats.
Conditions. Nominal gas pressure 0.30 ats. Impact pressure 0.34 ats.				
Partial oxygen pressure 0.34 ats. Gas velocity 7000 cms/sec.				
10	14	1000	0.01	0.33
11	52	1150	0.05	0.29
12	88	1280	0.07	0.27
13	120	1390	0.09	0.25
14	152	1530	0.10	0.24
15	174	1640	0.11	0.23
16	190	1800	0.11	0.23
17	192	1880	0.10	0.24
18	174	2010	0.09	0.25
19	150	2130	0.07	0.27
20	120	2200	0.06	0.28

Rates of Reaction versus Temperature at Fixed Oxygen Partial Pressure on the Graphite Surface.

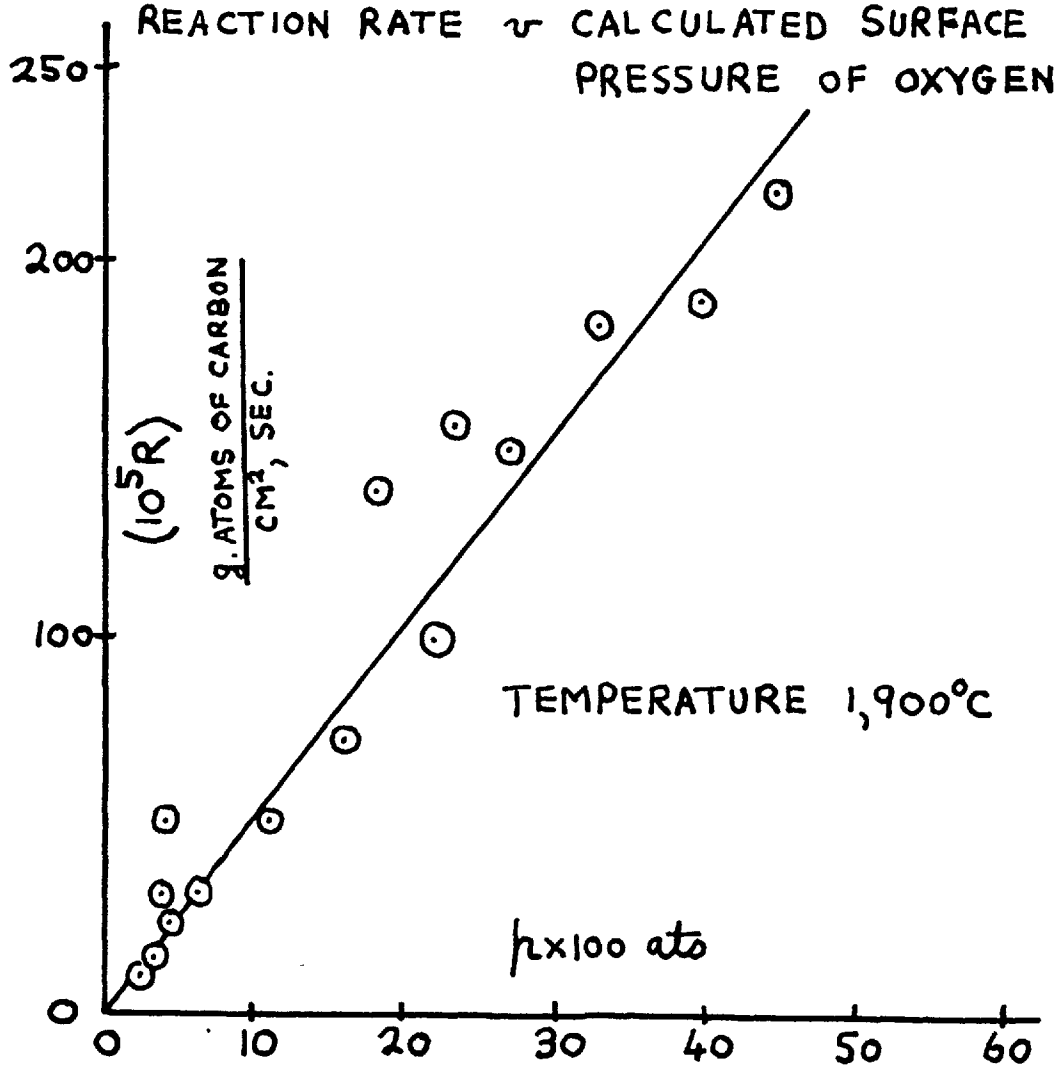
From the previous tables, graphs of the reaction rate versus surface oxygen partial pressure can be drawn for constant temperatures and from these graphs an indication of the order of the surface reaction at various temperatures can be obtained. Graphs 9 and 10 show variations of reaction order, with oxygen partial pressure and graphite surface temperature, which will be discussed in detail later. It is now possible to find how the reaction rate varies with temperature at any given surface partial pressure of oxygen. Graph 11 shows the variation and the following tables give the variation for other oxygen partial pressures.

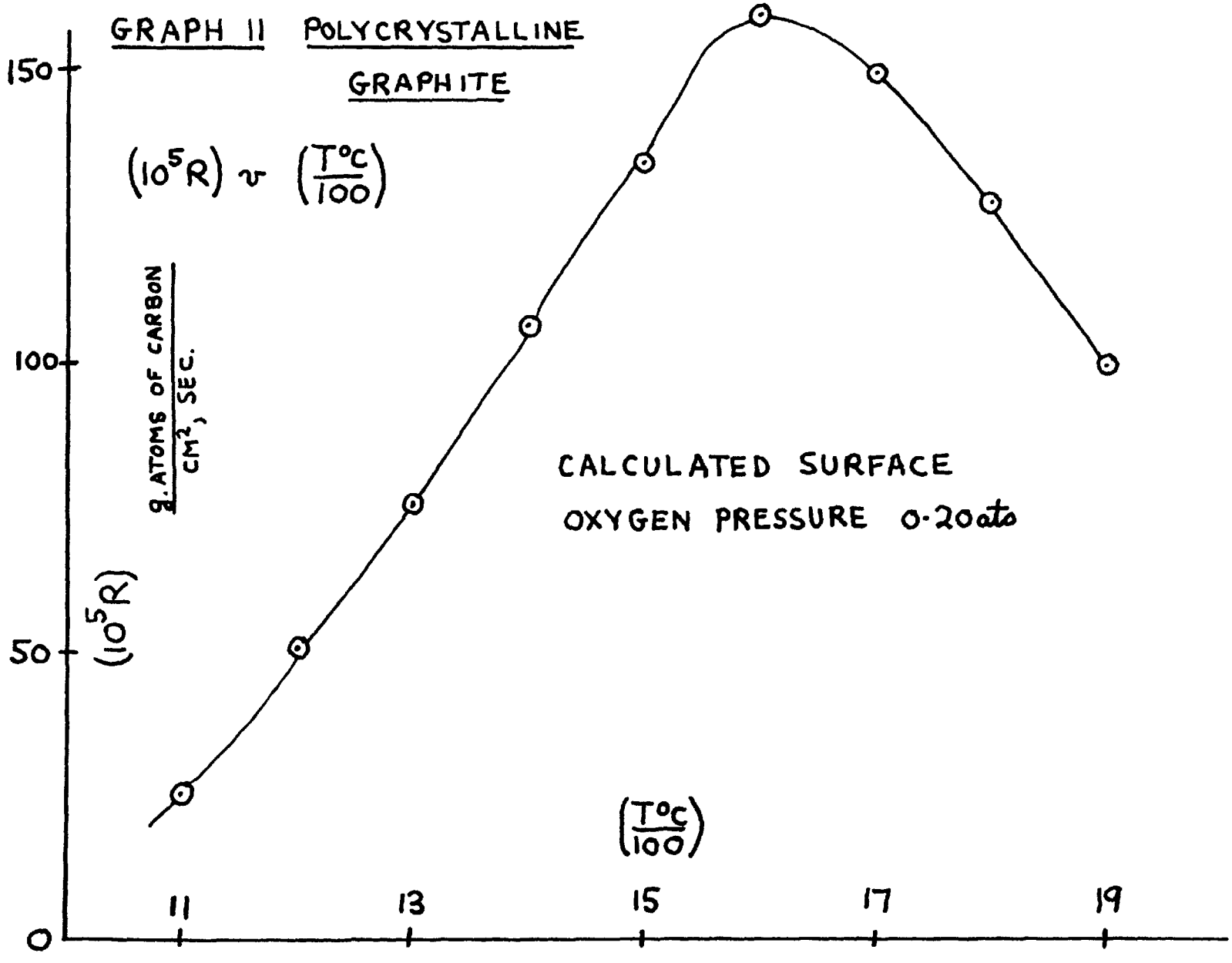
GRAPH 9 POLYCRYSTALLINE GRAPHITE

REACTION RATE v CALCULATED SURFACE PRESSURE OF OXYGEN



GRAPH 10 POLYCRYSTALLINE GRAPHITE




GRAPH II POLYCRYSTALLINE GRAPHITE
(10^5R) v $\left(\frac{T°C}{100}\right)$
g. ATOMS OF CARBON / CM², SEC.
(10^5R)
CALCULATED SURFACE
OXYGEN PRESSURE 0·20 ato
$\left(\frac{T°C}{100}\right)$
150
100
50
0
11
13
15
17
19

When p = 0.05 ats O_2

(T°C/100)	10^5R
11	4
12	11
13	14
14	23
15	36
16	43
17	38
18	33
19	26

When p = 0.10 ats. O_2

(T°C/100)	10^5R
11	9
12	22
13	30
14	46
15	68
16	75
17	75
18	65
19	50

When p = 0.20 ats O_2

11	25
12	50
13	70
14	106
15	134
16	160
17	150
18	128
19	100

When p = 0.30 ats O_2

11	48
12	90
13	135
14	182
15	224
16	248
17	220
18	190
19	152

When p = 0.40 ats O_2

(T°C/100)	10^5R
11	53
12	99
13	146
14	190
15	234

(T°C/100)	10^5R
16	272
17	290
18	252
19	200

G. Dependence of the Reaction Rate of Pyrographite with Oxygen on Temperature and Nominal Gas Velocity.

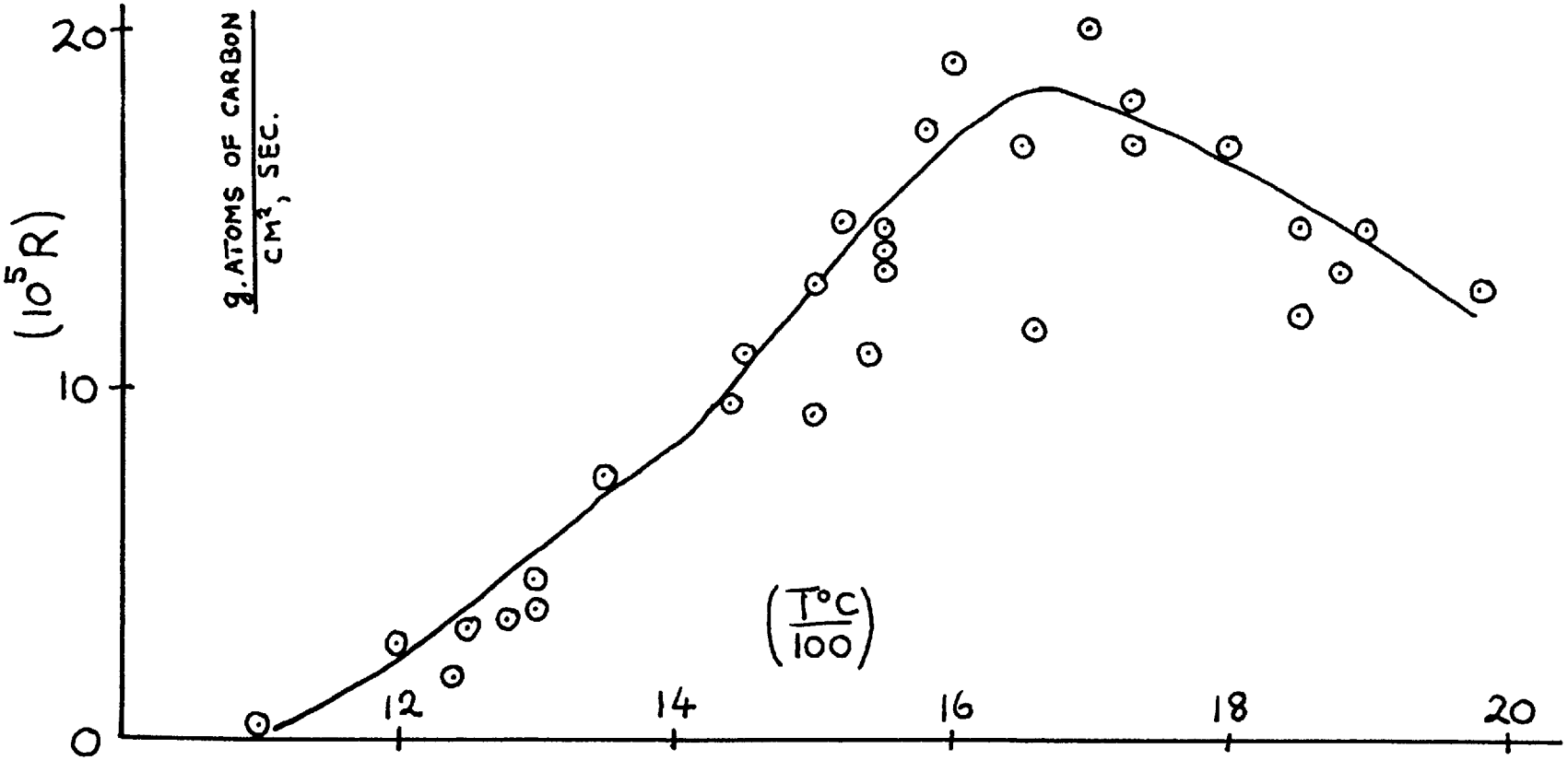
The results are taken from Appendix 1, Table 8.

The reaction rates were measured at two gas velocities of 1090 cms/sec and 7000 cms/sec., and corresponding oxygen partial pressures at the impact point of 0.20 ats. and 0.23 ats. In both cases the reaction rates were about the same and the reaction rates were very much slower than the corresponding reaction rates of the polycrystalline graphite obtained under similar conditions. Graphs 12 and 13 show that the general pattern of behaviour of pyrographite is similar to the results obtained with the polycrystalline graphite and the reaction rates are so much slower that there seems to be little doubt that the reaction rates are chemically controlled.

GRAPH 12 PYROGRAPHITE. OXYGEN AT 0·20 ATS.

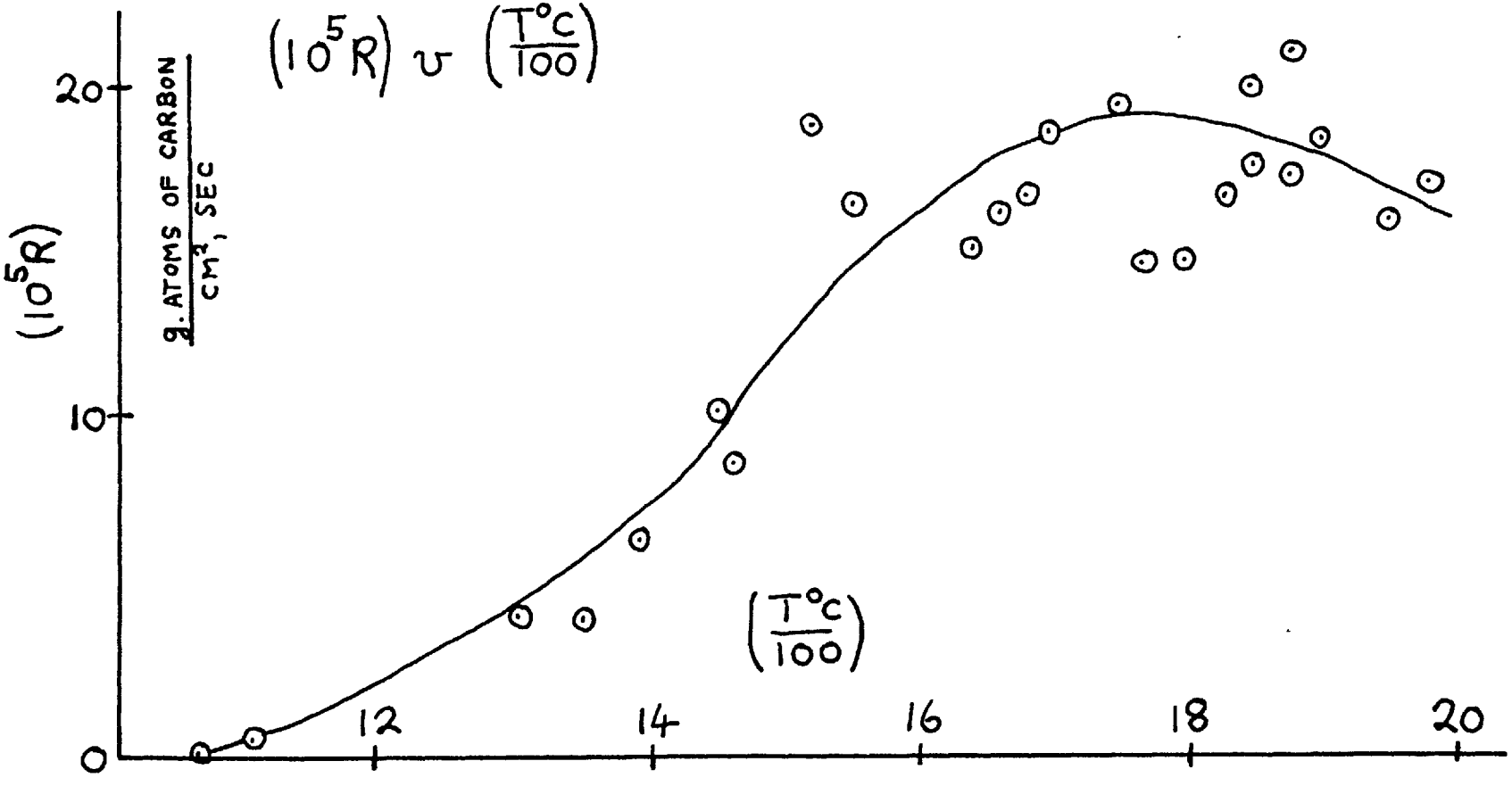
NOMINAL GAS VELOCITY 1,090 cms/sec

$(10^5 R) v \left(\frac{T°C}{100}\right)$



GRAPH.13 PYROGRAPHITE. OXYGEN AT 0·13 ATS.

NOMINAL GAS VELOCITY 7,000 cms/sec



THEORIES PROPOSED TO ACCOUNT FOR THE CHEMICAL SURFACE KINETICS OF THE HIGH TEMPERATURE OXIDATION REACTIONS OF GRAPHITE.

There are two main theories which can be distinguished by the part the reactant gas is thought to play in the reaction kinetics.

A. Eyring's theory [21] suggests that hydrogen as an impurity can activate the low temperature reaction and the reactive sites are therefore not created directly by the attack of the oxidising gas. A simple derivation of Eyring's theory will be given but it must be said that Eyring has taken Meyer's results [19,20] as being correct and has arranged his kinetic expressions to give a zero order reaction at high temperature. It will be easy to see that other arrangements of his terms could give first order reaction on the graphite when the hydrogen has been removed by the high temperature of the graphite surface.

B. An alternative explanation of the appearance of a maximum in the reaction rate as the temperature is increased is that at high temperatures carbon atoms can migrate fairly easily to heal the surface which would otherwise be very reactive. The attacking gas can in this case combine with relatively unreactive surface in a slow

reaction thereby providing sites which are much more reactive. A simple mathematical development of this theory will be given and the theory will be used to compare numerically the results of the author's work carried out at high oxygen partial pressures with Strickland-Constable's results [15] obtained at low pressures. For the above purpose plausible activation energies of the various rate constants in the expressions have been assumed.

A. Eyring's Theory.

Eyring assumes the existence of type 1 and type 2 sites.

Type 1 sites are associated with hydrogen.

Type 2 sites are pure graphite.

Let N = the total number of sites per cm^2.

f = the fraction of sites of type 1.

$(1-f)$ = the fraction of sites of type 2.

A_1 = fraction of type 1 sites which is covered by oxygen.

A_2 = fraction of type 2 sites which is covered by oxygen.

k_{-1} = rate constant for type 1 surface oxide leaving the surface.

k_{-2} = rate constant for type 2 surface oxide leaving the surface.

A_1 and A_2 are determined by the Langmuir equations :

$$A_1 = \frac{k_1 p}{k_{-1} + k_1 p} \qquad A_2 = \frac{k_2 p}{k_{-2} + k_2 p}$$

where k_1 = rate constant for the formation of a type 1 surface oxide,

k_2 = rate constant for the formation of a type 2 surface oxide,

and p = oxygen partial pressure.

The rate of reaction $v = k_{-1} A_1 f N + k_{-2} A_2 (1-f) N$

Eyring then considered seven possible processes which could influence (f) and from the rates of these processes he deduced the steady state condition for (f).

	Process.	Effect on N $\frac{df}{dt}$
1.	Formation of Type 1 surface oxide	none
2.	Formation of Type 2 surface oxide	none
3.	Type 1 surface oxide leaves the surface.	$(n-1) k_{-1} f N A_1$
4.	Type 2 surface oxide leaves the surface.	$n' k_{-2} (1-f) N A_2$
5.	Bare type 1 sites are converted to type 2 sites, with first order reaction rate constant k_3.	$-k_3 f N (1-A_1)$
6.	Type 1 surface oxide becomes type 2 site. First order constant k_4.	$-k_4 f N A_1$
7.	Type 2 sites are converted to type 1 sites at a rate proportional to the number of type 2 sites and to the rate at which a type 1 site leaves the surface; b is a proportionality constant	$\frac{1}{b} k_{-1} A_1 (1-f) N$

where n = number of type 1 sites formed when a type 1 oxide leaves the surface

n' = number of type 1 sites formed when type 2 oxide leaves the surface.

Eyring interprets the previous work on the combustion of graphite at high temperatures as showing the reaction is zero order. As a consequence of this condition the reaction rate $= k_1 f N p + k_{-2} (1-f) N$

and $$f = \frac{n' k_{-2} + 1/b\, k_1 p}{n k_{-2} + k_3 + \frac{k_3 k_4}{k_{-1}} p + \frac{1}{b} k_1 p}$$

To obtain a maximum in the reaction rate the value of (f) is thought to decrease with increasing temperature because certain processes act in competition in the formation or destruction of type 1 sites.

B.1. Active sites created by the attack of the reactant gas.

If there are two kinds of sites on the surface, reactive A sites and less reactive B sites :

Let x = the fraction of the surface occupied by A sites

Let σ = the fraction of the A surface occupied by adsorbed oxygen.

Then the Langmuir equation gives a value for σ

$$\sigma = \frac{k_c p}{k_e + k_c p}$$

where k_c = the rate of adsorption of oxygen on the surface
k_e = the rate of desorption of oxygen from the surface
p = the oxygen partial pressure.

Processes.

1. Reaction of oxygen with type A sites, leaving the number of type A sites unchanged.

$$\text{Rate of reaction} = k_3 \sigma x$$

$$= \frac{k_A}{1 + k_z p} \; p \; x$$

where k_A and k_z are composite rate constants.

2. Reaction of oxygen with type B sites to form type A sites.

The type B reaction has been assumed to be first order with respect to the oxygen pressure, corresponding to low adsorption coverage according to the Langmuir theory.

$$\text{Rate of reaction} = k_B (1 - x) p$$

3. The destruction of type A sites to form type B sites is assumed to proceed at a rate proportional to the surface concentration of type A sites.

$$\text{Rate of destruction of type A sites} = k_T x$$

In the steady state condition when there is no net change in the number of type A sites

$$x = \frac{k_B p}{k_T + k_B p}$$

$$\text{and Total Rate of Reaction (R)} = \left(\frac{k_A}{1 + k_z p} \; x + k_B (1-x) \right) p$$

At Low Temperatures.

x is large

$$R = \frac{k_A p x}{1 + k_z p}$$

The reaction rate could be first or zero order at low temperatures, depending on the relative magnitude of 1 and $k_z p$. The reaction occurs on type A sites.

At High Temperatures.

x is small

$$R = k_B p$$

The reaction rate is first order and occurs on type B sites.

B.2. Calculation of Reaction Rates from Surface Healing Theory.

In the calculations, it is assumed that all rate constants can be expressed as a function of the absolute temperature by the Arrhenius equation. Suitable numerical values have been chosen for the rate constants to enable the calculated reaction rates to fit the reaction rates observed by Strickland-Constable [15] and by the author.

$$k_A = 20\, e^{-30000/RT} = 20 \times 10^{-6500/T}$$

$$k_T = 1.51 \times 10^5\, e^{-97000/RT} = 1.51 \times 10^5 \times 10^{-21320/T}$$

$$k_z = 21.3\, e^{4100/RT} = 21.3 \times 10^{900/T}$$

$$k_B = 446 \times 10^{-5}\, e^{-15200/RT} = 446 \times 10^{-5} \times 10^{-3320/T}$$

Calculations.

Oxygen pressure = 2.5×10^{-5} ats.

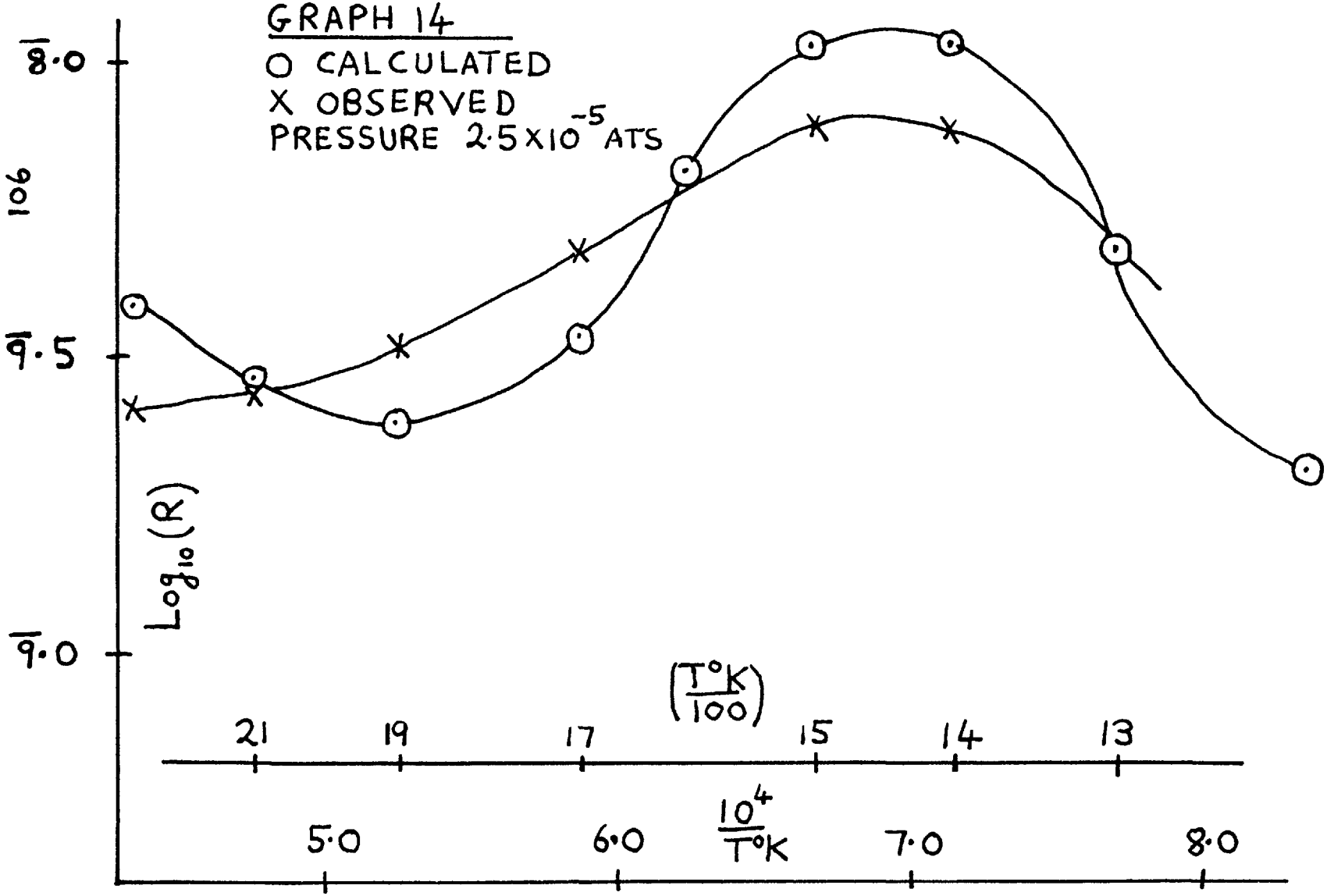
Temperature °K.	12	13	14	15	17	18	21	23	By a Factor of 100°k
A. 18000/T	15.0	13.8	12.9	12.0	10.6	9.5	8.6	7.84	-
B. 7.53-18000/T $=\log_{10}(k_T/k_B)$	-7.5	-6.3	-5.4	-4.5	-3.1	-2.0	-1.1	-0.3	-
C. $\log_{10} k_T/k_B p$ (add 4.6 to B)	-2.9	-1.6	-0.8	+0.1	+1.5	+2.6	+3.5	+4.3	-
D. $k_T/k_B p$	.00126	.025	0.16	1.26	31.6	400	3160	20000	-
E. x = 1/1 + D	1	.975	0.86	0.44	.0307	.0025	0	0	-
F. k_A	8	20	50	92	312	800	1600	3040	10^{-5}
G. k_A x (FxE)	8	19.5	43	40.5	9.6	2.0	0	0	10^{-5}
H k_B		1.2	1.8	2.7	5	8	12	16	10^{-5}
I (1-x)	0	.025	0.14	0.56	0.97	1	1	1	
J $k_B(1-x)$ = HxI	0	0	0.25	1.5	4.85	8	12	16	10^{-5}
K. $[k_A x + k_B(1-x)]$	8	19.5	43	42	14.4	10	12	16	10^{-5}
L [ ] p	20	47	107	105	36	25	30	40	10^{-10}
M $\log_{10}$[ ] p $= \log_{10}$ (R)	$\bar{9}.3$	$\bar{9}.67$	$\bar{8}.03$	$\bar{8}.02$	$\bar{9}.56$	$\bar{9}.40$	$\bar{9}.48$	$\bar{9}.60$	-

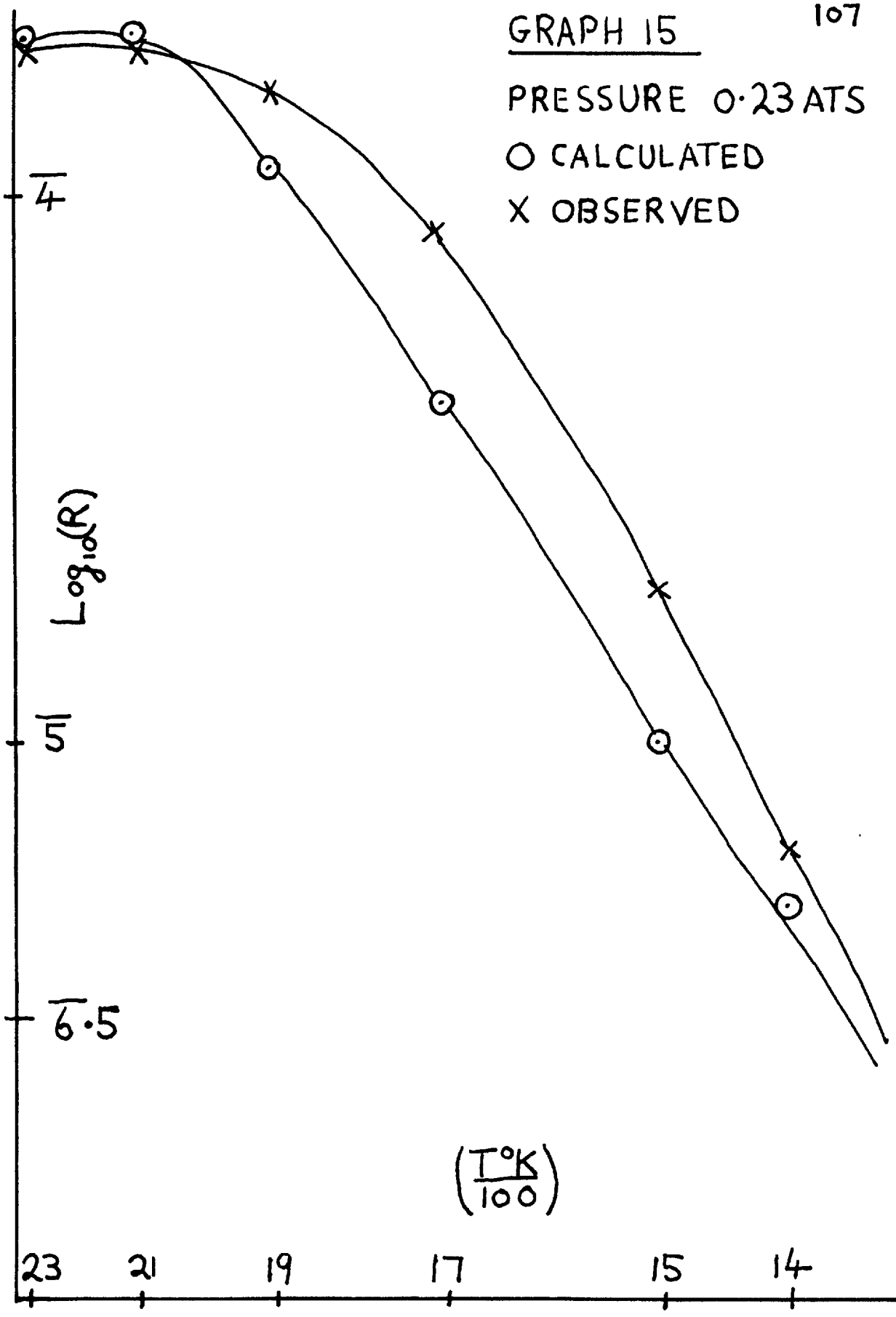
Oxygen pressure = 0.23 ats.

Temperature °K	12	13	14	15	17	19	21	23	By a factor of 100°K.
N. $\log_{10} \frac{k'_T}{k_B 0.23}$ = B + 0.64					-2.46	-1.36	-0.46	+0.34	
O. $k_T/0.23\ k_B$					0.0035	0.044	0.35	2.19	
P. x = 1/1+O)	1	1	1	1	1	0.96	0.74	0.314	
Q. (1-x)	0	0	0	0	0	0.04	0.26	0.69	
R. $k_A x$ = PxF		20	50	92	312	770	1190	960	10^{-5}
S. k_z		104	95.5	87	70	63	56.5	52	
T. $k_z p$		24	22	20	16	14½	13	12	
U. $k_A x/1+k_z p$		0.8	2.2	4.4	18.4	50	85	74	10^{-5}
V. $k_B(1-x)$ =QxH						0.3	3.1	11	10^{-5}
W. = U + V		0.8	2.2	4.4	18.4	50	88	85	10^{-5}
X. Wp = 0.23W = R		0.185	0.5	1.0	4.2	11.5	20.2	19.5	10^{-5}
Y. $\log_{10}$ (R)		$\bar{6}.27$	$\bar{6}.7$	$\bar{5}.0$	$\bar{5}.62$	$\bar{4}.06$	$\bar{4}.30$	$\bar{4}.29$	

Graphs 14 and 15 show how the calculated curves agree with the curves observed for pyrographite at low oxygen partial pressures (Strickland-Constable [15]) and for pyrographite at fairly high oxygen pressures (this work). In each case the agreement is good and the shift in the position of the maximum from 1,200°C. at 2.5×10^{-5} atm. O_2

to about 1700°C. at 0.23 atm. O_2 is accounted for by the calculations. The phsyical explanation of the shift in the position of the maximum rate with increasing oxygen partial pressure is that a much greater rate of surface healing, which will be available at higher temperatures, is required to overcome the increased rate of attack on the surface resulting from the increased oxygen concentration. Although insufficient measurements were made on pyrographite to establish the reaction order at various temperatures and oxygen pressures there will be a tendency for the reaction at 0.23 ats., if it is at all similar to the polycrystalline graphite reaction, to have an order less than unity especially at lower temperatures. The actual calculations in this case suggest that the (A) reaction is zero order for the high oxygen partial pressures at all temperatures up to 2,000°C., though the total reaction at high temperature will be of a greater order than zero because of the part played by the first order (B) reaction. It would seem that the chosen values of the rate constants do give a general picture of the behaviour of the reaction at pressures different by a factor of about ten thousand. The maximum in the reaction rate and the temperature shift of the maximum with increasing oxygen partial pressure agree with experimental observations


GRAPH 14
O CALCULATED
X OBSERVED
PRESSURE 2·5 X 10⁻⁵ ATS
8·0
9·5
9·0
Log10 (R)
(T°K / 100)
21
19
17
15
14
13
10⁴ / T°K
5·0
6·0
7·0
8·0


GRAPH 15
PRESSURE 0·23 ATS
O CALCULATED
X OBSERVED
$\overline{4}$
$\overline{5}$
$\overline{6}\cdot5$
$\log_{10}(R)$
$\left(\frac{T°K}{100}\right)$
23
21
19
17
15
14

and even the reaction orders which are probably not in perfect agreement with experiment show the correct tendency of first order reaction at low pressure and all temperatures and more zero order behaviour at high oxygen partial pressure and low temperatures.

It is difficult to give complete justification for the chosen activation energies. The value of 30 kcal/mole ascribed to k_A to account for the low temperature portion of the reaction rate curve is supported by Wicke and others [4,9,13] as being the activation energy of the reaction of oxygen with porous graphite at temperatures above about 700°C. Diffusion of carbon atoms on the surface of pyrographite is a process about which nothing is known but values of 90 kcal/mole have been calculated by Dienes [32] to be the activation energy of volume diffusion of carbon atoms in a graphite lattice and Feldman [33] using a carbon-14 tracer measured the self diffusion in graphite in the range 1800°C. to 2400°C. and found an effective activation energy for the combined volume diffusion-grain boundary diffusion to be 40 kcal/mole. In the calculations a value of 97 kcal/mole was given to the activation energy of the surface diffusion process.

There is no evidence to support the values given

to the activation energies of k_z and k_B and all that can be said for the particular choice is that the orders of magnitude are not unreasonable. k_B has an activation energy of about 15 kcal/mole and k_z which is the ratio of the adsorption rate constant / the desorption rate constant for oxygen on the type A graphite surface has been ascribed the small activation energy of about 4 kcal/mole.

DISCUSSION.

The apparent mass transfer coefficients given in Table 1 have been shown on analysis to depend only slightly on temperature and to be strongly influenced by gas velocity. Throughout the velocity range 100 to 10,000 cms/sec., the velocity dependence is not uniform. There is a definite change in velocity dependence about a gas velocity of 1500 cms/sec. and as the velocity is increased the dependence changes from the 0.6 power of velocity to the 0.16 power of velocity. Behaviour of this type is characteristic of a mass transfer controlled process and the change in velocity dependence immediately suggests a transition from a streamline boundary layer control to a turbulent boundary layer control of the diffusion process. The low temperature dependence of the apparent mass transfer coefficient shown by the activation energy of only 3 kcal/mole is consistent with the explanation of diffusion control because the diffusivity of a gas is only slightly temperature dependent and certainly does not change with temperature as quickly as a chemical reaction rate. Increasing influence of chemical reaction would explain the slightly higher temperature coefficient of the combustion rate found in the high velocity range.

Further support for the idea that the attack of

oxygen or porous carbon at atmospheric pressure is mass transfer controlled comes from the results of Table 2. Table 2 shows how at a constant total gas pressure of one atmosphere, the combustion rate of porous carbon changes with the partial oxygen pressure. The apparent first order reaction with respect to the oxygen partial pressure, while not being alone an indication of mass transfer control of the combustion rate is in fact a consequence of this suggestion on the grounds that most of the oxygen partial pressure would be used to drive the oxygen through the boundary layer to the reacting carbon surface.

The mass transfer rate must equal the combustion rate R

$$R = h (p_o - p)$$

where h = mass transfer coefficient $\frac{\text{gm. atoms of carbon used}}{\text{cm}^2, \text{ sec, atmosphere of } O_2}$

p_o = the main stream oxygen partial pressure (ats.)

p = the oxygen partial pressure on the carbon surface (ats.).

If the surface chemical reaction is very fast then the rate of combustion is controlled by the rate of mass transfer since it is the slower step in the series of processes and in addition p is very much smaller than p_o.

$R = h p_o$ an apparent first order reaction.

The diffusivity of a gas is known to be inversely proportional to the absolute gas pressure so that if the combustion rate of porous carbon could be shown to have this pressure dependence it could be said that the reaction of porous carbon with oxygen is mass transfer controlled. Analysis of the results of Table 3 does in fact show that the combustion rate is inversely proportional to the absolute gas pressure.

The dependence of the combustion rate of porous carbon, on carbon temperature, gas velocity, oxygen partial pressure and total gas pressure within the experimental ranges of these variables is the dependence that would be expected from a boundary layer diffusion controlled process.

These measurements of the combustion rate of porous carbon provide estimates of the mass transfer coefficients (on the basis of the carbon reacted) for the experimental system. Mass transfer coefficients calculated in this way from experimental correlations will provide perhaps the best available values which could be used to estimate the concentration driving force required to overcome the mass transfer resistance to the combustion of a much slower reacting carbon or graphite where there is a large measure of chemical control of the combustion rate.

The two systems are in geometrical, dynamic and thermal similarity and it is only assumed that in each case the ratio of carbon monoxide to carbon dioxide produced is the same for both carbons at any temperature. This assumption may not be unreasonable because other workers have shown that at high temperatures the product of the reaction is mainly carbon monoxide and that the nature of the carbon has not much influence on the ratio of the amounts of carbon monoxide to carbon dioxide. The ratio is chiefly temperature dependent [5, 10, 15].

Wicke and Rossberg [4] studying the reaction of oxygen with spectroscopic graphite have reported that the combustion rate is diffusion controlled between 1300°C. and 1400°C. Evidence for their claim was the velocity dependence of the combustion rate, the low activation energy of the reaction, the inverse proportionality between the combustion rate and the total gas pressure and the existence of concentration gradients in the gas phase. Walker [24] and his co-workers have found a mass transfer controlled oxidation of graphite between temperatures of 1200°C. and 1700°C. and Watt [22] has shown that the reaction of water vapour with carbon at 2300°C. is largely mass transfer controlled. The findings of this work are in general

agreement with the results obtained by the above mentioned authors.

When polycrystalline graphite is attacked by air and oxygen-nitrogen mixtures at a total gas pressure of one atmosphere there is a partial chemical control of the reaction rate as analysis of Tables 4 and 5 shows. At low temperatures of about 1000°C. the apparent activation energies of the reaction rates are rather high, of the order of 30 kcal/mole, but at higher temperatures around 1800°C. the apparent activation energies drop to about 10 kcal/mole. The reaction rate is very dependent on gas velocity at higher temperatures; when the velocity of the gas is changed from 100 cms/sec. to 7000 cms/sec. the reaction rate changes by a factor of about 10 at 1800°C. but about 1000°C. there is no appreciable change in the reaction rate for the same change in gas velocity. Comparison of the rates of combustion of polycrystalline graphite with the rates of combustion of porous carbon at similar gas velocities shows that the rate of attack of oxygen on polycrystalline graphite rapidly approaches the limiting mass transfer rate as the temperature is raised.

The apparent order of reaction with respect to the oxygen partial pressure in the combustion of

polycrystalline graphite had to be measured by finding the change in the reaction rate, over a temperature range 1000°C. to 1800°C., at different oxygen partial pressures when the gas velocities were the same. Differences in the regression of $\log_{10}(10^5 R)$ on $10^4/T°A$ were found at the same gas velocity for different oxygen partial pressures. The order of reaction varied irregularly with both gas velocity and temperature but the values always lay between 0.75 and 1.25. Even with this mixed regime control of the reaction rate it would seem that the overall order of reaction is about unity.

It is not possible to make a good correction for the mass transfer influence on the combustion of polycrystalline graphite at one atmosphere pressure over a wide temperature range because at higher temperatures about 90% of the resistance to combustion comes from the mass transfer resistance so that the remaining chemical resistance cannot be established with great precision.

At reduced pressures of the order of 1/10 atmosphere the calculated mass transfer rates become high compared with the measured rates of reaction of the polycrystalline graphite with both oxygen and oxygen-nitrogen mixtures shown in Tables 6 and 7. The observed reaction

rate can be seen to increase with temperature over the range 1000°C. to about 1600°C. and from about 1700°C. to 2000°C. to decrease appreciably; there is a maximum in the reaction rate about a temperature of 1650°C. While it can be calculated that the combustion rate is not fully mass transfer controlled there is probably about 50% mass transfer control at the maximum reaction rate in the least favourable cases.

Because of the partial mass transfer control of the reaction rates it is not possible to compare directly the rates of reaction obtained with different main stream oxygen partial pressures (p_o). At any single gas velocity and main stream oxygen partial pressure (p_o) the effective partial pressure of oxygen at the graphite surface (p) varies greatly with temperature because the degree of mass transfer resistance is related to the closeness of the observed reaction rate to the possible mass transfer rate. At the maximum observed reaction rate, for given conditions of gas velocity and main stream oxygen partial pressure (p_o) the effective oxygen partial pressure at the graphite surface (p) will be the least, for a bigger fraction of the main stream oxygen concentration is required to overcome the mass transfer resistance.

The mass transfer and chemical reaction processes are sequential, therefore

the observed reaction rate $R = h(p_o - p) = kp^n$,
mass transfer rate = chemical reaction rate,
n = order of reaction, k = reaction rate constant.

Since R increases with temperature very quickly compared with h then $(p_o - p)$ also increases with temperature therefore $p = p_o - (p_o - p)$ decreases as the observed reaction rate increases. When the temperature is increased beyond the point of the maximum reaction rate then the effective oxygen partial pressure on the graphite surface (p) increases again from the value obtained at the maximum reaction rate.

By using estimates of the mass transfer coefficient (h) one can calculate the effective oxygen partial pressures (p) corresponding to the observed reaction rates (R) obtained for different graphite temperatures, nominal gas velocities and main gas stream oxygen partial pressures (p_o). This type of calculation provides values of R and p at temperatures of 1000°C., 1100°C., etc. to 2000°C. Graphs of (R) versus (p) at constant temperatures immediately give an indication of the order of reaction at these temperatures and show how the order of reaction changes with the value of (p). At all temperatures and values of (p) up to 0.30 atmospheres the reaction is approximately first order with respect to the oxygen partial pressure (p) but at low temperatures there is a tendency for the reaction order to

decrease as the partial pressure is increased further. This tendency to low order of reaction at low temperature and high oxygen partial pressures can be explained by supposing that a Langmuir adsorption type of process occurs, the individual steps being the attack of the oxygen on the surface followed by the desorption of the gaseous products of the reaction.

If a fraction σ of the more reactive surface is covered by the adsorbed product of the reaction and if the rate of adsorption coupled with the rate of reaction is first order with respect to the oxygen partial pressure

Rate of attack on the surface = $k_c\ p\ (1 - \sigma)$

Rate of removal of reaction products = $k_e \sigma$

At steady state

$$\sigma = \frac{k_c\ p}{k_e + k_c p}$$

At high pressure and low temperature if $(k_c p)$ is greater than (k_e) then (σ) tends to unity and is zero order.

The observed rate of reaction = $k_e \sigma$ and is therefore zero order also.

Strong adsorption of reaction products giving a zero order reaction with respect to the partial pressures of the reactant gases is a phenomenon frequently met in the field of heterogeneous catalysis.

Another use of the graphs of (R) versus (p) can be made. Values of (R) at constant values of (p) can be chosen for each temperature and thus a graph of the reaction rate for a constant partial pressure of oxygen on the graphite surface can be plotted against the graphite surface temperature. This is a plot of the effective chemical reaction rate versus temperature. The reaction rate increases sharply with temperature, reaches a maximum and then decreases quickly as the temperature rises further.

Pyrographite was reacted with oxygen under conditions in which the true velocity dependence of the reaction rate could be tested. Table 8 shows that the reaction was carried out at 0.20 atmospheres of oxygen and 1090 cms/sec. nominal gas velocity and at 0.13 atmospheres of oxygen ambient gas pressure and 7000 cms/sec. nominal gas velocity when in fact the impact pressure at the point of attack would be 0.23 atmospheres of oxygen. Comparison of the reaction rates measured under the above conditions showed that the reaction rate was independent of the gas velocity and so it may be inferred that there is no great mass transfer resistance to the reaction rate. Polycrystalline graphite reacting under the conditions of the pyrographite experiment does show some velocity

dependence and in the case of the experiment carried out at 0.13 atmospheres of oxygen ambient gas pressure and nominal gas velocity of 7000 cms/sec., the polycrystalline graphite reaction rate is about nine times greater than the pyrographite rate. For the pyrographite reaction rectangular strips of pyrographite were used and to find out if any geometrical effect caused the reaction rate to fall, rectangular bars of polycrystalline graphite were used at 0.13 atmospheres of oxygen ambient gas pressure and 7000 cms/sec nominal gas velocity and the measured reaction rates were found to be the same as the rates measured on cylindrical rods of polycrystalline graphite reacted under the same conditions.

The estimations of the mass transfer coefficients and the subsequent estimation of the true reaction rate of the polycrystalline graphite were not susceptible to direct experimental test, but even if it was assumed that the polycrystalline graphite at 0.13 atmospheres of oxygen ambient gas pressure and 7000 cms/sec. nominal gas velocity was completely mass transfer controlled then the pyrographite reaction rate measured under the same gas phase conditions could only be about 10% mass transfer controlled. There is such a great similarity in the shapes of the reaction rate

versus temperature curves for the polycrystalline graphite and pyrographite that it is reasonable to suppose that the polycrystalline graphite reaction rates at low pressures are not mass transfer controlled to a very great extent. There is sufficient chemical control of the reaction rate to make the reaction rate show many of the characteristics of a chemically controlled process. The behaviour of the rates of reaction of pyrographite contributes strong experimental evidence for the conclusion of the mass transfer estimations, that there is considerable chemical control of the polycrystalline graphite reaction rates measured at low pressures.

There is no evidence which would exclude either Eyring's theory that the maximum in the reaction rate is the result of the competition between the reaction rate increasing with temperature and the loss of a catalysing impurity as the temperature is raised or the 'surface healing theory' which suggests that the attacking gas can create surface reactive sites and that the diffusion of carbon atoms on the surface can remove reactive sites. Duval [2] however, points out that Eyring's theory can explain the maximum in the reaction rate and the hysteresis found in the low pressure experiments but that it must explain how

different authors find rates of the same order and how a filament after long treatment at high temperature finds its reserve of impurity, remembering that the impurity concentration on the surface will depend on the evaporation from the surface and the diffusion to the surface from the bulk, processes which will have different thermal coefficients. The effect of oxygen pressure on the position of the maximum rate is easier to foresee in the case of the 'surface healing theory' but it can be accounted for by Eyring's theory if the ease of evaporation of the catalysing impurity from the surface is considered. The mean free path of the evaporating atoms would be inversely proportional to the total gas pressure so that at any temperature the surface concentration of impurity would be higher at high pressures than at low pressures. Preheating the polycrystalline graphite does not affect the reaction rate at the high oxygen partial pressures whereas at low oxygen partial pressures Strickland-Constable [15] and Duval [17] have shown that a hysteresis in the reaction rate can be caused. The high pressure reaction removes much of the graphite whereas the low pressure reaction has been calculated to remove only a few atomic layers and thus it would seem that the maximum and the hysteresis in the

reaction rate versus temperature curve are the result of processes occurring in the surface layers of the graphite. Because so much fresh surface is uncovered in the high pressure reaction, the thermal history of the surface cannot influence the overall reaction rate very greatly. That the polycrystalline graphite has about 1000 times as much impurity as the pyrographite, which has only one part in ten million of impurity, and yet the general behaviour of both on oxidation is the same, is an indication that impurities may not be the source of increased activity at the lower temperatures.

This work shows that mass transfer is the rate controlling process of the oxidation of more reactive carbons at high temperatures and pressures and at low gas velocities but when pressures of the order of one tenth of an atmosphere and less reactive graphites are used a large measure of chemical control of the reaction rate is achieved. The chemical kinetics of the graphite oxidation are not typical of the behaviour shown by chemical reactions, for the reaction rate does not increase continuously with temperature but reaches a maximum and then decreases as the temperature is raised. These unusual kinetics have been found previously by Strickland-Constable [15] and Duval [17]

whose experiments were carried out at low pressures, but the temperature corresponding to the maximum rate at the high oxygen partial pressures used in this research is about 500°C. higher than the temperature of the maximum rate in the low pressure experiments.

APPENDIX 1.

EXPERIMENTAL OBSERVATIONS.

A. Reactions of Oxygen with Porous Carbon.

Table 1. Dependence of apparent mass transfer coefficients on carbon temperature and gas velocity in air.

Table 2. Dependence of the reaction rate on the oxygen partial pressure at atmospheric pressure.

Table 3. Dependence of the reaction rate on the total gas pressure.

B. Reactions of Oxygen with Polycrystalline Graphite.

Table 4. Dependence of the reaction rate on gas velocity and graphite temperature in air.

Table 5. Dependence of the reaction rate on gas velocity and graphite temperature in 50% oxygen at total gas pressure of one atmosphere.

Table 6. Dependence of the reaction rate on graphite temperature, oxygen partial pressure and total gas pressure at a nominal gas velocity of 1,090 cms./sec.

Table 7. Dependence of the reaction rate on graphite temperature, oxygen partial pressure and total gas pressure at a nominal gas velocity of 7,000 cms./sec.

C. Reactions of Oxygen with Pyrographite.

Table 8. Dependence of the reaction rate on graphite temperature at nominal gas velocities of 1,090 cms./sec. and 7,000 cms./sec. and corresponding ambient oxygen pressures of 0.20 atmospheres and 0.13 atmospheres.

A. Reaction of Oxygen with Porous Carbon.

The reaction of oxygen with porous carbon is thought to be mass transfer controlled under the present experimental conditions.

h = mass transfer coefficient referred to the amount of carbon reacted.

$$\frac{\text{gm. atoms of carbon}}{\text{cm}^2\text{, sec., atm. of oxygen}}$$

The reaction rate $R = h\, p_o$

p_o = oxygen partial pressure (ats.)

The assumption here is that the surface reaction rate is so great compared with the rate of mass transfer that the oxygen partial pressure on the surface is almost zero.

TABLE 1.

Total Gas Pressure = 1 atmosphere

Oxygen partial pressure = 0.20 ats.

$h \times 10^5$	T°C.	T°A.	$1/T°A \times 10^4$	$\log_{10}(10^5 h)$
Gas Velocity 100 cms/sec.			Log_{10} (gas vel.) 2.00	
45.6	1000	1273	7.87	1.66
43.5	970	1243	8.06	1.64
59.5	1120	1393	7.19	1.78
45.0	1170	1443	6.94	1.65
45.4	1400	1673	5.98	1.66
33.0	1320	1593	6.28	1.52
52.8	1470	1743	5.74	1.72
74.5	1550	1823	5.49	1.87
57.5	1640	1913	5.23	1.76
79.0	1650	1923	5.20	1.90
54.5	1720	1993	5.02	1.74
93.5	1720	1993	5.02	1.97
93.5	1780	2053	4.87	1.97
76.0	1620	1893	5.29	1.88
76.0	1380	1653	6.06	1.88
46.2	1280	1563	6.41	1.66
Gas velocity 250 cms./sec.			Log_{10} (gas vel.) 2.40	
218	1120	1393	7.19	2.34
238	1250	1523	6.57	2.38
182	1320	1593	6.28	2.26
207	1350	1623	6.17	2.32
203	1420	1693	5.91	2.31
177	1500	1773	5.65	2.25
177	1500	1773	5.65	2.25
164	1500	1773	5.65	2.21
252	1540	1813	5.52	2.40
244	1640	1913	5.23	2.39
218	1660	1933	5.18	2.34
248	1770	2043	4.90	2.40
131	1080	1353	7.40	2.12
142	1090	1363	7.35	2.15
136	1020	1293	7.75	2.13
131	1030	1303	7.61	2.12

Table 1 (continued)

$h \times 10^5$	T°C.	T°A.	$1/T°A \times 10^4$	$\log_{10}(10^5 h)$
Gas velocity 400 cms./sec.			$\log_{10}$ (gas vel.)	2.60
187	1290	1563	6.41	2.27
229	1330	1603	6.25	2.36
229	1480	1753	5.71	2.36
187	1590	1863	5.37	2.27
228	1560	1833	5.46	2.36
222	1600	1873	5.34	2.35
228	1620	1893	5.29	2.36
222	1670	1943	5.15	2.35
195	1800	2073	4.83	2.29
214	1700	1973	5.07	2.33
216	1680	1953	5.12	2.34
180	1210	1483	6.75	2.26
180	1160	1453	6.89	2.26
144	1120	1393	7.19	2.16
166	1040	1313	7.63	2.22
148	1050	1323	7.57	2.17
Gas velocity 560 cms./sec.			$\log_{10}$ (gas vel.)	2.75
214	1050	1323	7.57	2.33
201	1060	1333	7.51	2.30
209	1150	1423	7.04	2.32
228	1160	1433	6.99	2.36
236	1250	1523	6.57	2.37
217	1230	1503	6.66	2.34
240	1420	1693	5.91	2.38
210	1480	1753	5.71	2.32
228	1480	1753	5.71	2.32
221	1500	1773	5.65	2.34
289	1560	1833	5.46	2.46
281	1600	1873	5.34	2.45
252	1660	1933	5.18	2.40
252	1680	1953	5.12	2.40
222	1780	2053	4.87	2.34
256	1740	2013	4.97	2.41
Gas velocity 800 cms./sec.			$\log_{10}$ (gas vel.)	2.90
277	1150	1423	7.04	2.44
252	1150	1423	7.04	2.40
221	1080	1353	7.40	2.34
238	1070	1343	7.46	2.38
266	1200	1473	6.80	2.43
238	1240	1513	6.62	2.38
282	1270	1543	6.49	2.45
266	1210	1483	6.75	2.43
282	1400	1673	5.98	2.45

$h \times 10^5$	T°C.	T°A.	$1/T°A \times 10^4$	$\log_{10}(10^5 h)$
284	1410	1683	5.95	2.45
258	1450	1723	5.81	2.41
302	1590	1863	5.37	2.48
312	1560	1833	5.46	2.49
332	1600	1873	5.34	2.52
292	1770	2043	4.90	2.47
277	1770	2043	4.90	2.44
Gas velocity 970 cms./sec.			$\log_{10}$ (gas vel.)	2.99
348	1750	2023	4.95	2.54
285	1770	2043	4.90	2.45
276	1800	2073	4.83	2.44
308	1670	1943	5.15	2.49
277	1600	1873	5.34	2.44
302	1560	1833	5.46	2.48
319	1500	1773	5.65	2.50
250	1500	1773	5.65	2.40
236	1400	1673	5.98	2.37
265	1420	1593	6.28	2.42
305	1320	1593	6.28	2.48
304	1300	1573	6.36	2.48
242	1220	1493	6.71	2.38
277	1200	1473	6.80	2.44
238	1100	1373	7.29	2.38
222	1100	1373	7.29	2.44
Gas velocity 2,000 cms./sec.			$\log_{10}$(gas vel.)	3.30
514	1760	2033	4.92	2.71
485	1800	2073	4.83	2.69
485	1660	1933	5.18	2.69
520	1620	1893	5.29	2.72
542	1600	1873	5.34	2.73
499	1420	1693	5.91	2.70
525	1530	1803	5.55	2.72
494	1500	1773	5.65	2.69
418	1400	1673	5.98	2.62
418	1400	1673	5.98	2.62
444	1300	1573	6.36	2.65
434	1220	1493	6.71	2.64
347	1170	1443	6.94	2.54
356	1150	1423	7.04	2.55
285	1140	1413	7.09	2.46
293	1100	1373	7.29	2.47

$h \times 10^5$	T°C.	T°A.	$1/T°A \times 10^4$	$\log_{10}(10^5 h)$
Gas velocity 1280 cms./sec.			$\log_{10}$ (gas vel.)	3.11
222	1060	1333	7.51	2.34
238	1070	1343	7.46	2.38
289	1230	1503	6.66	2.46
265	1120	1393	7.19	2.42
320	1220	1493	6.71	2.51
320	1250	1529	6.57	2.51
319	1230	1503	6.66	2.50
270	1290	1563	6.41	2.43
320	1400	1673	5.98	2.51
346	1440	1713	5.84	2.54
370	1560	1833	5.46	2.57
370	1430	1703	5.88	2.57
420	1640	1913	5.23	2.62
344	1710	1983	5.05	2.54
370	1680	1953	5.12	2.57
370	1770	2043	4.90	2.57
Gas velocity 2630 cms./sec.			$\log_{10}$ (gas vel.)	3.42
296	1160	1433	6.99	2.47
332	1210	1483	6.75	2.51
332	1200	1473	6.80	2.51
400	1240	1513	6.62	2.60
410	1250	1523	6.57	2.61
426	1320	1593	6.28	2.63
400	1320	1593	6.28	2.60
395	1320	1593	6.28	2.60
353	1300	1573	6.36	2.55
539	1540	1813	5.52	2.73
532	1550	1823	5.49	2.73
514	1670	1943	5.15	2.71
532	1620	1893	5.29	2.73
532	1740	2013	4.97	2.73
521	1800	2073	4.83	2.72
512	1780	2053	4.87	2.71
Gas velocity 3900 cms./sec.			$\log_{10}$ (gas vel.)	3.59
555	1620	1893	5.29	2.74
566	1800	2073	4.83	2.75
531	1740	2073	4.97	2.73
566	1620	1893	5.29	2.75
566	1600	1873	5.34	2.75
538	1520	1793	5.58	2.73
500	1600	1873	5.34	2.70

$h \times 10^5$	T°C.	T°A.	$1/T°A \times 10^4$	$\log_{10}(10^5 h)$
526	1490	1763	5.68	2.72
537	1550	1823	5.49	2.73
515	1410	1683	5.95	2.71
565	1460	1733	5.78	2.75
475	1360	1663	6.13	2.68
452	1360	1633	6.13	2.66
454	1300	1573	6.36	2.66
370	1210	1483	6.75	2.57
399	1190	1463	6.84	2.60
Gas velocity	5500 cms/sec.		$\log_{10}$ (gas vel.)	3.86
404	1250	1523	6.57	2.61
434	1250	1523	6.57	2.64
475	1300	1573	6.36	2.68
549	1430	1703	5.88	2.74
520	1420	1693	5.91	2.72
560	1460	1733	5.78	2.75
545	1520	1793	5.58	2.74
526	1560	1833	5.46	2.72
604	1640	1913	5.23	2.78
544	1620	1893	5.29	2.74
600	1600	1873	5.34	2.78
600	1670	1943	5.15	2.78
574	1740	2013	4.97	2.76
635	1720	1993	5.02	2.80
599	1800	2073	4.83	2.78
604	1740	2013	4.97	2.78
Gas velocity	7300 cms/sec.		$\log_{10}$ (gas vel.)	3.86
579	1680	1953	5.12	2.76
604	1740	2013	4.97	2.78
635	1720	1993	5.02	2.80
635	1670	1943	5.15	2.80
604	1550	1823	5.49	2.78
634	1520	1793	5.58	2.80
635	1540	1813	5.52	2.80
605	1450	1723	5.81	2.78
520	1420	1693	5.91	2.72
621	1450	1723	5.81	2.79
492	1280	1553	6.45	2.69
631	1380	1653	6.04	2.80
512	1340	1613	6.21	2.64
434	1340	1613	6.21	2.64
631	1510	1783	5.61	2.80
665	1440	1713	5.84	2.82

$h \times 10^5$	T°C.	T°A.	$1/T°A \times 10^4$	$\log_{10}(10^5 h)$
Gas velocity 9400 cms/sec.			$\log_{10}$ (gas vel.)	3.97
610	1700	1973	5.07	2.79
665	1770	2043	4.90	2.82
614	1800	2073	4.83	2.79
665	1670	1943	5.15	2.82
665	1700	1973	5.07	2.82
665	1600	1873	5.34	2.82
700	1550	1823	5.49	2.85
700	1490	1763	5.68	2.85
739	1540	1813	5.52	2.87
602	1490	1763	5.68	2.78
633	1500	1773	5.65	2.80
665	1650	1923	5.20	2.82
781	1590	1863	5.37	2.89
740	1720	1993	5.02	2.87
776	1740	2013	4.97	2.90
740	1770	2043	4.90	2.87
830	1620	1893	5.29	2.92
782	1620	1893	5.29	2.89

TABLE 2.

R = reaction rate $\frac{\text{gm. atoms of carbon}}{\text{cm}^2\text{, sec.}}$

Total gas pressure = 1 atmosphere.

$R \times 10^5$	T°C.	T°A.	$1/T°A \times 10^4$	$\log_{10}(10^5 R)$
54.5	1110	1383	7.24	1.74
67.0	1150	1423	7.04	1.83
61.0	1080	1353	7.40	1.79
41.0	1220	1493	6.71	1.62
41.0	1300	1573	6.36	1.62
45.0	1430	1703	5.88	1.65
55.0	1430	1703	5.88	1.74
43.0	1450	1723	5.81	1.63
70.0	1580	1853	5.40	1.85
69.2	1490	1753	5.71	1.84
52.8	1630	1923	5.20	1.72
72.5	1400	1673	5.98	1.86
61.0	1770	2043	4.90	1.79
65.2	1800	2073	4.83	1.81
54.0	1740	2013	4.97	1.73
67.0	1740	2013	4.97	1.83
Gas velocity 200 cms/sec.			$\log_{10}$ (gas vel.)	2.30
Oxygen partial pressure = 0.50 ats.			$\log_{10}(10p)$	0.70

$R \times 10^5$	T°C.	T°A.	$1/T°A \times 10^4$	$\log_{10}(10^5 R)$
Gas velocity 800 cms./sec.			$\log_{10}$(gas vel.)	2.90
Oxygen partial pressure = 0.50 ats.			$\log_{10}$ (10p)	= 0.70
123	1800	2073	4.83	2.09
139	1800	2073	4.83	2.14
143	1760	2033	4.92	2.16
169	1770	2043	4.90	2.23
139	1600	1873	5.34	2.14
117	1460	1733	5.78	2.05
152	1600	1873	5.34	2.18
127	1500	1773	5.65	2.10
109	1370	1643	6.09	2.04
119	1400	1673	5.98	2.08
152	1730	2003	5.00	2.18
169	1760	2033	4.92	2.23
Gas velocity 450 cms/sec.			$\log_{10}$ (gas vel.)	2.65
Oxygen partial pressure = 0.50 ats.			$\log_{10}$ (10p)	0.70
84.5	1400	1673	5.98	1.93
101	1340	1613	6.21	2.00
118	1450	1723	5.81	2.07
109	1500	1773	5.65	2.04
118	1460	1733	5.78	2.07
101	1570	1843	5.43	2.00
130	1640	1913	5.23	2.11
114	1650	1923	5.20	2.06
117	1740	2013	4.97	2.07
127	1760	2033	4.92	2.10
127	1640	1913	5.23	2.10
109	1470	1743	5.74	2.04
Gas velocity 1050 cms/sec.			$\log_{10}$ (gas vel.)	3.02
Oxygen partial pressure = 0.50 ats.			$\log_{10}$ (10p)	= 0.70
106	1370	1643	6.09	2.03
152	1470	1743	5.74	2.18
171	1530	1803	5.55	2.18
137	1490	1763	5.68	2.14
169	1550	1823	5.49	2.23
152	1570	1843	5.43	2.18
152	1650	1923	5.20	2.18
152	1720	1993	5.02	2.18
171	1780	2053	4.87	2.23
166	1800	2073	4.83	2.22
114	1370	1643	6.09	2.06
166	1600	1873	5.34	2.22

$R \times 10^5$	T°C.	T°A.	$1/T°A \times 10^4$	$\log_{10}(10^5 R)$
Gas velocity 100 cms/sec.		$\log_{10}$ (gas vel.)	2.00	
Oxygen partial pressure 0.50 ats.		$\log_{10}$ (10p)	0.70	
22.8	1290	1563	6.41	1.36
33.0	1350	1623	6.17	1.52
38.0	1280	1553	6.45	1.58
29.2	1200	1473	6.80	1.47
34.5	1580	1853	5.40	1.54
24.5	1520	1793	5.58	1.39
42.2	1620	1893	5.29	1.63
29.2	1650	1923	5.20	1.47
31.7	1720	1993	5.02	1.50
24.3	1570	1843	5.43	1.38
33.2	1720	1993	5.02	1.52
26.8	1740	2013	4.97	1.42
Gas velocity 100 cms/sec.		$\log_{10}$ (gas vel.)	2.00	
Oxygen partial pressure = 0.20 ats.		$\log_{10}$ (10p)	.0.30	
9.14	1000	1273	7.87	0.96
8.7	970	1243	8.06	0.94
11.9	1120	1393	7.19	1.08
9.0	1170	1443	6.94	0.95
9.1	1400	1673	5.98	0.96
6.6	1320	1593	6.28	0.82
10.5	1470	1743	5.74	1.02
14.9	1550	1823	5.49	1.17
11.5	1640	1913	5.23	1.06
15.8	1650	1923	5.20	1.20
10.9	1720	1993	5.02	1.04
18.7	1720	1993	5.02	1.27
18.7	1780	2053	4.87	1.27
15.2	1620	1893	5.29	1.18
15.2	1380	1653	6.06	1.18
9.25	1280	1563	6.41	0.97
Gas velocity 250 cms/sec.		$\log_{10}$ (gas vel.)	2.40	
Oxygen partial pressure 0.20 ats.		$\log_{10}$ (10p)	0.30	
43.6	1120	1393	7.19	1.64
47.6	1250	1523	6.57	1.68
36.5	1320	1593	6.28	1.56
41.4	1350	1623	6.17	1.62
40.5	1420	1693	5.91	1.61
35.4	1500	1773	5.65	1.55
35.4	1500	1773	5.65	1.55

$R \times 10^5$	T°C.	T°A.	$1/T°A \times 10^4$	$\log_{10}(10^5 R)$
32.8	1500	1773	5.65	1.52
50.4	1540	1813	5.52	1.70
48.9	1640	1913	5.23	1.69
43.5	1660	1933	5.18	1.64
49.6	1770	2043	4.90	1.70
26.2	1080	1353	7.40	1.42
28.4	1090	1363	7.35	1.45
27.2	1020	1293	7.75	1.43
26.2	1030	1303	7.69	1.42
Gas velocity 560 cms/sec.			$\log_{10}$ (gas vel.)	2.75
Oxygen partial pressure 0.20 ats.			$\log_{10}$ (10p)	0.30
42.9	1050	1323	7.57	1.63
40.2	1060	1333	7.51	1.61
41.8	1150	1423	7.04	1.62
45.6	1160	1433	6.99	1.66
47.2	1250	1523	6.57	1.67
43.5	1230	1503	6.66	1.64
48	1420	1693	5.91	1.68
42	1480	1753	5.71	1.62
45.6	1480	1753	5.71	1.66
44.1	1500	1773	5.65	1.64
57.8	1560	1833	5.46	1.76
56.2	1600	1873	5.34	1.73
50.5	1660	1933	5.18	1.70
50.5	1680	1953	5.12	1.70
44.5	1780	2053	4.87	1.65
51.2	1740	2013	4.97	1.71
Gas velocity 1280 cms/sec.			$\log_{10}$ (gas vel.)	3.11
Oxygen partial pressure 0.20 ats.			$\log_{10}$ (10p)	0.30
44.5	1060	1333	7.51	1.65
47.6	1070	1343	7.46	1.68
57.9	1230	1503	6.66	1.76
53.0	1120	1393	7.19	1.72
64	1220	1493	6.71	1.81
64	1250	1523	6.57	1.81
63.9	1230	1503	6.66	1.81
54.0	1290	1563	6.41	1.73
64	1400	1673	5.98	1.81
69.2	1440	1713	5.84	1.84
74	1560	1833	5.46	1.87
74	1430	1703	5.88	1.87
84	1640	1913	5.23	1.92
69	1710	1983	5.05	1.84
74	1680	1953	5.12	1.87
74	1770	2043	4.90	1.87

TABLE 3.

Nominal Gas Velocity 250 cms/sec. Log_{10} (gas vel.) 2.40.
Total gas pressure = 0.31 ats. Log_{10} (10P) 0.49
Partial oxygen pressure = 0.062 ats. Log_{10} (100p) 0.79

R x 10^5	T°C.	T°A.	1/T°A x10^4	$log_{10}(10^5R)$
33	1570	1843	5.43	1.52
36	1800	2073	4.83	1.56
35	1740	2013	4.97	1.54
35	1600	1873	5.34	1.54
38	1720	1993	5.02	1.58
29	1350	1623	6.17	1.46
29.5	1540	1813	5.52	1.47
25	1280	1553	6.45	1.40
25.4	1300	1573	6.36	1.41
35	1440	1713	5.84	1.54
26.2	1550	1823	5.49	1.42
25.2	1650	1923	5.20	1.40

Nominal gas velocity 100 cms/sec. Log_{10} (gas vel.) 2.00
Total gas pressure = 0.31 ats. Log_{10} (10P) 0.49
Partial gas pressure = 0.062 ats. Log_{10} (100p) 0.79

15.6	1720	1993	5.02	1.19
13.5	1750	2023	4.95	1.13
17.2	1620	1893	5.29	1.24
12.4	1630	1903	5.26	1.09
13.8	1690	1963	5.10	1.14
14.1	1440	1713	5.84	1.15
12.4	1570	1843	5.43	1.09
10.0	1420	1693	5.91	1.00
10.6	1340	1613	6.21	1.03
10.3	1250	1523	6.57	1.01
15.2	1650	1923	5.20	1.18
13.8	1640	1913	5.23	1.14

Nominal gas velocity 560 cms/sec. Log_{10} (gas vel.) 2.75
Total gas pressure 0.31 ats. Log_{10} (10P) 0.49
Partial oxygen pressure 0.062 ats. Log_{10} (100p) 0.79

32.8	1340	1613	6.21	1.52
42	1440	1713	5.84	1.62
38	1380	1653	6.06	1.58
36.7	1490	1763	5.68	1.56
32.5	1360	1633	6.13	1.51

$R \times 10^5$	T°C.	T°A.	$1/T°A \times 10^4$	$\log_{10}(10^5 R)$
39.0	1360	1633	6.13	1.59
39.4	1590	1863	5.37	1.60
40.2	1730	2003	5.00	1.60
41.5	1720	1993	5.02	1.62
45.6	1700	1973	5.07	1.66
35.2	1320	1593	6.28	1.55
43.5	1600	1873	5.34	1.64

Nominal gas velocity 840 cms/sec. $\log_{10}$ (gas vel.) 2.92

Total gas pressure 0.31 ats. $\log_{10}$ (10P) 0.49

Partial oxygen pressure 0.062 ats. $\log_{10}$ (100p) 0.79

31.6	1300	1573	6.36	1.50
35.4	1300	1573	6.36	1.55
45.2	1360	1633	6.13	1.66
49.0	1400	1673	5.98	1.69
43.5	1450	1723	5.81	1.64
54.1	1500	1773	5.65	1.73
50.5	1660	1933	5.18	1.70
49.0	1580	1853	5.40	1.69
49.0	1660	1933	5.18	1.69
52.5	1740	2013	4.97	1.72
50.5	1700	1973	5.07	1.70
50.5	1750	2023	4.93	1.70

Nominal gas velocity 1150 cms/sec. $\log_{10}$ (gas vel.) 3.06

Total gas pressure 0.32 ats. $\log_{10}$ (10P) 0.51

Partial gas pressure 0.064 ats. $\log_{10}$ (100p) 0.81

49.0	1360	1633	6.13	1.69
60.8	1400	1673	5.98	1.78
60.8	1440	1713	5.84	1.78
47.5	1350	1623	6.17	1.68
63.2	1630	1903	5.26	1.80
57.8	1570	1843	5.43	1.76
60.8	1550	1823	5.49	1.78
61.8	1690	1963	5.10	1.79
62.5	1620	1893	5.29	1.80
64.5	1640	1913	5.23	1.81
61.8	1730	2003	5.00	1.79
67.5	1800	2073	4.83	1.83

$R \times 10^5$	T°C.	T°A.	$1/T°A \times 10^4$	$\log_{10}(10^5 R)$
Nominal gas velocity 1200 cms/sec. $\log_{10}$ (gas vel.) 3.08				
Total gas pressure = 1 at. $\log_{10}$ (10P) = 1				
Partial oxygen pressure = 0.20 ats. $\log_{10}$ (100p) = 1.3				
84	1460	1733	5.98	1.92
64	1220	1493	6.71	1.81
71.2	1260	1533	6.53	1.85
70.5	1150	1423	7.04	1.85
62.5	1170	1443	6.94	1.80
55.0	1120	1393	7.19	1.74
70	1390	1663	6.02	1.85
88.8	1470	1743	5.74	1.95
86	1520	1793	5.58	1.93
86.4	1750	2023	4.95	1.94
85	1740	2013	4.97	1.93
88.8	1680	1953	5.12	1.95
Nominal gas velocity 780 cms/sec $\log_{10}$ (gas vel.) 2.89				
Total gas pressure = 1 at. $\log_{10}$ (10P) = 1				
Partial oxygen pressure = 0.20 ats. $\log_{10}$ (100p) 1.3				
69.4	1760	2033	4.92	1.84
76	1760	2033	4.92	1.88
66.4	1600	1873	5.34	1.82
69.4	1440	1713	5.84	1.84
72.4	1730	2033	5.00	1.86
69.8	1490	1763	5.68	1.84
70	1740	2013	4.97	1.85
64	1600	1873	5.34	1.81
55.4	1270	1543	6.49	1.74
47.4	1160	1433	6.99	1.68
55	1190	1463	6.84	1.74
55	1200	1473	6.80	1.74
Nominal gas velocity 410 cms/sec. $\log_{10}$ (gas vel.) 2.61				
Total gas pressure = 1 at. $\log_{10}$ (10P) = 1				
Partial oxygen pressure = 0.20 ats. $\log_{10}$ (100p) = 1.3				
40.4	1240	1513	6.62	1.61
40.4	1150	1423	7.04	1.61
40.4	1150	1423	7.04	1.61
46.4	1240	1513	6.62	1.67
41.6	1460	1733	5.78	1.62
46.4	1370	1643	6.09	1.67
59.2	1580	1853	5.40	1.77
53.2	1600	1873	5.34	1.73
56	1600	1873	5.34	1.71

$R \times 10^5$	T°C.	T°A.	$1/T°A \times 10^4$	$\log_{10}(10^5 R)$
51.2	1660	1933	5.18	1.71
49	1700	1973	5.07	1.69
56	1800	2073	4.83	1.75

Nominal gas velocity 250 cms/sec. $\log_{10}$ (gas vel.) 2.40

Total gas pressure 1 at. $\log_{10}$ (10P) = 1

Partial oxygen pressure 0.20 ats. $\log_{10}(100p)$ 1.3

46.4	1740	2013	4.97	1.67
38.8	1730	2003	5.00	1.59
42.2	1500	1773	5.65	1.63
40	1560	1833	5.46	1.60
40.6	1600	1873	5.34	1.61
40.6	1460	1733	5.78	1.61
34.4	1400	1673	5.98	1.54
34.4	1350	1623	6.17	1.54
31	1100	1373	7.29	1.49
29.6	1270	1543	6.49	1.47
31.8	1170	1443	6.94	1.50
30.2	1110	1383	7.24	1.48

Nominal gas velocity 150 cms/sec. $\log_{10}$ (gas vel.) 2.18

Total gas pressure = 1 at. $\log_{10}$ (10P) = 1

Partial oxygen pressure 0.20 ats. $\log_{10}(100p)$ 1.3

16.6	1300	1573	6.36	1.22
13.3	1300	1573	6.36	1.12
19.5	1420	1693	5.91	1.29
26.6	1400	1673	5.98	1.42
20.2	1580	1853	5.40	1.31
18.1	1490	1763	5.68	1.26
21.2	1560	1833	5.46	1.33
25.6	1700	1973	5.07	1.41
22.2	1750	2023	4.95	1.35
17	1060	1333	7.51	1.23
19	1070	2033	4.95	1.35
22.8	1770	2043	4.90	1.36

B. Reactions of oxygen with polycrystalline graphite.

The reaction of oxygen with the polycrystalline graphite is chemically controlled to a degree dependent on the reaction conditions e.g. temperature and total gas pressure. Because of the existence of mixed regimes no apparent mass transfer coefficients or chemical reaction rate constants have been calculated.

TABLE 4.

Total gas pressure = 1 atmosphere.
Partial oxygen pressure = 0.20 ats.

$R \times 10^5$	T°C.	T°A	$1/T°A \times 10^4$	$\log_{10}(10^5 R)$
Gas Velocity	100 cms/sec.			
2.66	900	1173	8.54	0.43
4.56	1050	1323	7.57	0.66
6.71	1070	1343	7.46	0.83
17.0	1110	1383	7.24	1.23
24.4	1390	1663	6.02	1.39
7.86	1340	1613	6.21	0.90
9.5	1330	1603	6.25	0.98
13.0	1350	1623	6.17	1.11
23.0	1520	1793	5.58	1.36
11.5	1580	1853	5.40	1.06
12.2	1520	1793	5.58	1.07
9.75	1460	1733	5.78	0.99
19.5	1620	1893	5.29	1.29
13.8	1650	1923	5.20	1.14
13.7	1720	1993	5.02	1.14
13.0	1800	2073	4.83	1.11
9.75	1270	1543	6.49	0.99
11.9	1220	1493	6.71	1.08
5.45	1170	1443	6.94	0.74
10.4	1200	1473	6.80	1.02
3.9	1010	1283	7.81	0.59
2.13	980	1253	8.00	0.33

$R \times 10^5$	T°C.	T°A	$1/T°A \times 10^4$	$\log_{10}(10^5 R)$
6.0	1080	1353	7.40	0.78
4.87	1120	1393	7.19	0.69
11.2	1130	1403	7.14	1.05
9.0	1200	1473	6.80	0.95
6.24	1120	1393	7.19	0.80
10.4	1120	1393	7.19	1.02
9.0	1160	1433	6.99	0.95
12.1	1150	1423	7.04	1.09
Gas velocity	250 cms/sec.			
21.6	1300	1573	6.37	1.33
25.0	1300	1573	6.37	1.40
24.4	1300	1573	6.37	1.39
18.9	1150	1423	7.04	1.28
3.12	1000	1273	7.87	0.49
15.3	1140	1413	7.09	1.18
2.58	900	1173	8.55	0.41
16.6	1220	1493	6.71	1.22
1.74	920	1193	8.38	0.24
17.9	1100	1373	7.28	1.25
6.30	1040	1313	7.60	0.80
21.7	1300	1573	6.37	1.34
37.0	1700	1973	5.04	1.57
26.0	1450	1723	5.81	1.42
27.2	1380	1653	6.06	1.43
25.0	1300	1573	6.37	1.40
24.6	1300	1573	6.37	1.39
39.0	1400	1673	6.00	1.52
34.4	1420	1693	5.92	1.60
25.2	1320	1593	6.25	1.46
35.0	1600	1873	5.35	1.61
20.5	1150	1423	7.04	1.31
14.6	1160	1433	6.99	1.16
16.7	1180	1453	6.89	1.22
1.19	930	1203	8.33	0.08
22.1	1280	1553	6.45	1.34
21.6	1230	1503	6.66	1.33
7.1	1070	1343	7.46	0.85
17.2	1270	1543	6.49	1.24
19.5	1260	1533	6.53	1.29

$R \times 10^5$	T°C.	T°A.	$1/T°A \times 10^4$	$\log_{10}(10^5 R)$
Gas velocity 1,090 cms/sec.				
26.4	1300	1573	6.37	1.42
21.9	1280	1553	6.45	1.34
2.56	1060	1333	7.52	0.41
2.26	1010	1283	7.81	0.35
34.8	1260	1533	6.54	1.54
1.50	980	1253	8.00	0.18
32.6	1240	1513	6.62	1.51
11.0	1100	1383	7.24	1.04
6.5	1040	1313	7.63	0.81
43	1500	1773	5.65	1.63
10.4	1080	1353	7.40	1.02
9.75	1090	1363	7.35	0.99
16.2	1100	1373	7.29	1.21
28	1230	1503	6.66	1.45
36.6	1320	1593	6.28	1.56
55.6	1470	1743	5.74	1.75
67	1700	1973	5.07	1.83
39	1900	2173	4.60	1.59
51	1870	2143	4.67	1.71
58.5	1910	2183	4.58	1.77
49	1980	2253	4.44	1.69
65	1850	2123	4.71	1.81
56	1850	2123	4.71	1.75
49	1950	2123	4.50	1.69
65	1850	2123	4.71	1.81
65	1950	2223	4.50	1.81
69.5	1860	2133	4.69	1.84
65	1930	2203	4.54	1.81
73	1840	2113	4.73	1.86
58.5	1640	1913	5.23	1.77
43	1530	1803	5.55	1.63
43	1570	1843	5.43	1.63
56	1690	1963	5.10	1.75
49	1800	2073	4.83	1.69
33.5	1520	1793	5.58	1.53
18.8	1260	1533	6.53	1.27
28.3	1280	1553	6.45	1.45
21	1200	1473	6.80	1.32
15	1200	1473	6.80	1.18
33.2	1380	1653	6.06	1.52
33.4	1400	1673	5.98	1.52
34.0	1370	1643	6.09	1.53
34.4	1380	1653	6.06	1.54

$R \times 10^5$	T°C.	T°A	$1/T°A \times 10^4$	$\log_{10}(10^5 R)$
65	1700	1973	5.07	1.81
70.5	1750	2023	4.95	1.85
71.5	1670	1943	5.16	1.85
42.5	1520	1793	5.59	1.63
42.5	1520	1793	5.59	1.63
34.2	1550	1823	5.50	1.53
67.1	1680	1953	5.16	1.83
54.6	1600	1873	5.35	1.74
44.6	1520	1793	5.59	1.65
30	1400	1673	5.99	1.48
49.5	1550	1823	5.50	1.69
Gas velocity 7,000 cms/sec.				
2.3	900	1173	8.54	0.36
34	1280	1553	6.45	1.53
39.8	1300	1573	6.37	1.60
27.6	1250	1523	6.60	1.44
25.6	1300	1573	6.40	1.41
5.22	1050	1323	7.58	0.72
3.48	1030	1303	7.68	0.54
1.88	900	1173	8.55	0.27
2.61	1000	1273	7.87	0.42
22.3	1300	1573	6.37	1.35
4.85	1000	1273	7.87	0.69
2.34	900	1173	8.54	0.37
1.76	960	1233	8.13	0.25
48.7	1300	1573	6.36	1.69
31.6	1200	1473	6.80	1.50
25.8	1150	1423	7.04	1.41
47.1	1430	1703	5.88	1.67
43.5	1400	1673	5.98	1.64
58.5	1480	1753	5.71	1.77
69.6	1620	1893	5.29	1.84
104	1740	2013	4.97	2.02
80	1630	1903	5.26	1.90
87.1	1700	1973	5.04	1.94
38	1450	1723	5.81	1.58
43.6	1450	1723	5.81	1.64
42	1500	1773	5.65	1.62
78.1	1600	1873	5.35	1.89
53	1480	1753	5.71	1.72
106	1920	2193	4.56	2.03
159	1840	2113	4.73	2.20
130	1910	2183	4.58	2.11
102	1880	2153	4.65	2.01
94	1920	2193	4.56	1.97

$R \times 10^5$	T°C.	T°A.	$1/T°A \times 10^4$	$\log_{10}(10^5 R)$
106	1830	2103	4.76	2.03
109	1870	2143	4.67	2.04
84	1910	2183	4.58	1.92
122	1830	2103	4.76	2.09
106	1980	2253	4.44	2.03
98	1910	2183	4.58	1.99
117	1870	2143	4.67	2.07
30.2	1270	1523	6.57	1.48
29.2	1230	1503	6.66	1.47
63.5	1480	1753	5.71	1.80
35	1340	1613	6.21	1.54
40	1370	1643	6.09	1.60
100	1720	1993	5.02	2.00
43	1440	1713	5.84	1.63
90	1800	2073	4.83	1.95
97.5	1750	2023	4.95	1.99
58.5	1640	1913	5.23	1.77
135	1800	2073	4.83	2.13
135	1780	2053	4.87	2.10
125	1800	2073	4.83	2.10

TABLE 5.

Total gas pressure = 1 atm. Partial oxygen pressure =0.50

$R \times 10^5$	T°C	T°A	$1/T°A \times 10^4$	$\log_{10}(10^5 R)$
26.6	1230	1503	6.66	1.43
23.4	1080	1353	7.40	1.37
1.6	950	1223	8.19	0.19
16.0	1060	1333	7.51	1.20
16.2	1120	1393	7.19	1.21
14.6	1150	1423	7.04	1.16
13.9	1100	1373	7.29	1.14
38.3	1450	1723	5.81	1.58
39.0	1400	1673	5.98	1.59
53	1510	1783	5.61	1.72
34	1560	1833	5.46	1.53
30	1700	1973	5.07	1.48
49	1720	1993	5.02	1.69
42	1760	2033	4.92	1.62
50	1750	2023	4.95	1.70
16.7	1080	1353	7.40	1.22
4.9	990	1263	7.93	0.69

Gas velocity 100 cms/sec.

$R \times 10^5$	T°C.	T°A.	$1/T°A \times 10^4$	$\log_{10}(10^5 R)$
10.6	1020	1293	7.75	1.03
14	1070	1343	7.46	1.15
41.6	1430	1703	5.88	1.62
49	1440	1713	5.84	1.69
9.2	1050	1323	7.57	0.96
24.4	1200	1473	6.80	1.39
24.4	1240	1513	6.62	1.39
24.4	1230	1503	6.66	1.39
27.0	1270	1543	6.49	1.43
36.5	1350	1623	6.17	1.56
29.2	1350	1623	6.17	1.47
29.2	1650	1923	5.20	1.47
26.6	1740	2013	4.97	1.43
Gas Velocity 250 cms/sec.				
97.5	1600	1873	5.34	1.99
107	1770	2043	4.90	2.03
68.0	1560	1833	5.46	1.83
97.5	1620	1893	5.29	1.99
73.1	1560	1833	5.46	1.86
97.5	1630	1903	5.36	1.99
41.8	1130	1403	7.14	1.62
33.2	1170	1443	6.94	1.52
33.4	1170	1443	6.94	1.52
17.6	1060	1333	7.51	1.25
24.5	1120	1393	7.19	1.39
33.4	1140	1413	7.09	1.52
0.9	870	1143	8.77	$\bar{1}$.95
14.6	1030	1303	7.69	1.16
26	1120	1393	7.19	1.42
19.5	1030	1303	7.19	1.29
18.3	1050	1323	7.57	1.26
71.5	1480	1713	5.84	1.85
84	1620	1893	5.29	1.92
54	1270	1543	6.49	1.73
84	1560	1833	5.46	1.92
32.6	1290	1563	6.41	1.51
65.2	1360	1633	6.13	1.81
58.5	1440	1713	5.84	1.77
36.0	1350	1623	6.17	1.57
61.5	1400	1673	5.98	1.79
30	1280	1553	6.45	1.48
40.5	1200	1473	6.80	1.61
52.5	1300	1573	6.36	1.72
75.1	1460	1733	5.78	1.88

$R \times 10^5$	T°C.	T°A.	$1/T°A \times 10^4$	$\log_{10}(10^5 R)$
Gas Velocity 1,090 cms/sec.				
44	1200	1473	6.80	1.64
168	1720	1993	5.02	2.23
143	1740	2013	4.97	2.14
130	1650	1923	5.20	2.11
130	1620	1893	5.29	2.11
130	1750	2023	4.95	2.11
102	1420	1693	5.91	2.01
146	1620	1893	5.29	2.16
117	1370	1643	6.09	2.07
97.5	1440	1713	5.84	1.99
97.5	1390	1663	6.09	1.99
80	1370	1643	6.09	2.07
65	1240	1513	6.62	1.81
83.5	1320	1593	6.28	1.92
73	1300	1573	6.36	1.86
65	1260	1533	6.53	1.81
65	1220	1493	6.71	1.81
83.5	1250	1523	6.57	1.92
15.6	1030	1303	7.69	1.19
25.1	1060	1333	7.51	1.40
78	1260	1533	6.53	1.89
29.2	1110	1383	7.24	1.47
48.7	1160	1433	6.99	1.69
16.4	1020	1293	7.75	1.21
30.8	1100	1373	7.29	1.49
63.5	1220	1493	6.71	1.80
27.8	1080	1353	7.40	1.44
44	1170	1443	6.94	1.64
23.4	1040	1313	7.63	1.34
80	1250	1523	6.57	1.90
Gas Velocity 7,000 cms/sec.				
39	1100	1373	7.29	1.59
50	1160	1433	6.99	1.70
68.4	1180	1453	6.89	1.84
180	1720	1993	5.02	2.26
146	1600	1873	5.34	2.16
207	1770	2043	4.90	2.32
161	1600	1873	5.34	2.21
88	1330	1603	6.25	1.94
75.5	1300	1573	6.36	1.88
123	1600	1873	5.34	2.09
159	1580	1853	5.40	2.20
69.6	1300	1573	6.36	1.84

$R \times 10^5$	T°C.	T°A.	$1/T°A \times 10^4$	$\log_{10}(10^5 R)$
122	1550	1823	5.49	2.09
97.5	1380	1653	6.06	1.99
132	1490	1763	5.68	2.12
76	1310	1583	6.32	1.88
97.5	1260	1533	6.53	1.99
73	1200	1473	6.80	1.86
51	1230	1503	6.66	1.71
19.5	1070	1343	7.46	1.29
88	1300	1573	6.36	1.94
133	1440	1713	5.84	2.12
117	1440	1713	5.84	2.07
209	1580	1853	5.40	2.30
146	1500	1773	5.65	2.16
128	1370	1643	6.09	2.11
167	1470	1743	5.74	2.22
195	1660	1933	5.18	2.29
154	1550	1823	5.49	2.19
110	1370	1643	6.09	2.04

TABLE 6.

Nominal Gas Velocity 1,090 cms/sec.

$R \times 10^5$	T°C.	T°A.	$1/T°A \times 10^4$	$\log_{10}(10^5 R)$
No preheating of graphite. Total gas pressure = 0.13 ats. Partial oxygen pressure = 0.026 ats.				
14.2	1430	1703	5.88	1.15
0.78	1030	1303	7.69	$\bar{1}$.89
9.6	1250	1523	6.57	0.98
0.81	1070	1343	7.46	$\bar{1}$.91
3.44	1200	1473	6.80	0.54
2.44	1180	1453	6.89	0.39
10.4	1380	1653	6.06	1.02
11	1330	1603	6.25	1.04
2.16	1180	1453	6.89	0.33
7.5	1420	1693	5.91	0.88
8	1370	1643	6.09	0.90
13	1470	1743	5.74	1.11
18.9	1550	1823	5.49	1.28
11	1400	1673	5.98	1.04
19.5	1590	1863	5.37	1.29
18.9	1570	1843	5.43	1.28

$R \times 10^5$	T°C.	T°A.	$1/T°A \times 10^4$	$\log_{10}(10^5 R)$
10.1	1680	1953	5.12	1.00
15.8	1610	1883	5.31	1.20
11.7	1980	2253	4.44	1.07
9.0	1970	2243	4.46	0.95
13.7	1930	2203	4.54	1.14
18.3	1750	2023	4.95	1.26
8.2	1950	2223	4.50	0.91
12.2	1910	2183	4.58	1.09
19.5	1780	2053	4.87	1.29
13.3	1930	2203	4.54	1.14
6.0	1920	2193	4.56	0.78
21.2	1700	1973	5.07	1.33
16.2	1860	2133	4.69	1.21
11.7	1880	2153	4.65	1.07
13	1600	1873	5.34	1.11
12	1700	1973	5.07	1.08
11.7	1720	1993	5.02	1.07
12.4	1630	1903	5.26	1.09
14.6	1600	1873	5.34	1.16
9.75	1780	2053	4.87	0.99
8.4	1800	2073	4.83	0.92
13.6	1760	2033	4.92	1.13
12.7	1720	1993	5.02	1.10
19.5	1660	1933	5.18	1.29
10.8	1700	1973	5.07	1.03
20.8	1500	1773	5.65	1.32
18.7	1500	1773	5.65	1.27
19.5	1670	1943	5.15	1.29
14.6	1510	1783	5.61	1.16
17.2	1580	1953	5.12	1.24
6.5	1800	2073	4.83	0.81
9.4	1800	2073	4.83	0.97

Graphite preheated at 2,000°C. for about 30 seconds. The reaction times were 30 seconds or less. $T_o$tal gas pressure = 0.13 ats. Partial oxygen pressure = 0.026 ats.

10.2	1660	1933	5.18	1.01
14.6	1620	1893	5.29	1.16
5.9	1780	2053	4.87	0.77
5.1	1800	2073	4.87	0.71
15.4	1650	1923	5.20	1.19
11.7	1760	2033	4.92	1.07
17	1660	1933	5.18	1.23
7.0	1780	2063	4.85	0.85
18.1	1720	1993	5.02	1.26

$R \times 10^5$	T°C.	T°A.	$1/T°A \times 10^4$	$\log_{10}(10^5 R)$
11.4	1670	1943	5.15	1.06
20.8	1630	1903	5.26	1.32
17.1	1640	1913	5.23	1.23
6.3	1280	1553	6.45	0.80
2.1	1070	1343	7.46	0.32
1.2	1080	1353	7.40	0.08
3.7	1190	1463	6.84	0.57
15.8	1450	1723	5.81	1.20
15.2	1470	1743	5.74	1.18
13.3	1400	1673	5.98	1.12
2.4	1190	1463	6.84	0.38
17.7	1400	1673	5.98	1.25
21.6	1490	1763	5.68	1.33
17.5	1500	1773	5.65	1.24
20.8	1560	1833	5.46	1.32
11.9	1470	1740	5.74	1.08
15.4	1460	1733	5.78	1.19
2.54	1150	1423	7.04	0.40
11.1	1420	1693	5.91	1.04
17.3	1540	1813	5.52	1.24
22.6	1640	1913	5.23	1.35

Ambient nominal gas pressure = 0.063 ats. Impact pressure = 0.069 ats.
Partial oxygen pressure = 0.069 ats.

3.0	1060	1333	7.51	0.48
22.2	1280	1553	6.45	1.35
16.5	1260	1533	6.53	1.22
1.2	1050	1323	7.57	0.8
13	1180	1453	6.89	1.11
1.25	1020	1293	7.75	0.10
30.8	1910	2183	4.58	1.49
37.4	1930	2203	4.54	1.57
26	1910	2183	4.58	1.42
55	1830	2103	4.76	1.74
50	1880	2153	4.65	1.70
39	1890	2163	4.63	1.59
43	1740	2013	4.97	1.63
42.5	1820	2093	4.78	1.63
23.4	1920	2193	4.56	1.37
37.6	1820	2093	4.78	1.58
47	1840	2113	4.73	1.67
38	1800	2073	4.83	1.58
13.2	1210	1483	6.74	1.67
26.6	1430	1703	5.88	1.42
10.0	1250	1523	6.57	1.00

$R \times 10^5$	T°C.	T°A.	$1/T°A \times 10^4$	$\log_{10}(10^5 R)$
27.4	1400	1673	5.98	1.44
26.6	1370	1643	6.09	1.42
41.7	1470	1743	5.74	1.62
39	1490	1763	5.68	1.59
15.2	1300	1573	6.36	1.18
42	1450	1723	5.81	1.62
40.5	1690	1963	5.10	1.61
42	1720	1993	5.02	1.62
39	1600	1873	5.34	1.59
51	1660	1933	5.15	1.71
51	1700	1973	5.07	1.71
51	1690	1963	5.10	1.71
19	1800	2073	4.83	1.28
24	1800	2073	4.83	1.38
25.4	1790	2063	4.85	1.40
46.8	1640	1913	5.23	1.67
41	1750	2023	4.95	1.61
52.5	1620	1893	5.29	1.72
36.6	1700	1973	5.07	1.56
48.6	1720	1993	5.02	1.69
56	1450	1723	5.81	1.75
25	1300	1573	6.36	1.40
15.4	1200	1473	6.80	1.19
13.5	1080	1353	7.40	1.13
6.5	1130	1403	7.14	0.81
21.4	1280	1553	6.45	1.33
39	1700	1973	5.07	1.59
53	1600	1873	5.34	1.72
34	1770	2043	4.90	1.53
58	1520	1793	5.58	1.76
52	1450	1723	5.81	1.72
51	1500	1773	5.65	1.71
36	1700	1973	5.07	1.56
Total gas pressure = 0.13 ats.			Partial oxygen pressure = 0.13 ats.	
52	1940	2213	4.52	1.72
58.5	1830	2103	4.76	1.77
52	1820	2093	4.78	1.72
69	1800	2073	4.83	1.84
56	1840	2113	4.73	1.75
58.5	1880	2153	4.65	1.77
51.5	1830	2103	4.76	1.71
58.5	1860	2113	4.69	1.77
48.5	1820	2093	4.78	1.69
38	1980	2253	4.44	1.58

$R \times 10^5$	T°C.	T°A.	$1/T°A \times 10^4$	$\log_{10}(10^5 R)$
41	1900	2173	4.60	1.61
51	1940	2213	4.52	1.70
68	1740	2043	4.90	1.83
80.5	1600	1873	5.34	1.91
81	1670	1943	5.34	1.91
61.5	1800	2073	4.83	1.79
73	1740	2013	4.97	1.86
55	1800	2073	4.83	1.79
68	1550	1823	5.49	1.83
61.5	1470	1743	5.74	1.79
58.5	1460	1733	5.78	1.77
76	1570	1843	5.43	1.88
65	1490	1763	5.68	1.81
91	1660	1993	5.18	1.96
70	1570	1843	5.43	1.85
26	1400	1673	5.98	1.42
23	1360	1633	6.13	1.36
28.4	1370	1643	6.09	1.45
41.6	1430	1703	5.88	1.62
58.5	1520	1793	5.58	1.77
61.6	1580	1853	5.40	1.79
75.4	1630	1903	5.26	1.88
58.5	1600	1873	5.34	1.77
76.5	1770	2043	4.90	1.88
73	1640	1913	5.23	1.86
90.5	1670	1943	5.15	1.96
63.6	1620	1893	5.29	1.80
58.5	1800	2073	4.83	1.77
11.7	1110	1383	7.24	1.07
16.0	1130	1403	7.14	1.20
28.6	1320	1593	6.28	1.46
33.8	1400	1673	5.98	1.53
29.2	1360	1633	6.13	1.47
9.4	1070	1343	7.46	0.97
15.1	1090	1363	7.35	1.18
25	1230	1503	6.66	1.40
36	1290	1563	6.41	1.56
62.6	1740	2013	4.97	1.80
73	1620	1893	5.29	1.86
65	1480	1753	5.71	1.81
73	1800	2073	4.83	1.86
62.5	1800	2073	4.83	1.80
66	1780	2053	4.87	1.82

$R \times 10^5$	T°C.	T°A.	$1/T°A \times 10^4$	$\log_{10}(10^5 R)$
Total pressure = 0.20 ats.			Partial oxygen pressure = 0.20 ats	
109	1800	2073	4.83	2.04
65	1550	1823	5.49	1.81
88	1750	2023	4.95	1.94
67.6	1560	1833	5.46	1.83
99	1620	1893	5.29	2.00
99	1680	1953	5.12	2.00
86	1700	1973	5.07	1.93
62.5	1660	1933	5.18	1.80
34	1160	1433	6.99	1.53
34.1	1170	1443	6.94	1.53
67.6	1370	1643	6.09	1.83
68.6	1440	1713	5.84	1.84
72	1910	2183	4.58	1.86
90	1870	2143	4.67	1.95
69	1900	2173	4.60	1.84
78	1930	2203	4.54	1.89
69	1850	2123	4.71	1.84
90	1850	2123	4.71	1.95
72	1880	2153	4.65	1.86
81	1860	2133	4.69	1.91
69	1980	2253	4.44	1.84
64	1960	2233	4.48	1.81
74.5	1870	2143	4.67	1.87
81	1750	2023	4.95	1.91
54.6	1270	1543	6.49	1.74
78	1400	1673	5.98	1.89
88	1440	1713	5.84	1.94
80	1560	1833	5.46	1.90
89	1580	1853	5.40	1.95
73	1600	1873	5.34	1.86
75	1780	2053	4.87	1.88
36	1160	1433	6.99	1.56
46.5	1220	1493	6.71	1.67
23.4	1100	1373	7.29	1.37
67.5	1280	1553	6.45	1.83
43	1180	1453	6.89	1.63
75.5	1660	1933	5.18	1.88
83.5	1500	1773	5.65	1.92
96	1590	1863	5.37	1.98
90	1450	1723	5.81	1.95
108	1600	1873	5.34	2.03
110	1640	1913	5.23	2.04
85	1560	1833	5.46	1.93
93.5	1680	1953	5.12	1.97

$R \times 10^5$	T°C.	T°A.	$1/T°A \times 10^4$	$\log_{10}(10^5 R)$
91	1540	1813	5.52	1.96
83.5	1800	2073	4.83	1.92
87	1520	1793	5.58	1.94
94	1590	1863	5.37	1.97
91	1560	1833	5.46	1.96
78	1800	2073	4.83	1.89
81.5	1750	2023	4.95	1.91
107	1670	1943	5.15	2.03
73	1800	2073	4.83	1.86
92.5	1630	1903	5.26	1.97
Total pressure = 0.30 ats.			Oxygen partial pressure = 0.06 at.	
31.3	1570	1843	5.43	1.50
33.6	1670	1943	5.15	1.53
40	1730	2003	5.00	1.60
28.2	1780	2053	4.87	1.45
20.8	1460	1733	5.78	1.32
29.2	1730	2003	5.00	1.47
31.8	1720	1993	5.02	1.50
19.5	1800	2073	4.83	1.29
36	1650	1923	5.20	1.56
25.5	1770	2043	4.90	1.41
29.2	1750	2023	4.95	1.47
18.8	1790	2063	4.85	1.21
19.5	1770	2043	4.90	1.29
1.12	1000	1273	7.87	0.05
17.6	1420	1693	5.91	1.25
21.7	1400	1673	5.98	1.34
30.2	1540	1813	5.52	1.48
16.8	1420	1693	5.91	1.22
19.5	1900	2173	4.60	1.29
31	1850	2123	4.71	1.49
31	1870	2143	4.67	1.49
32.4	1830	2103	4.76	1.51
37.8	1820	2093	4.78	1.58
37	1570	1843	5.43	1.57
34.4	1860	2133	4.69	1.54
22.5	1870	2143	4.67	1.35
20.4	1890	2163	4.63	1.31
13	1980	2253	4.44	1.11
27.5	1920	2193	4.56	1.44
28.2	1950	2223	4.50	1.45
19.5	1400	1673	5.98	1.29
9.1	1170	1443	6.94	0.96
9.8	1150	1423	7.04	0.99

$R \times 10^5$	T°C.	T°A.	$1/T°A \times 10^4$	$\log_{10}(10^5 R)$
9.8	1150	1423	7.04	0.99
15.3	1300	1473	6.37	1.18
10.3	1210	1483	6.75	1.01
9.8	1200	1473	6.80	0.99
3.9	1030	1303	7.69	0.59
6.2	1160	1433	6.99	0.79
20.4	1350	1623	6.17	1.31
8.4	1200	1473	6.80	0.92
29	1560	1833	5.46	1.46
39	1680	1953	5.12	1.59
19.5	1500	1773	5.65	1.29
17.8	1380	1653	6.06	1.25
20	1370	1643	6.09	1.30
9.8	1320	1593	6.28	0.99
16.8	1360	1633	6.13	1.23
Total pressure = 0.30 ats.			Partial oxygen pressure = 0.30 ats	
26	1060	1333	7.51	1.42
35.4	1080	1353	7.40	1.55
55.7	1170	1443	6.94	1.75
61	1220	1493	6.71	1.79
66.5	1210	1483	6.75	1.82
47.1	1110	1383	7.24	1.67
93.5	1300	1573	6.36	1.97
117	1400	1673	5.78	2.07
117	1420	1693	5.91	2.07
70	1250	1523	6.57	1.85
125	1400	1673	5.98	2.10
111	1400	1673	5.98	2.05
74.6	1280	1553	6.45	1.87
138	1660	1933	5.18	2.14
122	1680	1953	5.12	2.09
108	1660	1933	5.18	2.03
105	1620	1893	5.29	2.02
129	1640	1913	5.23	2.11
108	1670	1943	5.15	2.03
112	1730	2003	5.00	2.05
123	1780	2053	4.87	2.09
111	1750	2023	4.95	2.05
117	1710	1983	5.05	2.07
134	1700	1973	5.07	2.13
121	1630	1903	5.26	2.08
102	1640	1913	5.23	2.01
129	1700	1973	5.07	2.11
114	1520	1793	5.58	2.06
126	1650	1923	5.20	2.10

R x10^5	T°C.	T°A.	1/T°A. x10^4	$\log_{10}(10^5 R)$
71	1300	1573	6.36	1.85
69	1930	2203	4.54	1.84
86	1980	2253	4.44	1.94
90	1900	2173	4.60	1.95
97.5	1880	2153	4.65	1.99
129	1850	2123	4.71	2.11
104	1830	2103	4.65	2.02
104	1830	2103	4.76	2.02
99	1810	2083	4.80	2.00
110	1880	2153	4.65	2.04
129	1850	2123	4.71	2.11
117	1890	2163	4.63	2.07
92	1950	2223	4.50	1.94
108	1400	1673	5.98	2.03
114	1530	1803	5.55	2.06
121	1570	1843	5.43	2.08
110	1480	1753	5.71	2.04
111	1530	1803	5.55	2.04
58.5	1270	1543	6.49	1.77
117	1640	1913	5.23	2.07
80	1350	1623	6.17	1.90
77	1350	1623	6.17	1.89
103	1460	1733	5.78	2.01
132	1590	1863	5.37	2.12
58.5	1280	1553	6.45	1.77
Total pressure = 0.20 ats.			Partial oxygen pressure = 0.04 a	
13.6	1430	1703	5.88	1.13
13.6	1750	2023	4.95	1.13
25.8	1690	1963	5.10	1.41
25.1	1630	1903	5.26	1.40
11.7	1470	1743	5.74	1.07
23.4	1600	1873	5.34	1.37
14.6	1730	2003	5.00	1.16
24.4	1690	1963	5.10	1.39
15.6	1720	1993	5.02	1.19
21.4	1780	2053	4.87	1.33
25.4	1700	1973	5.07	1.40
26.7	1700	1973	5.07	1.43
13.6	1400	1673	5.98	1.13
10.5	1280	1553	6.45	1.02
10.8	1300	1573	6.36	1.03
15.4	1360	1633	6.13	1.18
9.0	1320	1593	6.28	0.95
9.8	1400	1673	5.98	0.99
19.5	1460	1733	5.78	1.29

R x10^5	T°C.	T°A.	1/T°A x10^4	$\log_{10}(10^5 R)$
18.2	1440	1713	5.49	1.26
3.0	1110	1383	7.24	0.48
2.7	1080	1353	7.40	0.43
1.8	1040	1313	7.63	0.26
18.2	1400	1673	5.98	1.26
13	1870	2143	4.67	1.11
14.6	1900	2173	4.60	1.16
12.3	1900	2173	4.60	1.09
26.8	1800	2073	4.83	1.43
14.6	1830	2103	4.76	1.16
22.8	1760	2033	4.92	1.35
11.7	1370	1643	6.09	1.07
7.75	1180	1453	6.89	0.89
8.6	1280	1553	6.45	0.93
2.0	1070	1343	7.46	0.30
23.4	1690	1963	5.10	1.37
25.8	1640	1913	5.23	1.40
22.5	1550	1823	5.49	1.35
22.5	1800	2073	4.83	1.35
17.6	1420	1693	5.91	1.25
20.3	1540	1813	5.52	1.31
23.4	1600	1873	5.34	1.37
21.2	1800	2073	4.83	1.33
16.7	1860	2133	4.69	1.22
15.5	1910	2183	4.58	1.19
13	1920	2193	4.56	1.11
12.8	1960	2233	4.48	1.11
24.4	1800	2073	4.83	1.39
17.7	1900	2173	4.60	1.25

TABLE 7.

Nominal gas velocity 7,000 cms/sec.

R x10^5	T°C.	T°A.	1/T°A x10^4	$\log_{10}(10^5 R)$
Ambient gas pressure = 0.13 ats. Impact pressure = 0.23 ats.				
Partial oxygen pressure = 0.046 ats.				
3.6	1130	1403	7.14	0.56
2.72	1080	1353	7.40	0.44
10.4	1220	1493	6.41	1.02
1.04	1010	1283	7.81	0.02
4.25	1160	1433	6.99	0.63
3.02	1110	1383	7.24	0.48
26.8	1500	1773	5.65	1.43

$R \times 10^5$	T°C.	T°A.	$1/T°A. \times 10^4$	$\log_{10}(10^5 R)$
44.4	1700	1973	5.07	1.65
21.6	1480	1753	5.71	1.34
42.8	1530	1803	5.55	1.63
10.9	1200	1473	6.80	1.04
16.2	1440	1713	5.84	1.21
13.6	1440	1713	5.84	1.13
51.5	1640	1913	5.23	1.71
37.8	1700	1973	5.07	1.58
36.6	1790	2063	4.85	1.56
27	1800	2073	4.83	1.43
26.6	1800	2073	4.83	1.43
35	1590	1863	5.37	1.54
24.4	1520	1793	5.58	1.39
2.3	1110	1383	7.24	0.26
17.5	1360	1633	6.13	1.24
14.7	1370	1643	6.09	1.17
24.4	1450	1723	5.81	1.39
29	1970	2243	4.46	1.46
34.6	1850	2123	4.71	1.54
27.4	1930	2203	4.54	1.44
39	1880	2153	4.65	1.59
45	1820	2093	4.78	1.65
28.2	1890	2163	4.63	1.45
36.4	1900	2173	4.60	1.56
39	1850	2123	4.71	1.59
29	1900	2173	4.60	1.46
48	1850	2123	4.71	1.68
25.4	1980	2253	4.44	1.40
35.4	1860	2133	4.69	1.55
10.6	1220	1493	4.71	1.03
46	1540	1813	5.52	1.66
27.8	1390	1663	6.02	1.44
36.6	1480	1753	5.71	1.56
32.5	1670	1943	5.15	1.51
43	1620	1893	5.29	1.63
45	1800	2073	4.83	1.65
25.1	1750	2023	4.95	1.40
53	1590	1863	5.34	1.72
24.4	1420	1693	5.91	1.39
45	1680	1953	5.12	1.65
22.5	1800	2073	4.83	1.35

$R \times 10^5$	T°C.	T°A.	$1/T°A \times 10^4$	$\log_{10}(10^5 R)$
Gas pressure = 0.13 ats. Impact pressure = 0.23 ats.				
Partial oxygen pressure = 0.23 ats.				
67	1230	1503	6.66	1.83
48.8	1170	1443	6.94	1.69
13.5	1000	1273	7.87	1.13
58.5	1190	1463	6.84	1.77
31.4	1060	1333	7.51	1.50
58.5	1300	1573	6.36	1.77
65.5	1350	1623	6.17	1.82
114	1510	1783	5.61	2.06
92	1400	1673	5.98	1.96
77	1370	1643	6.09	1.89
101	1500	1773	5.65	2.00
103	1470	1743	5.74	2.01
135	1500	1773	5.65	2.13
156	1620	1893	5.29	2.19
193	1680	1953	5.12	2.29
156	1690	1963	5.10	2.19
156	1730	2003	5.00	2.19
180	1720	1993	5.02	2.26
161	1780	2053	4.87	2.21
149	1680	1953	5.12	2.17
146	1500	1773	5.65	2.16
164	1680	1953	5.12	2.22
133	1560	1833	5.46	2.12
163	1800	2073	4.83	2.21
162	1900	2173	4.60	2.21
162	1880	2153	4.65	2.21
122	1850	2123	4.71	2.09
122	1870	2143	4.67	2.09
107	1930	2203	4.54	2.03
98	1970	2243	4.46	1.99
98	1920	2193	4.56	1.99
138	1890	2163	4.63	2.14
167	1820	2093	4.78	2.22
156	1940	2213	4.52	2.19
154	1850	2123	4.71	2.19
156	1860	2133	4.69	2.19
172	1740	2013	4.97	2.24
175	1750	2023	4.95	2.24
140	1470	1743	5.74	2.15
92	1330	1603	6.25	1.96
142	1480	1753	5.71	2.15
94	1320	1593	6.28	1.97

$R \times 10^5$	T°C.	T°A.	$1/T°A \times 10^4$	$\log_{10}(10^5 R)$
156	1660	1933	5.18	2.19
180	1570	1843	5.43	2.26
180	1570	1843	5.43	2.26
170	1610	1883	5.31	2.23
180	1730	2003	5.00	2.26
173	1780	2053	4.87	2.24
Ambient gas pressure = 0.20 ats. Impact pressure = 0.30 ats.				
Partial oxygen pressure = 0.30 ats.				
73.2	1280	1553	6.45	1.86
43.9	1090	1363	7.35	1.64
60.0	1150	1423	7.04	1.78
172	1700	1973	5.07	2.24
66.5	1170	1443	6.94	1.82
77	1220	1493	6.71	1.89
22.6	1020	1293	7.75	1.35
102	1260	1533	6.53	2.01
93.5	1250	1523	6.57	1.97
97.5	1320	1593	6.28	1.99
97.5	1300	1573	6.36	1.99
122	1620	1893	5.29	2.09
140	1640	1913	5.23	2.15
160	1500	1773	5.65	2.20
147	1620	1893	5.29	2.17
160	1580	1853	5.40	2.20
144	1670	1943	5.15	2.16
125	1640	1913	5.23	2.10
170	1690	1963	5.10	2.23
226	1700	1973	5.07	2.35
160	1750	2023	4.95	2.20
175	1700	1973	5.07	2.24
73.5	1220	1493	6.71	1.89
153	1550	1823	5.49	2.18
92	1440	1713	5.84	1.96
116	1380	1653	6.06	2.06
125	1350	1623	6.17	2.10
146	1400	1673	5.98	2.16
124	1370	1643	6.09	2.10
135	1360	1633	6.13	2.13
180	1850	2123	4.71	2.26
154	1830	2103	4.76	2.19
169	1870	2143	4.67	2.23
117	1960	2233	4.48	2.07
162	1820	2093	4.78	2.21
163	1920	2193	4.56	2.21
163	1840	2113	4.73	2.21

$R \times 10^5$	T°C.	T°A.	$1/T°A \times 10^4$	$\log_{10}(10^5 R)$
133	1910	2183	4.58	2.12
172	1920	2193	4.56	2.24
156	1980	2253	4.44	2.19
133	1900	2173	4.60	2.12
110	1960	2233	4.48	2.04
167	1790	2063	4.85	2.22
164	1550	1823	5.49	2.21
167	1600	1873	5.34	2.22
160	1580	1853	5.40	2.20
160	1540	1813	5.52	2.20
195	1530	1803	5.55	2.29

Ambient gas pressure = 0.20 ats. Impact pressure = 0.30 ats.

Partial oxygen pressure = 0.06 ats.

41.7	1940	2213	4.52	1.62
56	1930	2203	4.54	1.75
45.5	1960	2233	4.48	1.66
58.5	1840	2113	4.73	1.77
56	1850	2123	4.71	1.75
64	1800	2073	4.83	1.81
68	1820	2093	4.78	1.83
53	1820	2093	4.78	1.72
44	1980	2253	4.44	1.64
53	1880	2153	4.65	1.72
61.5	1860	2133	4.69	1.79
65	1830	2103	4.74	1.81
58.5	1640	1913	5.23	1.77
52.5	1550	1823	5.49	1.72
51.5	1660	1933	5.18	1.71
42	1780	2053	4.87	1.62
48	1700	1973	5.07	1.68
53	1740	2013	4.97	1.72
48	1770	2043	4.90	1.68
56	1690	1963	5.10	1.75
45	1800	2073	4.83	1.65
51	1790	2063	4.85	1.71
33.2	1470	1743	5.74	1.52
58.5	1640	1913	5.23	1.77
63.5	1580	1853	5.40	1.80
45	1520	1793	5.58	1.65
53	1630	1903	5.26	1.72
40.5	1550	1823	5.49	1.61
43.5	1500	1773	5.65	1.64
43.5	1520	1793	5.58	1.64
1.5	1050	1323	7.57	0.18
1.5	1060	1333	7.51	0.18

$R \times 10^5$	T°C.	T°A.	$1/T°A \times 10^4$	$\log_{10}(10^5 R)$
6.5	1180	1453	6.89	0.81
10.3	1100	1373	7.29	1.01
1.2	1030	1303	7.69	0.08
10.3	1080	1353	7.40	1.01
10.6	1200	1473	6.80	1.03
15.5	1230	1503	6.66	1.19
25.7	1280	1553	6.45	1.41
13.2	1180	1453	6.89	1.12
8.4	1180	1453	6.89	0.92
18.3	1300	1573	6.36	1.26
27.4	1440	1713	5.84	1.44
31.4	1460	1733	5.78	1.50
64.5	1620	1893	5.29	1.81
24.4	1420	1693	5.91	1.39
35.2	1480	1753	5.71	1.55
63	1660	1933	5.18	1.80

Ambient gas pressure = 0.40 ats. Impact pressure = 0.44 ats.
Partial oxygen pressure = 0.44 ats.

188	1400	1673	5.98	2.27
140	1350	1623	6.17	2.15
212	1440	1713	5.84	2.33
174	1350	1623	6.17	2.24
27.6	1020	1293	7.75	1.44
18.3	1010	1283	7.81	1.26
26.6	1000	1273	7.87	1.43
260	1600	1873	5.34	2.42
158	1340	1613	6.21	2.20
146	1420	1693	5.91	2.16
233	1570	1843	5.43	2.37
175	1380	1653	6.06	2.24
66	1150	1423	7.04	1.82
15	1050	1323	7.57	1.18
146	1230	1503	6.66	2.16
130	1250	1523	6.57	2.11
146	1400	1673	5.98	2.16
225	1480	1753	5.71	2.35
212	1630	1903	5.26	2.33
225	1760	2033	4.92	2.35
233	1660	1933	5.18	2.37
241	1800	2073	4.83	2.38
205	1730	2003	5.00	2.31
260	1680	1953	5.12	2.42
260	1710	1983	5.05	2.42
146	1400	1673	5.98	2.16
193	1460	1733	5.78	2.29

$R \times 10^5$	T°C.	T°A.	$1/T°A \times 10^4$	$\log_{10}(10^5 R)$
222	1600	1873	5.34	2.35
205	1900	2173	4.60	2.31
239	1550	1823	5.49	2.38
226	1850	2123	4.73	2.35
223	1800	2073	4.83	2.35
223	1739	2003	5.00	2.35
240	1750	2023	4.95	2.38
188	1780	2053	4.87	2.27
212	1700	1973	5.07	2.33
185	1870	2143	4.67	2.27
185	1810	2083	4.80	2.27
138	1920	2193	4.56	2.14
180	1970	2243	4.46	2.26
172	1930	2203	4.54	2.24
138	1880	2153	4.65	2.14
175	1870	2143	4.67	2.25
167	1840	2113	4.72	2.22
175	1930	2203	4.54	2.25
167	1830	2103	4.76	2.22
185	1930	2203	4.54	2.27
150	1950	2223	4.50	2.18

Ambient gas pressure = 0.60 ats. Impact pressure = 0.65 ats.

Partial oxygen pressure = 0.65 ats.

156	1800	2073	4.83	2.19
110	1260	1533	6.53	2.04
38	1030	1303	7.69	1.58
83.5	1160	1433	6.99	1.92
29.7	1020	1293	7.75	1.47
103	1180	1453	6.89	2.01
15	1000	1273	7.87	1.18
125	1350	1623	6.17	2.10
58.5	1100	1373	7.30	1.77
19.5	1010	1283	7.81	1.29
176	1600	1873	5.34	2.25
234	1500	1773	5.65	2.37
205	1840	2113	4.72	2.31
234	1870	2143	4.67	2.37
250	1850	2123	4.71	2.40
234	1820	2093	4.78	2.37
220	1800	2073	4.83	2.34
175	1900	2173	4.60	2.25
267	1740	2013	4.97	2.43
292	1660	1933	5.18	2.47
260	1720	1993	5.02	2.42
308	1650	1923	5.20	2.49

$R \times 10^5$	T°C.	T°A.	$1/T°A \times 10^4$	$\log_{10}(10^5 R)$
225	1630	1903	5.26	2.35
267	1570	1843	5.43	2.43
234	1900	2173	4.60	2.37
251	1670	1943	5.15	2.40
125	1360	1633	6.13	2.10
212	1480	1753	5.71	2.33
230	1800	2073	4.83	2.36
234	1780	2053	4.87	2.37
251	1550	1823	5.49	2.40
195	1400	1673	5.98	2.29
267	1550	1823	5.49	2.43
126	1250	1523	6.57	2.10
264	1600	1873	5.34	2.42
67	1100	1373	7.30	1.83
254	1760	2033	4.92	2.41
260	1580	1853	5.40	2.42
225	1480	1753	5.71	2.35
246	1820	2093	4.78	2.39
205	1970	2243	4.46	2.31
250	1930	2203	4.54	2.40
196	1930	2203	4.54	2.29
187	1900	2173	4.60	2.27
176	1910	2183	4.58	2.25

Ambient gas pressure = 0.50 ats. Impact pressure = 0.54 ats.

Partial oxygen pressure = 0.54 ats.

225	1450	1723	5.81	2.35
92.5	1180	1453	6.89	1.97
188	1500	1773	5.65	2.27
240	1580	1853	5.40	2.38
180	1440	1713	5.84	2.26
225	1580	1853	5.40	2.35
195	1420	1693	5.91	2.29
225	1570	1843	5.43	2.35
146	1260	1533	6.53	2.16
146	1300	1573	6.36	2.16
48.5	1060	1333	7.51	1.69
163	1320	1593	6.28	2.21
240	1540	1813	5.52	2.38
264	1550	1823	5.49	2.42
187	1360	1633	6.13	2.27
133	1360	1633	6.13	2.12
12	1000	1273	7.87	1.08
174	1540	1813	5.52	2.24
244	1720	1993	5.02	2.39
278	1650	1923	5.20	2.44
244	1720	1933	5.02	2.39
244	1730	2003	5.00	2.39

$R \times 10^5$	T°C.	T°A.	$1/T°A \times 10^4$	$\log_{10}(10^5 R)$
264	1800	2073	4.83	2.42
235	1700	1973	5.07	2.37
274	1730	2003	5.00	2.44
263	1600	1873	5.34	2.42
229	1760	2033	4.92	2.36
220	1840	2113	4.73	2.34
254	1660	1933	5.18	2.40
78	1230	1503	6.66	1.89
23.4	1010	1283	7.81	1.37
146	1220	1493	6.71	2.16
97	1100	1373	7.29	1.99
11	1000	1273	7.87	1.04
155	1300	1573	6.36	2.19
160	1850	2123	4.71	2.20
148	1920	2193	4.56	2.17
207	1850	2123	4.71	2.31
175	1870	2143	4.67	2.25
195	1920	2193	4.56	2.29
207	1870	2143	4.67	2.31
182	1850	2123	4.71	2.26
220	1890	2163	4.63	2.34
175	1880	2153	4.65	2.25
195	1860	2133	4.69	2.29
167	1830	2103	4.76	2.22

Ambient gas pressure = 0.30 ats. Impact pressure = 0.34 ats.

Partial oxygen pressure = 0.34 ats.

26.5	1030	1303	7.69	1.42
195	1670	1943	5.15	2.29
61	1130	1403	7.14	1.79
15.7	1000	1273	7.87	1.20
104	1290	1563	6.41	2.02
93.5	1160	1433	6.99	1.97
104	1230	1503	6.66	2.02
120	1310	1583	6.32	2.08
97.5	1250	1523	6.57	1.99
158	1540	1813	5.52	2.20
117	1270	1543	6.49	2.07
117	1250	1523	6.57	1.99
155	1470	1743	5.74	2.19
160	1360	1633	6.13	2.20
123	1340	1613	6.21	2.09
155	1480	1753	5.71	2.19
155	1520	1793	5.58	2.19
183	1500	1773	5.65	2.26

$R \times 10^5$	T°C.	T°A.	$1/T°A \times 10^4$	$\log_{10}(10^5 R)$
161	1620	1893	5.29	2.21
195	1640	1913	5.23	2.29
197	1630	1903	5.26	2.30
183	1780	2053	4.87	2.26
187	1760	2033	4.95	2.29
172	1800	2073	4.83	2.24
195	1750	2023	4.95	2.29
195	1770	2043	4.90	2.29
156	1860	2133	4.69	2.19
208	1760	2033	4.92	2.32
165	1580	1853	5.40	2.22
210	1670	1943	5.15	2.32
167	1630	1903	5.26	2.22
128	1410	1683	5.95	2.11
122	1300	1573	6.36	2.09
174	1530	1803	5.55	2.24
128	1300	1573	6.36	2.11
77	1200	1473	6.80	1.89
123	1880	2153	4.65	2.09
147	1900	2173	4.60	2.17
153	1860	2133	4.69	2.18
138	1850	2123	4.71	2.14
148	1880	2153	4.65	2.17
144	1900	2173	4.60	2.16
117	1870	2143	4.67	2.07
140	1870	2143	4.67	2.15
130	1970	2243	4.46	2.11
147	1930	2203	4.54	2.17
172	1950	2223	4.50	2.24
146	1930	2203	4.54	2.17
With 'squared' samples.			Ambient pressure 0.13 ats.	
Impact pressure 0.23 ats.			Partial oxygen pressure 0.23 ats.	
130	1980	2253	4.44	2.11
168	1660	1933	5.18	2.23
161	1740	2013	4.97	2.21
130	1880	2153	4.65	2.11
161	1690	1963	5.10	2.21
174	1680	1953	5.12	2.24
146	1650	1923	5.20	2.16
156	1700	1973	5.07	2.19
142	1850	2123	4.71	2.15
156	1640	1913	5.23	2.19
156	1660	1933	5.18	2.19
156	1670	1943	5.15	2.19

(C) Reactions of oxygen with pyrographite.

Pyrographite reacts with oxygen much more slowly than the other materials and the reaction is thought to be mainly chemically controlled. To test the velocity dependence the reaction rates have been measured at different velocities when the oxygen impact pressures have been about equal.

Table 8.

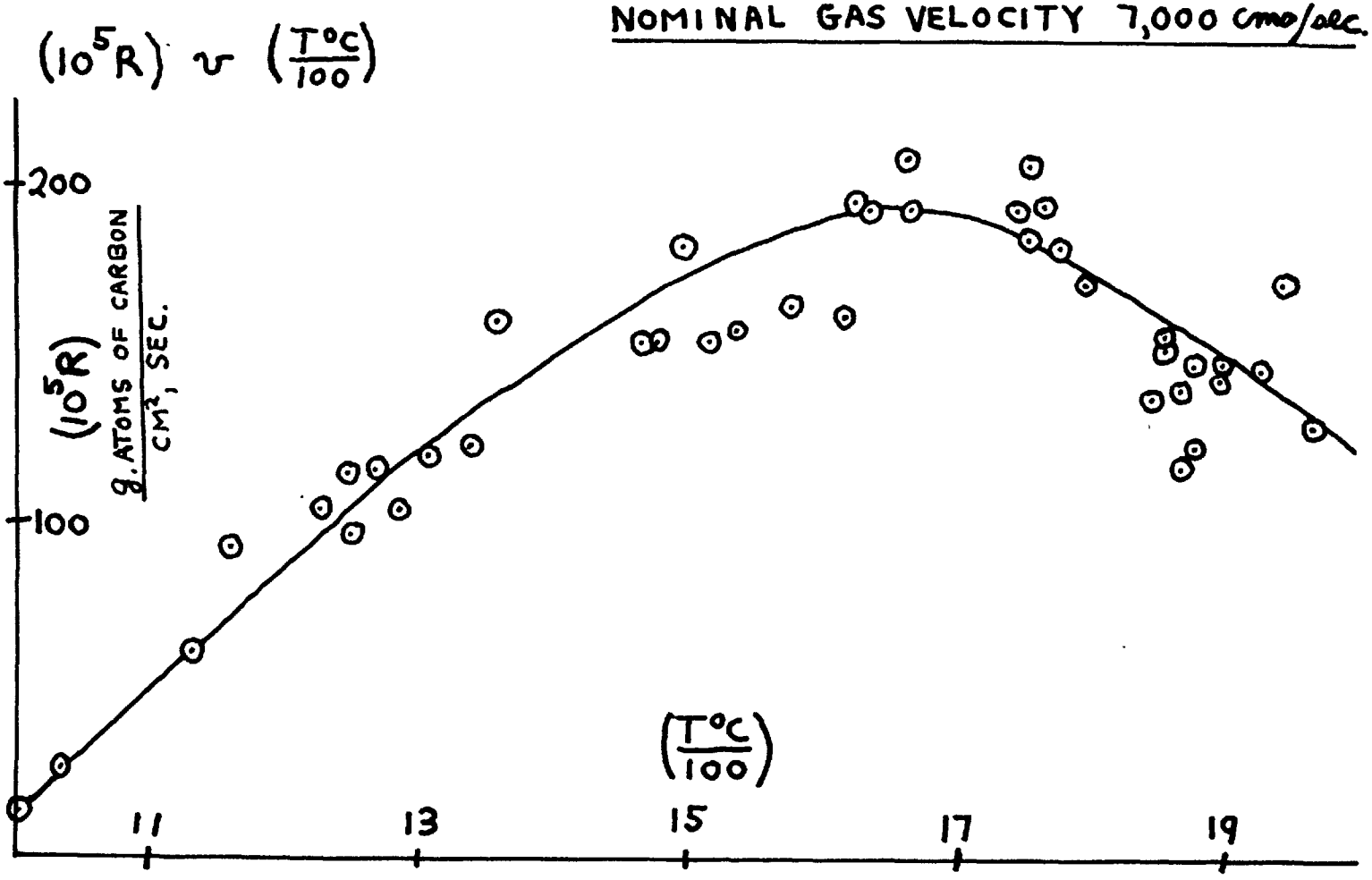
R x10^5	T°C.	T°A.	1/T°A x10^4	$\log_{10}(10^5 R)$
Nominal gas velocity 1090 cms/sec.				
Total gas pressure 0.20 ats.			Oxygen partial pressure 0.20 ats	
9.7	1440	1713	5.84	0.99
14.7	1900	2173	4.60	1.17
13	1980	2253	4.44	1.11
17.1	1800	2073	4.83	1.23
0.35	1100	1373	7.29	1.54
13.4	1880	2153	4.65	1.13
12.2	1850	2123	4.71	1.09
2.7	1200	1473	6.80	0.43
13.2	1500	1773	5.65	1.12
15	1520	1793	5.58	1.18
3.7	1300	1573	6.36	0.57
11.1	1540	1813	5.52	1.05
14.7	1550	1823	5.49	1.17
14	1550	1823	5.49	1.15
17.1	1730	2003	5.00	1.23
9.3	1500	1773	5.65	0.97
11.8	1660	1933	5.18	1.08
17.1	1650	1923	5.20	1.23
18.4	1730	2003	5.00	1.26
1.75	1240	1513	6.62	0.24
4.6	1300	1573	6.36	0.66
13.5	1550	1823	5.49	1.13
3.5	1280	1553	6.45	0.45
3.3	1250	1533	6.57	0.52
20.6	1700	1973	5.07	1.31
7.6	1350	1623	6.17	0.88
19.5	1600	1873	5.34	1.29
14.7	1850	2123	4.71	1.17
17.6	1580	1853	5.40	1.25
11.1	1450	1723	5.81	1.05

10^5R	T°C	T°A.	$1/T°A \times 10^4$	$\log_{10}(10^5R)$
Nominal gas velocity 7000 cms/sec.				
Ambient gas pressure 0.13 ats. Impact pressure 0.23 ats.				
Partial oxygen pressure 0.23 ats.				
4.2	1300	1573	6.36	0.62
17.3	1880	2153	4.65	1.24
18.6	1700	1973	5.07	1.27
18.8	1520	1793	5.58	1.27
0.2	1060	1333	7.51	$\bar{1}.3$
15.1	1640	1913	5.23	1.18
16.7	1680	1953	5.12	1.22
14.7	1800	2073	4.83	1.17
19.4	1750	2023	4.95	1.29
0.6	1100	1373	7.29	$\bar{1}.78$
10.5	1450	1723	5.81	1.02
20	1850	2123	4.71	1.30
14.7	1770	2043	4.90	1.17
16	1950	2233	4.48	1.20
18.3	1900	2173	4.60	1.26
4.1	1350	1623	6.17	0.61
17	1980	2253	4.44	1.23
21	1880	2153	4.65	1.32
16.7	1550	1823	5.49	1.22
16.2	1660	1933	5.18	1.21
16.8	1830	2103	4.76	1.22
8.8	1460	1733	5.78	0.94
17.6	1850	2123	4.71	1.25
1.1	1220	1493	6.71	$\bar{0}.04$
0.32	1080	1353	7.40	$\bar{1}.51$
1.63	1170	1443	6.94	0.21
4.6	1300	1573	6.36	$\bar{0}.66$
0.93	1150	1423	7.04	$\bar{1}.97$
1.33	1260	1533	6.53	0.12
2.5	1300	1573	6.36	$\bar{0}.40$
0.82	1190	1463	6.84	$\bar{1}.91$

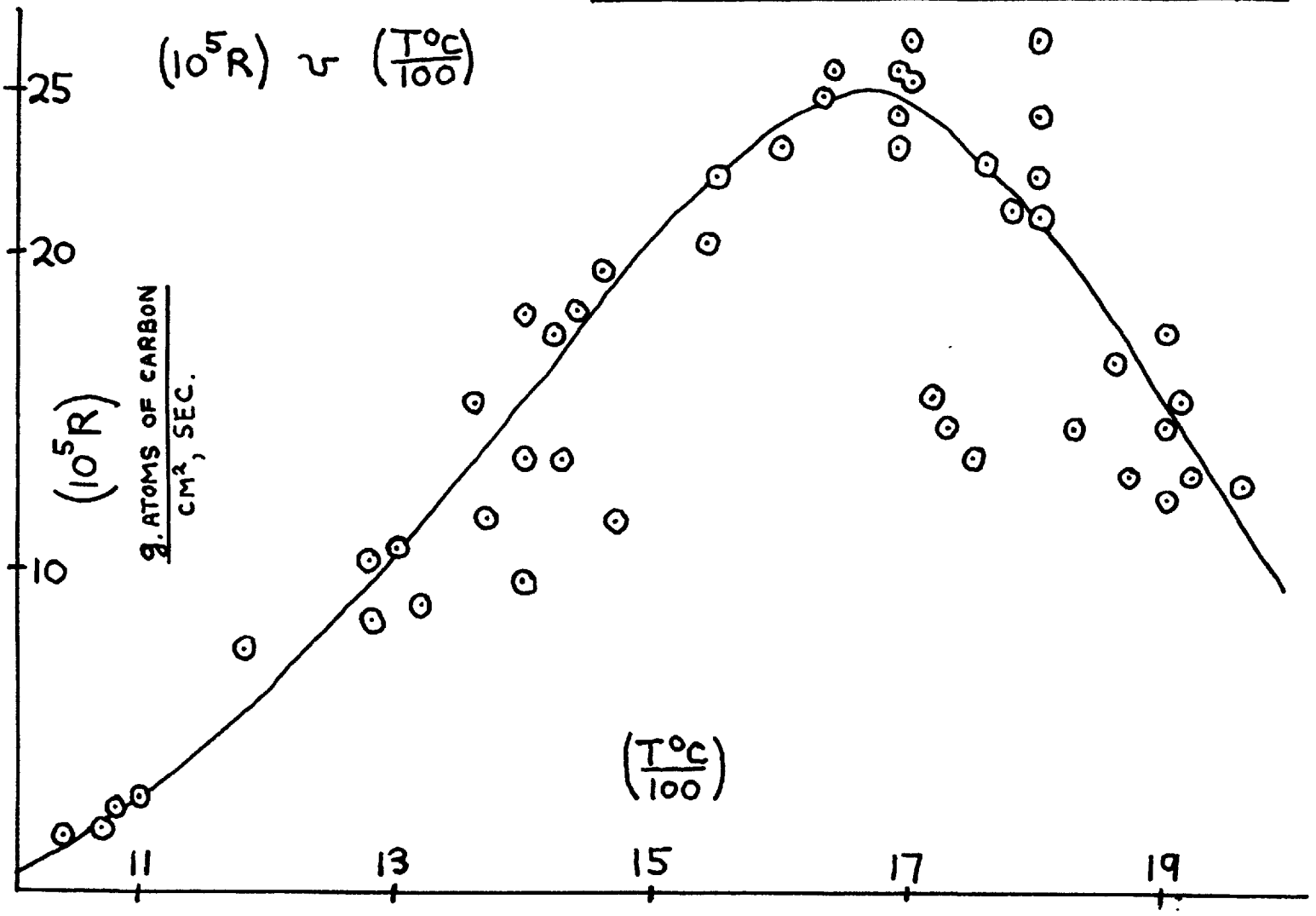
APPENDIX 2.

GRAPHS.

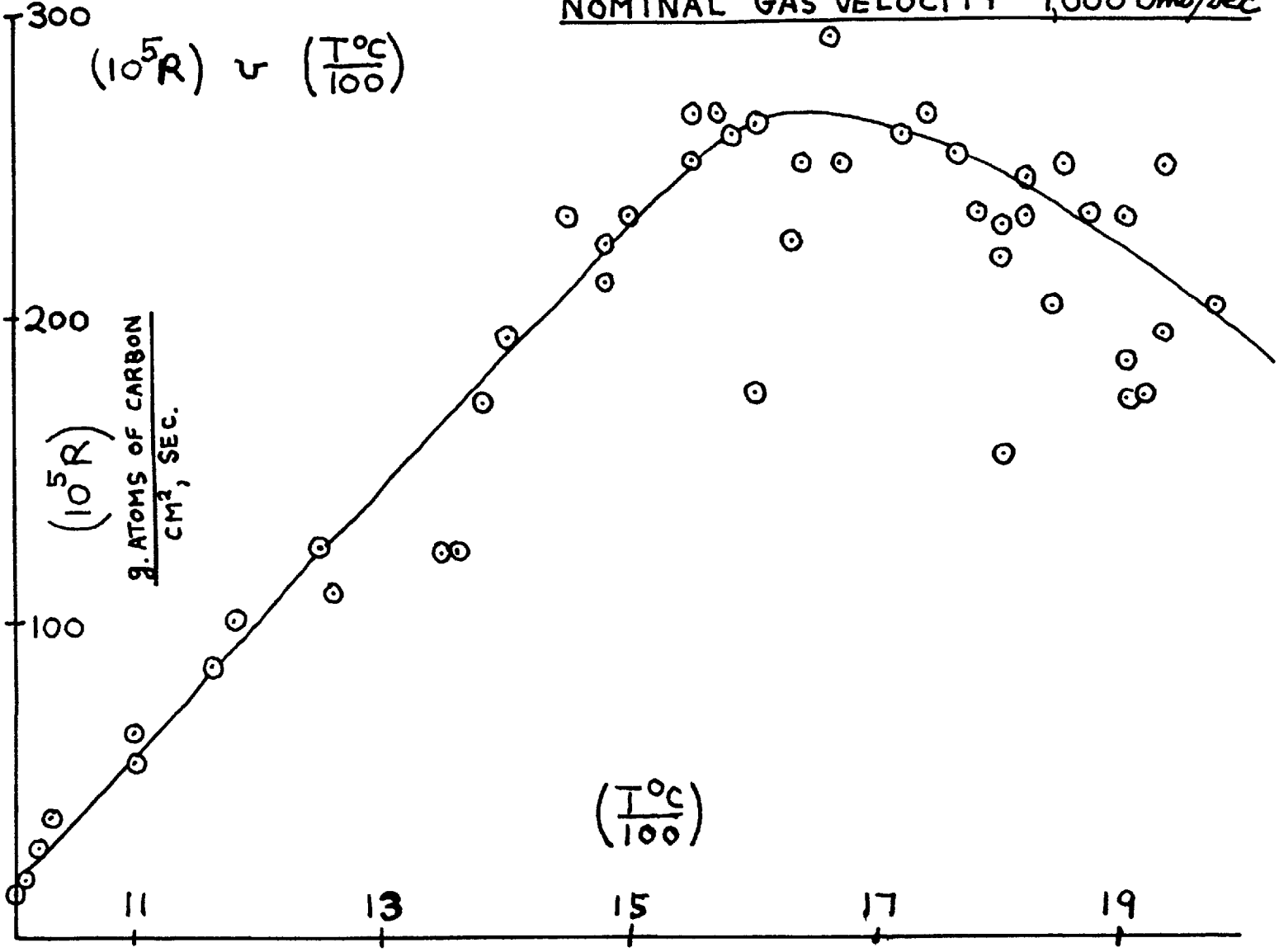
GRAPH 16 POLYCRYSTALLINE GRAPHITE. OXYGEN AT 0·30 ATS., NOMINAL GAS VELOCITY 7,000 cms/sec.



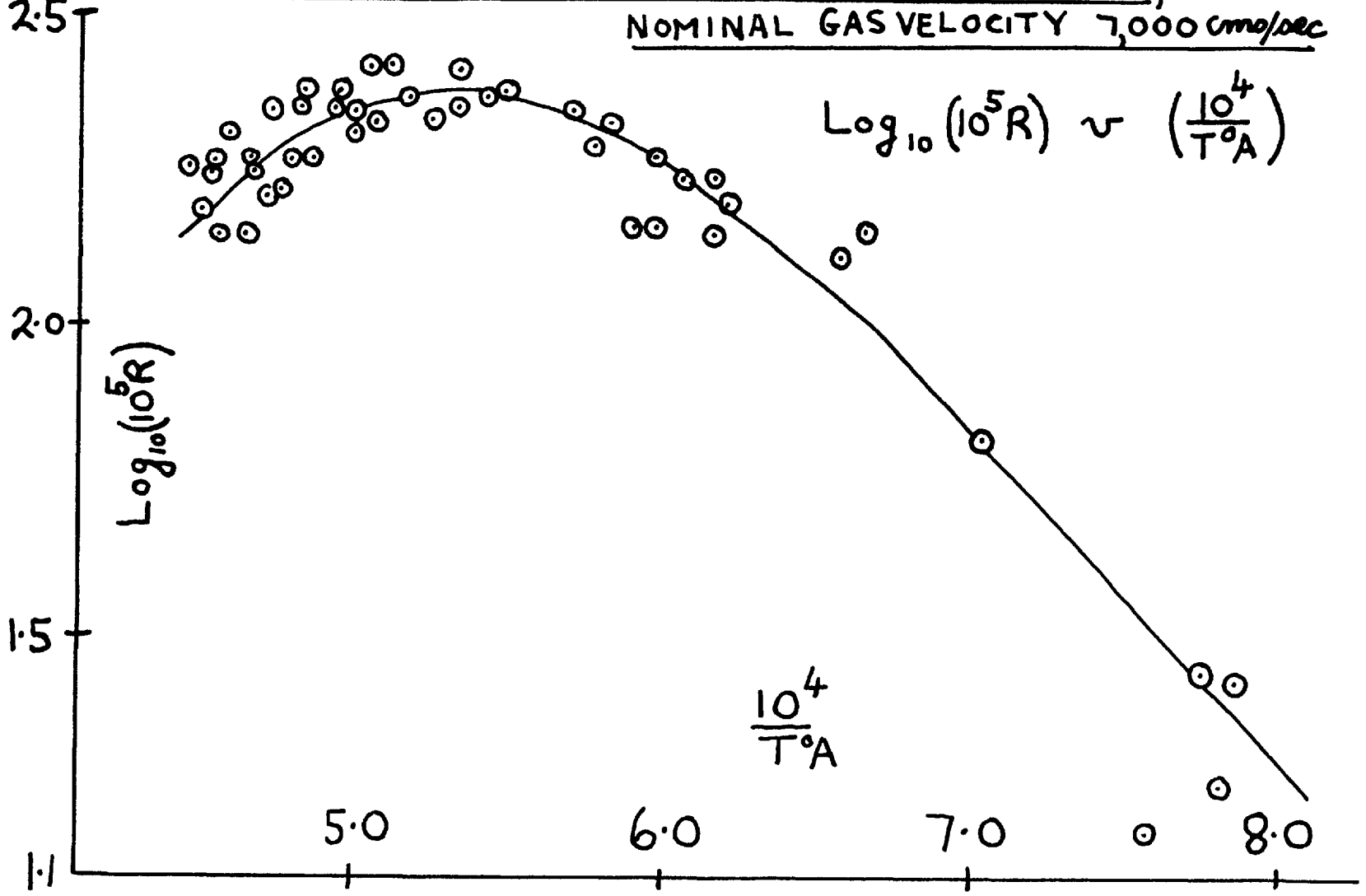
GRAPH 17 POLYCRYSTALLINE GRAPHITE. AIR AT 0·20 ATS.,
NOMINAL GAS VELOCITY 1,090 cms/sec



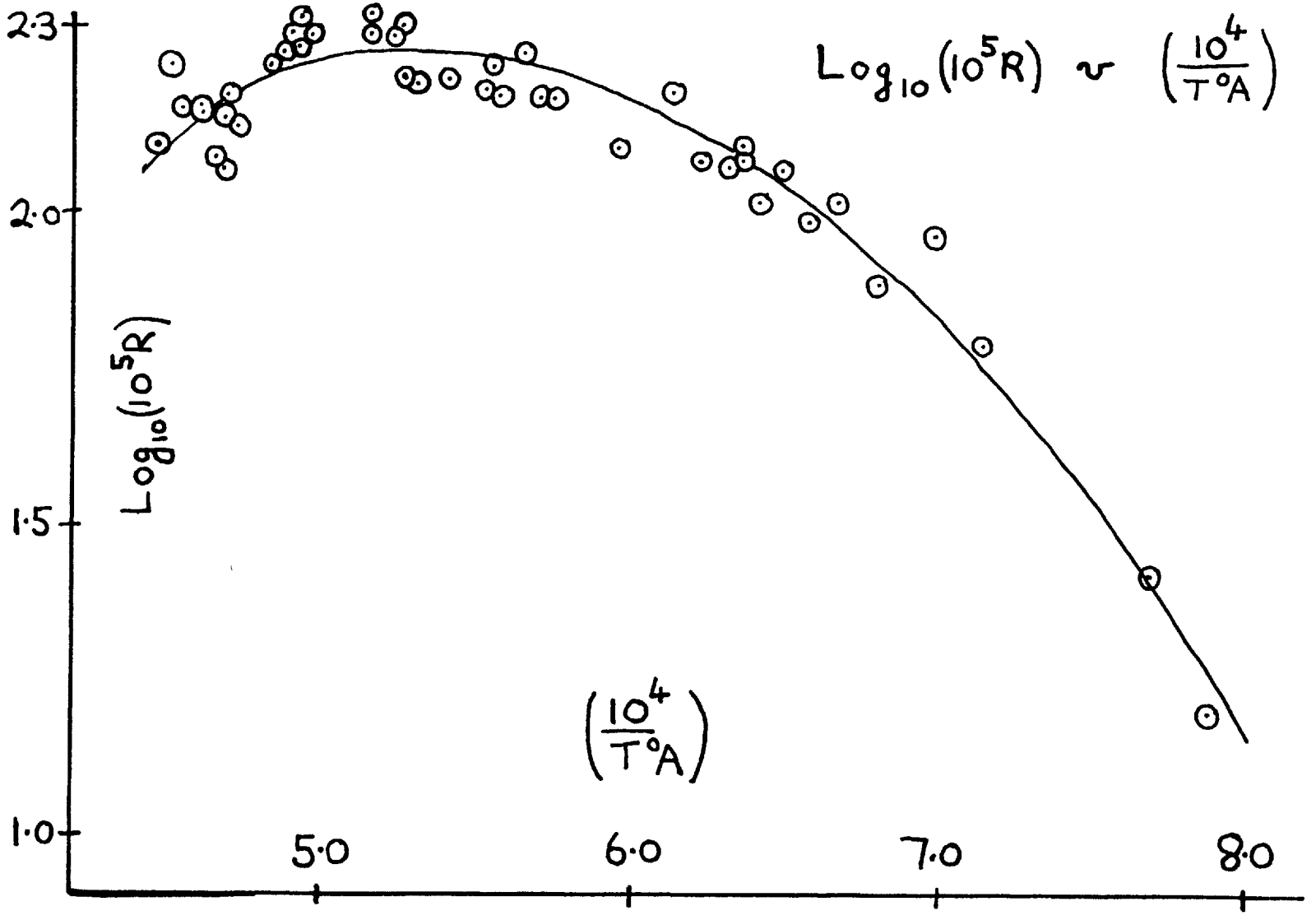
GRAPH 18 POLYCRYSTALLINE GRAPHITE, OXYGEN AT 0·60 ATS.,
NOMINAL GAS VELOCITY 7,000 cms/sec



GRAPH 19 POLYCRYSTALLINE GRAPHITE OXYGEN AT 0·40ATS.,
NOMINAL GAS VELOCITY 7,000 cms/sec

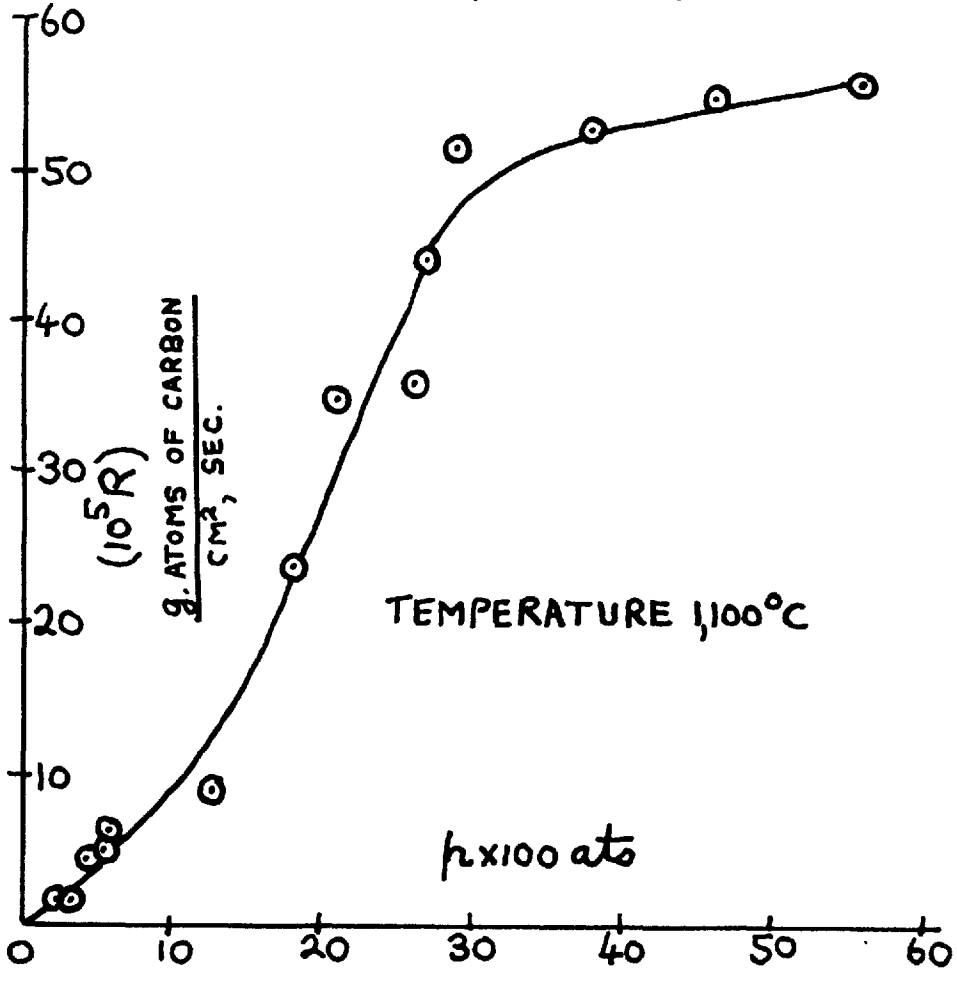


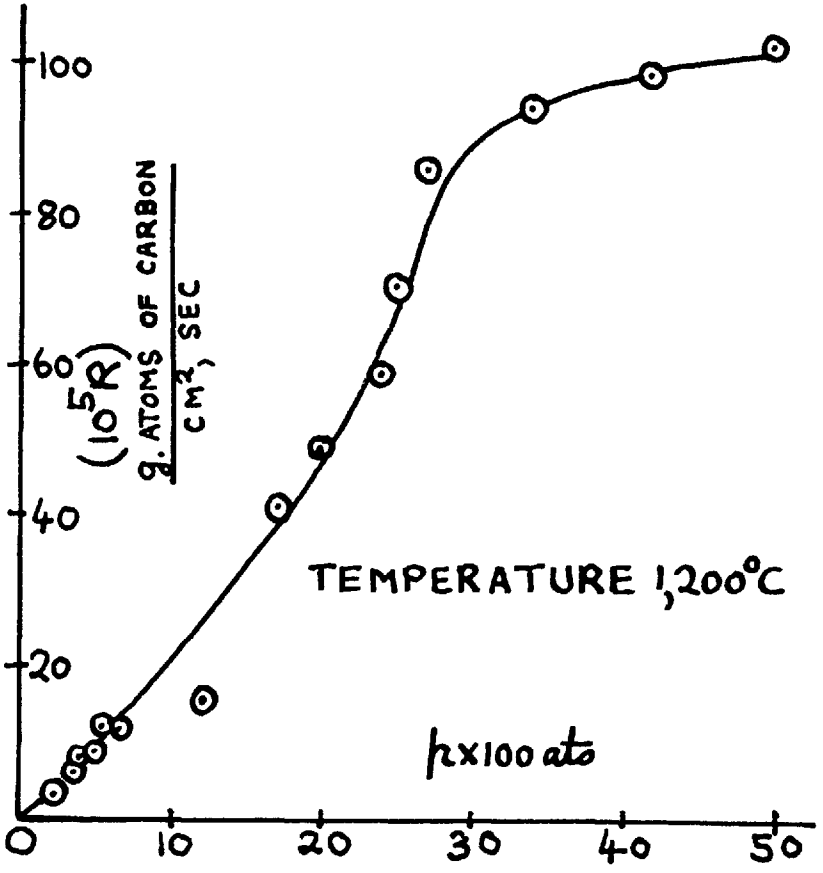
GRAPH 20 POLYCRYSTALLINE GRAPHITE. OXYGEN AT 0·30ATS.,
NOMINAL GAS VELOCITY 7,000 cms/sec



GRAPH 21 POLYCRYSTALLINE GRAPHITE

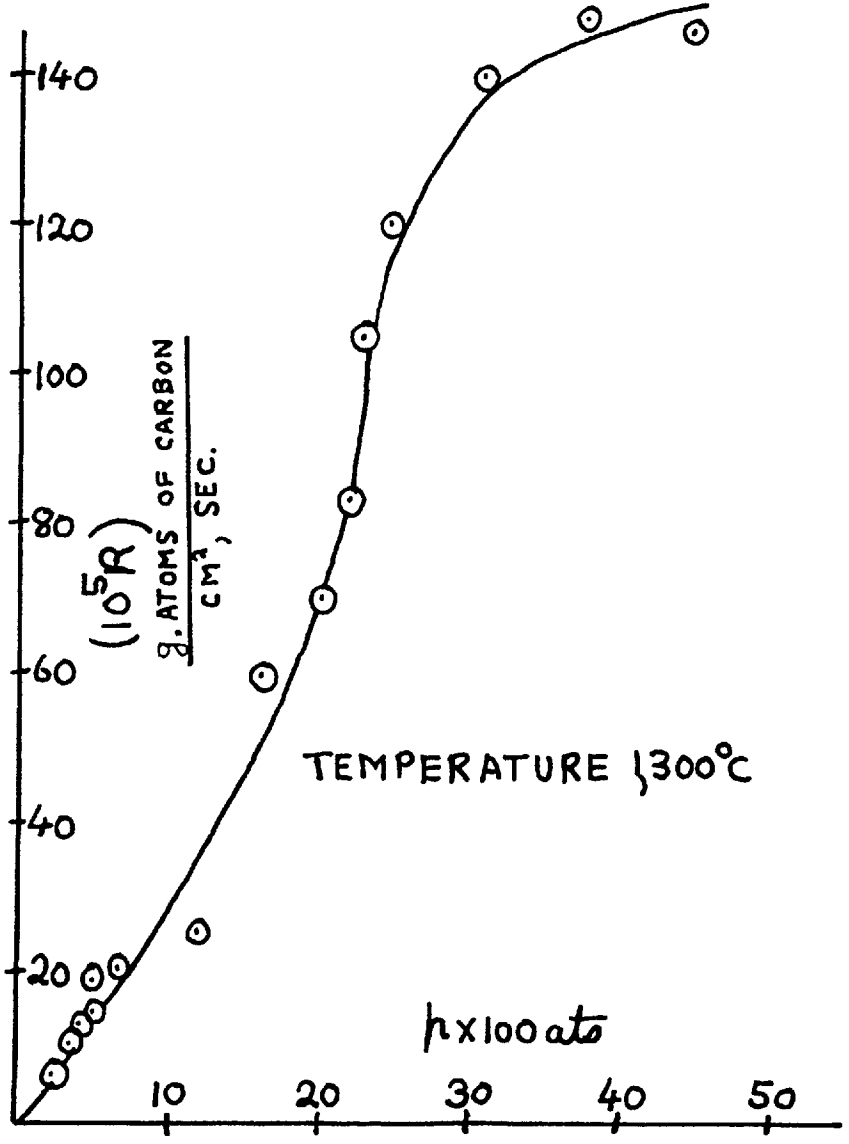
REACTION RATE ν CALCULATED SURFACE PRESSURE OF OXYGEN

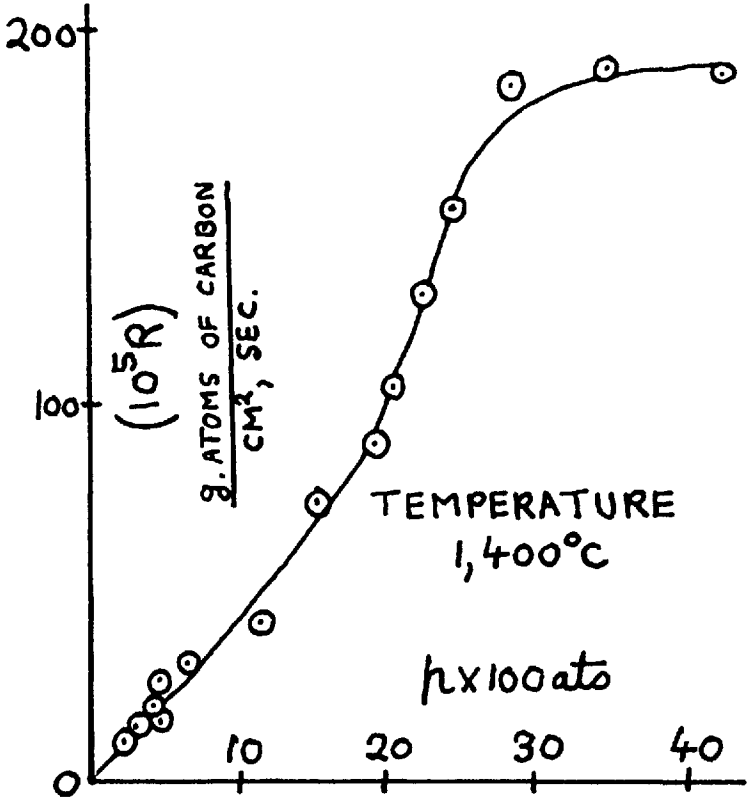




GRAPH 22 POLYCRYSTALLINE GRAPHITE

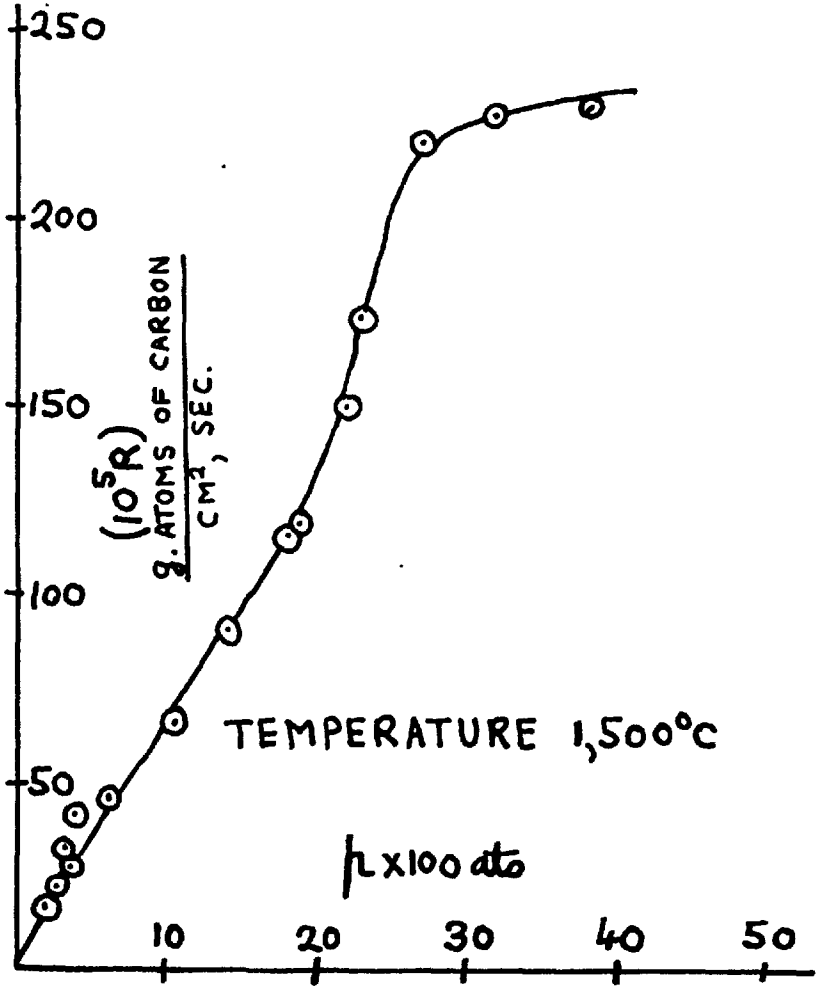
REACTION RATE ~ CALCULATED SURFACE PRESSURE OF OXYGEN

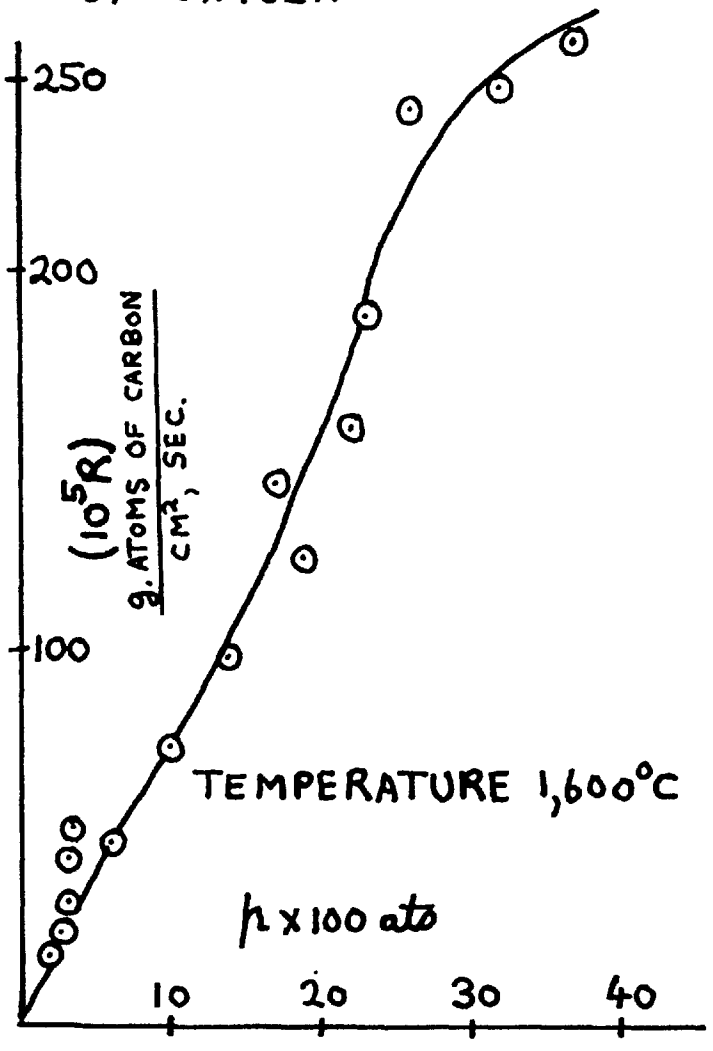




GRAPH 23 POLYCRYSTALLINE GRAPHITE

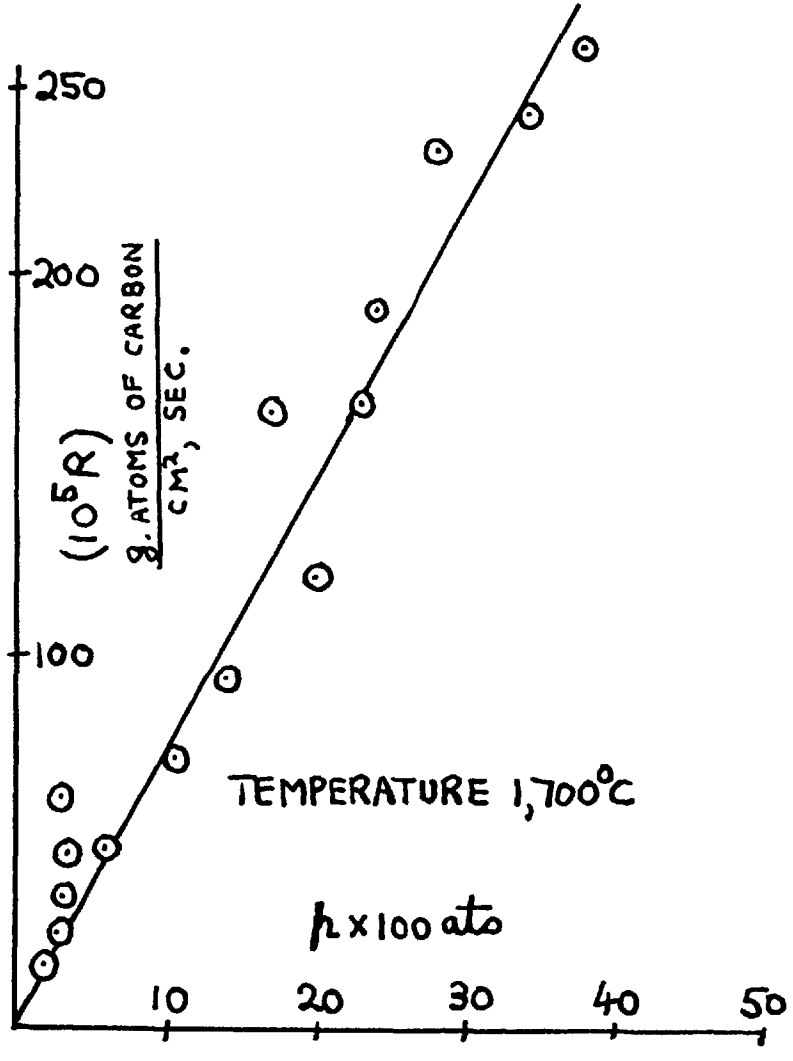
REACTION RATE ν CALCULATED SURFACE PRESSURE OF OXYGEN

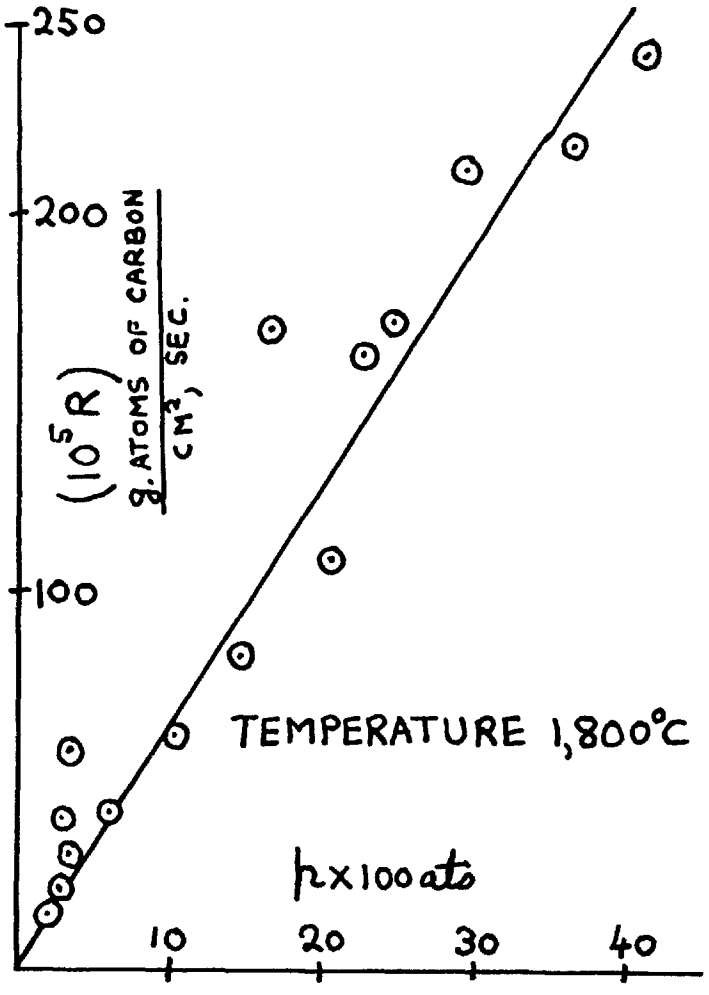




GRAPH 24 POLYCRYSTALLINE GRAPHITE

REACTION RATE v CALCULATED SURFACE PRESSURE OF OXYGEN

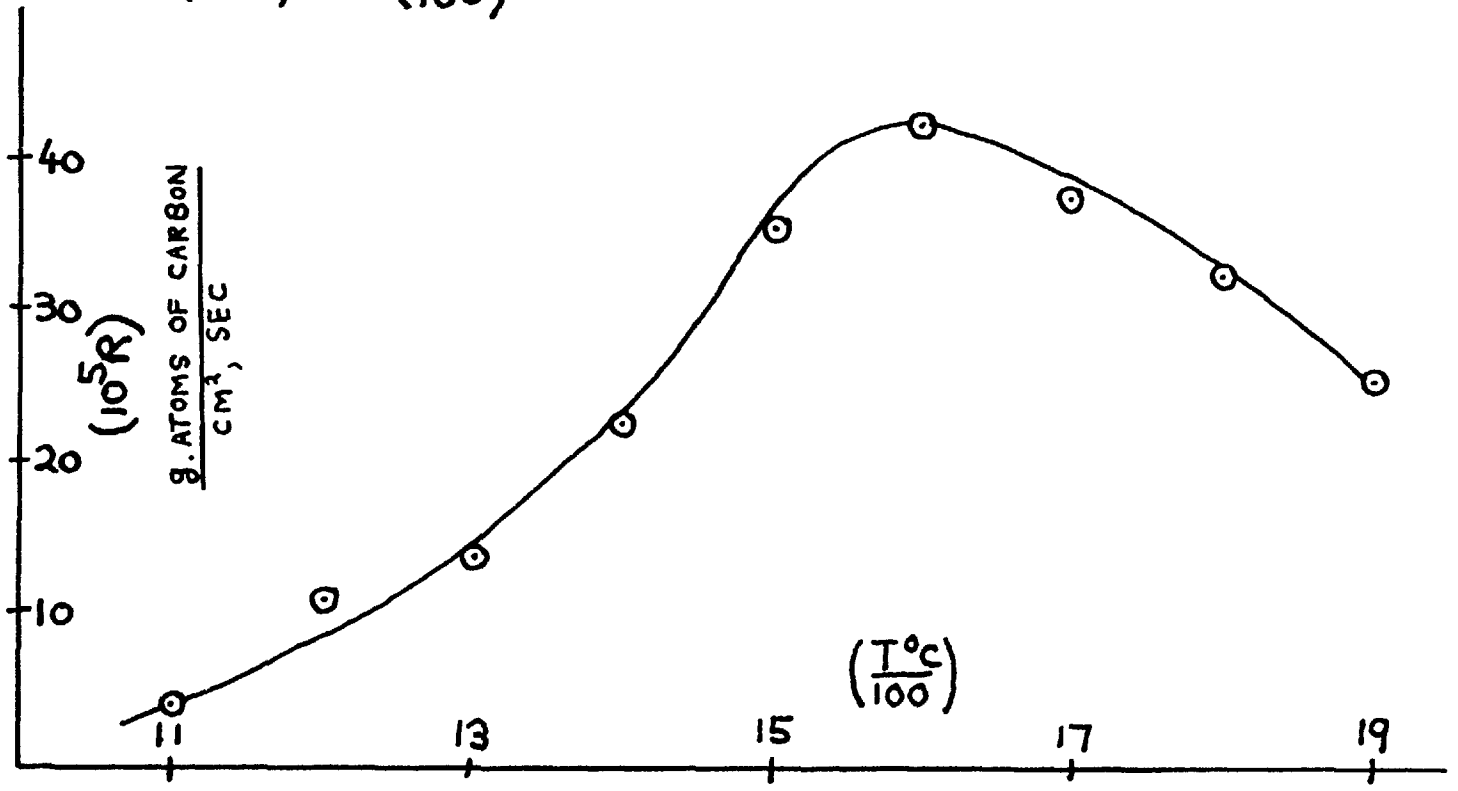




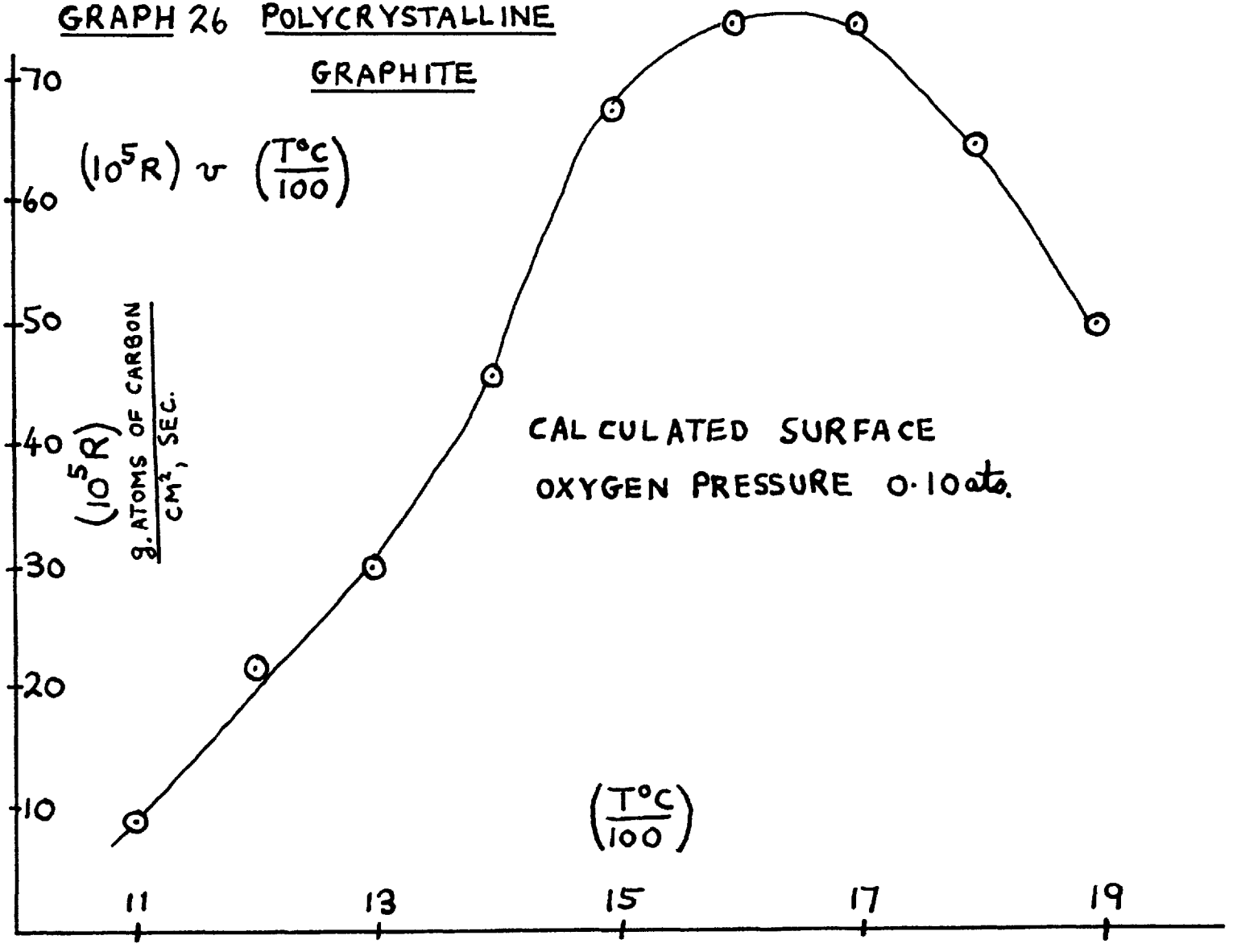
GRAPH 25 POLYCRYSTALLINE GRAPHITE

CALCULATED SURFACE OXYGEN PRESSURE 0·05 ato

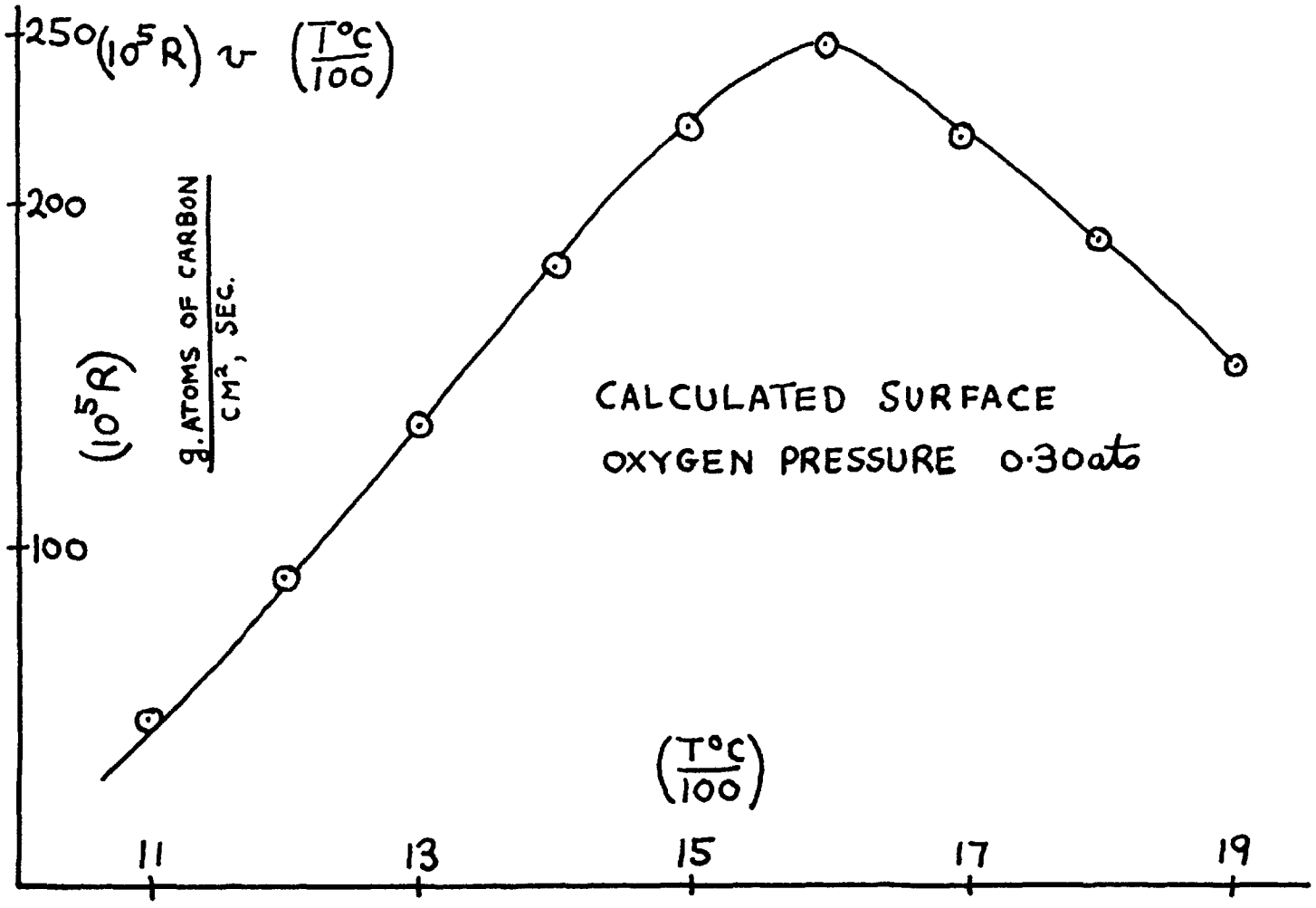
$(10^5 R)$ v $\left(\frac{T°C}{100}\right)$

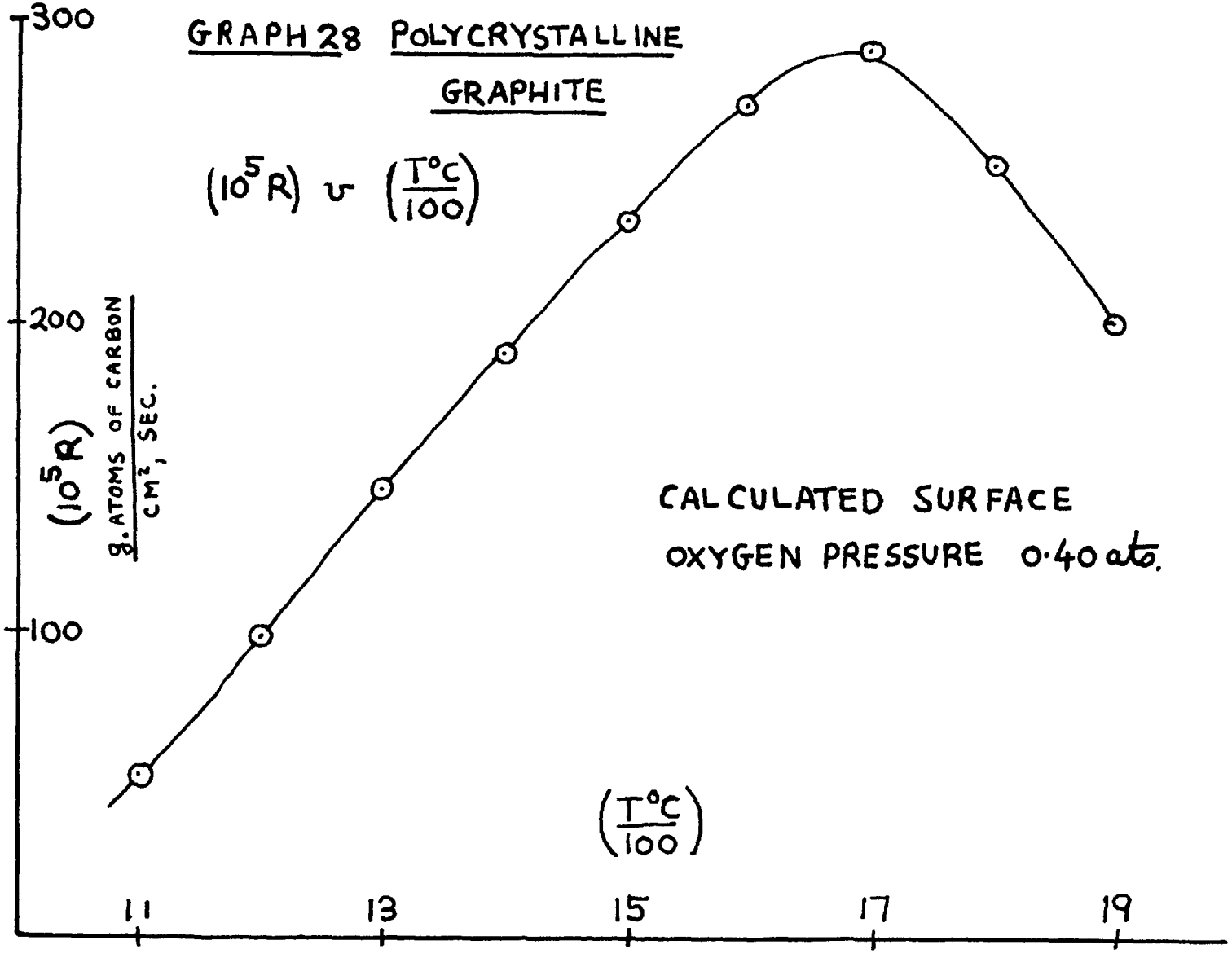


GRAPH 26 POLYCRYSTALLINE GRAPHITE



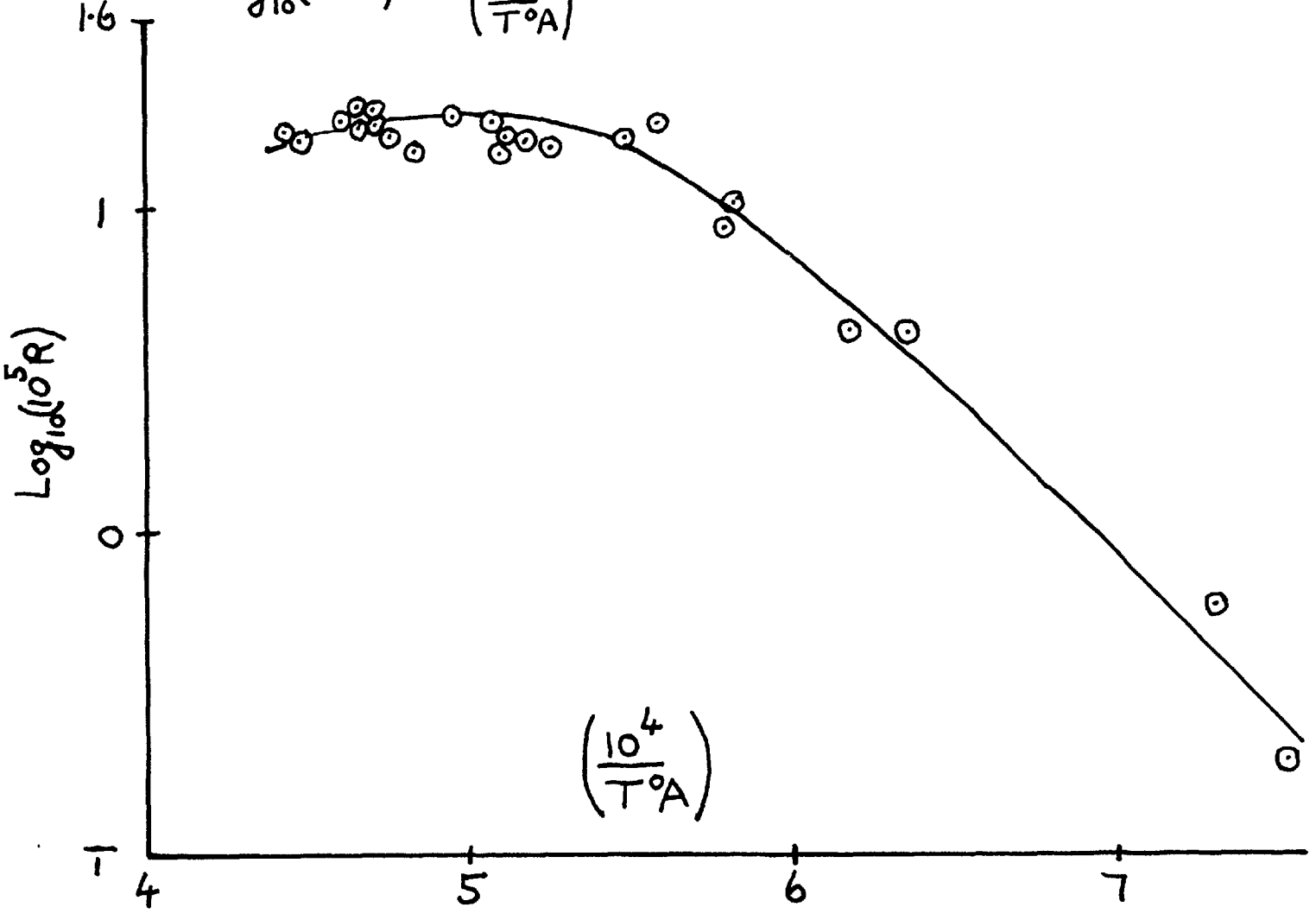
GRAPH 27 POLYCRYSTALLINE GRAPHITE




GRAPH 28 POLYCRYSTALLINE GRAPHITE
$(10^5 R)$ v $\left(\frac{T°C}{100}\right)$
300
200
100
$(10^5 R)$ g. ATOMS OF CARBON / CM², SEC.
CALCULATED SURFACE
OXYGEN PRESSURE 0·40 ato.
$\left(\frac{T°C}{100}\right)$
11
13
15
17
19

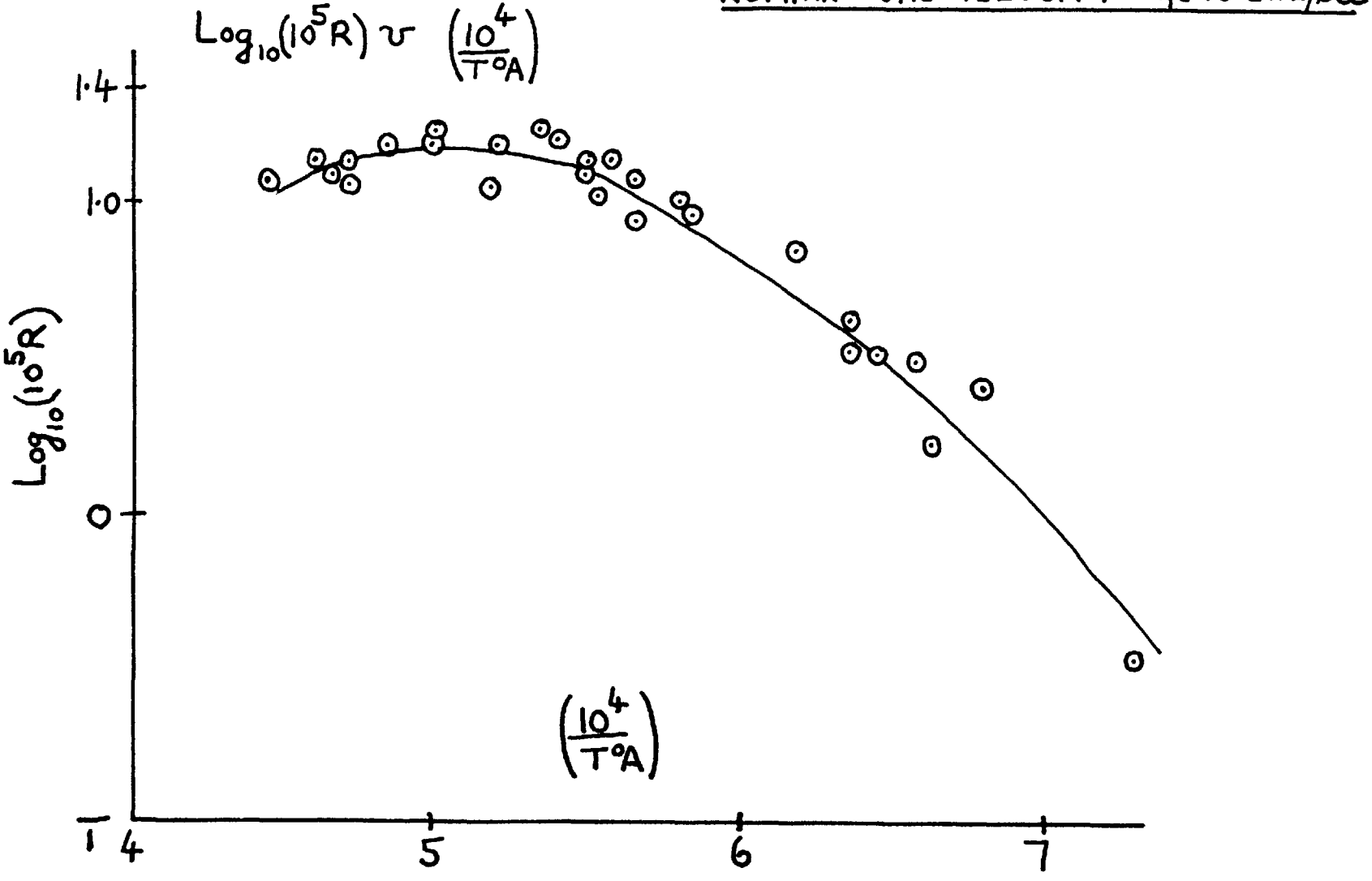
GRAPH29 PYROGRAPHITE. OXYGEN AT 0·13 ATS

NOMINAL GAS VELOCITY 7,000 cms/sec



GRAPH 30 PYROGRAPHITE. OXYGEN AT 0·20 ATS.

NOMINAL GAS VELOCITY 1,090 cms/sec



APPENDIX 3.

Gas Impact Pressures at the Leading Edge of a Cylinder.

A pitot tube was placed diametrically through a steel rod of the same size as the carbon rods. Gas at low pressure was allowed to flow radially across the rod.

The impact pressures were measured and compared with the values calculated from the conventional impact pressure formula

$$u_1^2 = 2p_1 v_1 \log_e \frac{p_2}{p_1}$$

in which it was assumed the gas impinges on the surface at velocity u_1

u_1 = the linear gas velocity at the pressure p_1.

v_1 = the specific volume of the gas at p_1.

p_2 = the impact pressure of the gas.

Nominal Gas Velocity (Proportional to Reynolds Number) cms/sec.	Gas Velocity at Ambient Gas Pressure	Ambient Pressure (ats.)	Calculated Impact Pressure (ats.)	Measured Impact Pressure (ats.)
7000	1.67 x7000	0.60	0.65	0.65
7000	2.5 x7000	0.40	0.51	0.44
7000	5 x7000	0.20	0.40	0.30
7000	7.7 x7000	0.13	0.65	0.23
7000	2 x7000	0.50	0.56	0.54
7000	3.3 x7000	0.30	0.40	0.34
1090	15 x1090	0.066	0.075	0.072
1090	7.7 x1090	0.13	0.133	0.13
1090	5 x1090	0.20	0.202	0.20

Sample Calculation.

If the nominal gas velocity = 7000 cms/sec.

Gas velocity at 0.13 ats. = 7.7 x7000 cms/sec.

Now $p_1 v_1 = p_2 v_2 = 9 \times 10^8$ cm^2/sec^2

$$\log_e \frac{p_2}{p_1} = \frac{u_1^2}{2 p_1 v_1} = \frac{59 \times 49 \times 10^6}{2 \times 9 \times 10^8} = 1.6$$

$$\log_{10} \frac{p_2}{p_1} = \frac{1.6}{2.303} = 0.7 \qquad \frac{p_2}{p_1} = 5$$

$$p_2 = 5 \times 0.13 = 0.65 \text{ ats.}$$

APPENDIX 4.

Error Analysis.

There are two types of source of error in the measured reaction rate (R); (A) errors in the direct measurements of length, time and density from which R is calculated and (B) errors in the independent variables temperature, gas velocity, etc of which R is a function. The error analysis shows the effect of errors in all the experimental observations on the error in R and in this way discovers which observations must be made most carefully. The total estimated error should agree approximately with the actual measured error in R.

(A) Errors arising from errors in direct measurements.

If the linear rate of removal of carbon at the point of attack is

$$\frac{x}{t} \quad \frac{\text{cms}}{\text{sec}}$$

The rate of removal of carbon per cm^2, $R = \frac{x\rho}{12t}$ $\frac{\text{g atoms}}{\text{cm}^2\,\text{sec}}$

where ρ = density of the carbon gms/cm^3.

$$R = \frac{x\rho}{12t}$$

$$\frac{\partial R}{\partial \rho} = \frac{1}{12}\,\frac{x}{t}, \qquad \frac{\partial R}{\partial x} = \frac{\rho}{12t}, \qquad \frac{\partial R}{\partial t} = -\frac{\rho x}{12t^2}$$

and $dR = \frac{\partial R}{\partial \rho}\,d\rho + \frac{\partial R}{\partial x}\,dx + \frac{\partial R}{\partial t}\,dt$

and $\sigma^2(R) = \sum \left(\frac{\partial R}{\partial i}\right)^2 \sigma^2(i)$

where $\sigma^2(R)$ = the variance of R

and R is a function of i independent variables.

$$\sigma^2(R) = \left(\frac{1}{12t}\right)^2 \left[x^2\sigma^2(\rho) + \rho^2\sigma^2(x) + \left(\frac{\rho x}{t}\right)^2 \sigma^2(t) \right]$$

Probable error in ρ = $\pm$ 0.1 gms/cc.

Probable error in x = $\pm$ 0.002 cms.

Probable error in t = $\pm$ 0.2 secs.

$\sigma^2(\rho) = 10^{-2}$ gm^2/cm

$\sigma^2(x) = 4 \times 10^{-6}$ cm^2

$\sigma^2(t) = 4 \times 10^{-2}$ sec^2

A typical value of the reaction rate is

$$R = 60 \times 10^{-5} \ \frac{\text{g atoms}}{\text{cm}^2 \text{ sec}}$$ when ρ = 1.75 gms/cc.
x = 0.04 cms.
t = 10 secs.

$$\sigma^2(R) = \frac{10^{-6}}{(120)^2} \left(4 + 12 + 2 \right)$$

Errors in length contribute most to the error in R

$$\sigma(R) = 4 \times 10^{-5} \ \frac{\text{g atoms}}{\text{cm}^2 \text{ sec}}$$

$$\text{Rate of Reaction} = (60 \pm 4) \times 10^{-5} \ \frac{\text{g atoms}}{\text{cm}^2 \text{ sec.}}$$

The measured error in R is closer to $\pm$ 10% so that it would seem that the method used to measure the amount of reaction is not the only source of error.

(B) Errors in R arising from errors in temperature, etc.

R is a function of temperature etc. but the form of the function will be dependent on the rate controlling process i.e. mass transfer or chemical reaction. These two cases will be discussed separately.

B.1. Mass Transfer Control of the Reaction Rate.

The following formula has been derived from the experimental results to express R as a function of gas velocity, temperature, partial oxygen pressure and total gas pressure. This equation comes from the regression equation accounting for mass transfer rates up to a nominal gas velocity of 1500 cms./sec.

$$R = \left(20\ Vel^{0.5}\ e^{\frac{-2000}{1.98\ T}}\ p_o'\ P^{-1} \right) x10^{-5}\ \frac{g\ atoms}{cm^2\ sec}$$

p_o = partial pressure of oxygen in ats.
T = absolute surface temperature of the carbon °K.
P = total ambient gas pressure in ats.

$$\frac{\partial R}{\partial V} = \left(\frac{20 \times 0.5}{V^{0.5}}\ e^{\frac{-2000}{1.98T}}\ p_o\ P^{-1} \right) x10^{-5}$$

$$\frac{\partial R}{\partial T} = \left(20\ V^{0.5}\ p_o\ P^{-1}\ \frac{2000}{1.98T^2} e^{\frac{-2000}{1.98T}} \right) x10^{-5}$$

$$\frac{\partial R}{\partial p_o} = \left(20\ V^{0.5}\ e^{\frac{-2000}{1.98T}}\ P^{-1} \right) x10^{-5}$$

$$\frac{\partial R}{\partial P} = -\left(20\ V^{0.5}\ e^{\frac{-2000}{1.98T}}\ p_o\ P^{-2} \right) x10^{-5}$$

The probable error in velocity because of a $\pm$ 1 mm. error in a flowmeter at about a velocity of 900 cms/sec. is about 10 cms./sec.

$$\sigma^2(V) = 100 \text{ cm}^2/\text{sec}^2$$

Probable error in temperature = $\pm$ 20°C.

$$\sigma^2(T) = 400 (^\circ C)^2$$

The probable error in p_o and P is $\pm$ 1 mm. mercury.

$$\sigma^2(p_o) = \sigma^2(P) = 1.7 \times 10^{-6} \text{ (atm.}^2\text{)}.$$

When V = 900 cms/sec.
T = 1,500°C. = 1773 °A
p_o = 0.06 ats.
P = 0.30 ats.
R = 67 x10^{-5} g.atoms/cm^2, sec.

$$\sigma^2(R) = \left[\left(\frac{\partial R}{\partial V}\right)^2 \sigma^2(V) + \left(\frac{\partial R}{\partial T}\right)^2 \sigma^2(T) + \left(\frac{\partial R}{\partial p_o}\right)^2 \sigma^2(p_o) + \left(\frac{\partial R}{\partial P}\right)^2 \sigma^2(P) \right]$$

$$= 10^{-10} \left(0.16 + 0.80 + 0.08 + 2.00 \right)$$

When there is mass transfer control the most important error is the error in the total pressure.

$$\text{Total Error in R} = \sigma^2_{\text{Total}}(R)$$

$$\sigma^2_{\text{Total}}(R) = \sigma^2_{\text{measurements}}(R) + \sigma^2_{\text{variables}}(R) = 15 \times 10^{-10}$$

$$\sigma_T(R) = 4 \times 10^{-5} \quad \text{i.e.} \quad \pm 7\%.$$

This magnitude of error is near the measured error in R, but errors in the direct measurements are the most important.

B.2. Chemical Control of the Reaction Rate.

The chemical reaction rate can be expressed in the usual way

$$R = k_o e^{-A/RT} p$$

A = the activation energy of the reaction, found to be about 30,000 cals/g. atom.

p = oxygen partial pressure in ats.

Now $\frac{\partial R}{\partial p} = \frac{R}{p}$ and $\frac{\partial R}{\partial T} = \frac{RA}{1.98T^2}$

A typical value of R is 60×10^{-5} $\frac{g \text{ atoms}}{cm^2 \text{ sec}}$ at 1,500°C.

and p = 0.18 ats.

$$\sigma^2(R) = (20 + 3600) \times 10^{-12}$$

The most important error is in the temperature

$$\sigma^2_{\text{Total}}(R) = \sigma^2_{\text{measurements}}(R) + \sigma^2_{\text{variables}}(R) = 5{,}000 \times 10^{-12}$$

$$\sigma_T(R) = 7 \times 10^{-5}$$

The error is ± 10% which is approximately the observed error. The errors in temperature contribute most to the total error.

APPENDIX 5.

Optical Pyrometry.

Apart from any reading error there is in most cases an error in temperature measurements made with optical pyrometers. The temperatures recorded by optical pyrometers are "apparent black body temperatures" and may require considerable correction to compensate for the emissivity of the surface at the wavelength of the emission [25,26,27]. From the definition of a black body and from Kirchoff's Law it follows that non black bodies are less bright than black bodies of the same temperature. If non-black bodies are assumed black the temperatures measured by an optical pyrometer are less than the true temperature.

Wien's formula is used to calculate the true temperature (T) from the apparent temperature (S) when the emissivity (ε) of the particular body is known, at the wavelength of emission (λ).

$$\frac{1}{T} - \frac{1}{S} = \frac{\lambda \log_e \varepsilon}{C_2} \qquad C_2 = 14{,}350 \text{ micron degrees}$$

The magnitude of the correction to the observed temperature increases as the observed temperature increases and as the deviations of the emissivity from unity increase. There is no need for any temperature correction when temperatures are measured on black body cavities but corrections are required when the temperatures of unenclosed radiating bodies are measured.

The following table [28] gives the corrections for a pyrometer having a wavelength of 0.65 μ

Emissivity	0.1	0.2	0.3	0.4	0.5	0.6	0.7	0.8	0.9
Observed Temperature °C	°C	°C	°C	°C	°C	°C	°C	°C	°C
600	88	63	44	35	25	18	13	8	4
800	135	91	66	50	37	27	19	12	6
1000	195	130	95	71	53	39	27	17	8
1200	267	177	128	96	71	52	36	22	10
1400	353	232	168	125	93	67	46	29	14
1600	454	295	213	157	117	85	58	36	17
1800	570	368	263	195	144	104	71	44	21
2000	705	450	263	236	174	126	87	54	25

Various values have been suggested for the average emissivity of carbon at $\lambda = 0.65\mu$

$\varepsilon = 0.53$ [29] and $\varepsilon = 0.85$ [28]

Correction tables [30] for the temperatures of carbon filaments are more in agreement with the value of ε of 0.85.

More recent measurements [31] made at wavelength $\lambda = 0.653\mu$ and temperatures 1,300°C. to 2,000°C. give values of ε in the range 0.75 to 0.80.

BIBLIOGRAPHY.

1. Strickland-Constable, Journal Chimie Physique, 47, 1950.
2. Duval, Paris Carbon Conference, 1960. 3 .
3. Gulbransen, Ind.Eng.Chem., 44, 1952, 1034.
4. Rossberg and Wicke, Chemie Ing.Techn., 28, 1956, 181.
5. Rossberg, Zeit.Elektrochem., 60, 1956, 952.
6. Thiele, Ind.Eng.Chem., 31, 1939, 917.
7. Wicke and Hedden, Zeit. Elektrochem., 57, 1953, 636.
8. Walker, Paris Carbon Conference, 1960. 10.
9. Rossberg and Wicke, Zeit. Elektrochem., 57, 1953, 641.
10. Arthur, Trans.Farad.Soc., 47, 1951, 164.
    Bridges, J.Soc.Chem.Ind., 67, 1948, 445.
11. Ramchandra, Ind.Eng.Chem., 50, 1958, 331.
12. Petersen and Wright, Ind.Eng.Chem., 47, 1955, 1624.
13. Hennig, Paris Carbon Conference, 1960. 12
14. Eyring and Blyholder, J.Phys.Chem., 1957, 61, 682.
15. Strickland-Constable, Trans.Faraday Soc., 40, 1944.
16. Strickland-Constable, Trans.Faraday Soc., 43, 1947.
17. Duval, Ann.Chim., 10, 1955, 903.
18. Duval, Proc.Third Carbon Conference, 257. 1957.
19. Meyer, Z.Physik.Chem., B, 1932, XVIII, 385.
20. Meyer, Z.Elektrochem., 41, 1935, 136.
21. Blyholder and Eyring, J.Phys.Chem., 1958, 62, 263.
22. Watt et alia, Carbon Conference, London, 1957.

23. Kuchta et alia, Ind.Eng.Chem., 44, 1952, 1559.

24. Walker and Day, Carbon Conference, London, 1957.

25. Trans.Inst.Gas Eng., 1932-33, 494.

26. Trans. Faraday Soc., 15, 1919-20, 36.

27. Emslie and Blau, J.Electrochem.Soc., 106, 1959, 877.

28. Kaye and Laby, Physical and Chemical Constants, 49.

29. Lummer, Z.Elektrochem., 34, 1913, 1428.

30. International Critical Tables, Vol.5, 245, Table 1.

31. Thorn and Simpson, J.Appl.Phys., 24, 1953, 633.

32. Dienes, J.Appl.Phys., 23, 1952, 1194.

33. Feldman, J.Appl.Phys., 23, 1952, 1200.